Supporting Information

Radical–Anion Coupling Through Reagent Design: Hydroxylation of Aryl Halides

Andrew J. Greener,‡ Patrycja Ubysz,‡ Will Owens-Ward, George Smith, Ivan Ocaña, Adrian C. Whitwood, Victor Chechik, Michael J. James*

Department of Chemistry, University of York, York, YO10 5DD, UK.

michael.james@york.ac.uk

Table of Contents

1. General Information

Except where stated, all reagents and anhydrous solvents were purchased from commercial sources and used without further purification.

NMR spectra were recorded on a Bruker AVIII300NB, JEOL ECX400, JEOL ECS400, or Bruker AVIIIHD500 spectrometer. All spectral data was acquired at the stated temperature. Chemical shifts (δ) are quoted in parts per million (ppm). The following residual solvent signals were used as references for ^{1}H and ^{13}C NMR spectra: δ_H 7.26 and δ_C 77.0 for $CDCl_3$, and δ_H 2.50 ppm, δ_C 39.52 ppm for DMSO-d_6. Coupling constants (*J*) are reported in Hertz (Hz) to the nearest 0.1 Hz. The multiplicity abbreviations used are: s singlet, d doublet, t triplet, q quartet, m multiplet.

Infrared (IR) spectra were recorded on a PerkinElmer UATR 2 spectrometer as a thin film dispersed from CH_2Cl_2 or $CDCl_3$. The wave numbers (*v*) of recorded IR-signals are quoted in cm^{-1}. UV/Vis absorption spectra were recorded on an Agilent Cary 60 spectrometer.

High-resolution mass-spectra were obtained by the University of York Mass Spectrometry Service, using electrospray ionisation (ESI) on a Bruker Daltonics, Micro-tof spectrometer.

EPR spectra were recorded on a Bruker EMX micro spectrometer.

Thin layer chromatography was carried out on Merck silica gel $60F_{254}$ pre-coated aluminium foil sheets and were visualised using UV light (254 nm) and stained with basic aqueous potassium permanganate. Column chromatography was carried out using Fluka silica gel (SiO_2), 35–70 μm, 60 Å under a light positive pressure, eluting with the specified solvent system.

All photochemical reactions were conducted in a fan cooled EvoluChem PhotoRedOx Box reactor using commercial LEDs purchased from HepatoChem Inc.

2. Experimental Procedures and Characterization Data

2.1. Oxime Synthesis

(*E*)-1-Methyl-1H-pyrrole-2-carboxaldehyde oxime (9d)

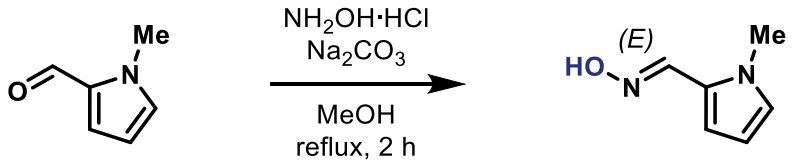

To a stirred solution of $NH_2OH{\cdot}HCl$ (1.67 g, 24.0 mmol), Na_2CO_3 (2.54 g, 24.0 mmol) in MeOH (100 mL) was added *N*-methyl-2-pyrrolecarboxaldehyde (2.15 mL, 20.0 mmol). The mixture was then heated to reflux and stirred for 2 hours. The reaction was allowed to cool to room temperature and MeOH was removed under reduced pressure. The residue was dissolved in EtOAc (50 mL) and H_2O (50 mL). The organic phase was separated and the aqueous phase was extracted with EtOAc (2 × 50 mL). The organics were combined, washed with brine (50 mL), dried ($MgSO_4$), and concentrated under reduced pressure. The crude product was dissolved in a minimum amount of CH_2Cl_2 and purified by column chromatography (30% EtOAc + 3% Et_3N in hexane) to afford the *title compound* **9d** (2.12 g, 17.1 mmol, 86%) as a white solid.

Note: Et_3N is added to the column eluent to prevent the decomposition of the oxime reagent.

***R*$_f$** 0.45 (30% EtOAc in hexane);

ATR-FTIR (thin film) ν_{max}/cm^{-1} 3312, 1619, 1482, 1416, 1309, 1057, 948, 817, 730;

^{1}H NMR (300 MHz, DMSO-D_6) δ_H 10.71 (s, 1H), 8.03 (s, 1H), 6.85 (dd, *J* = 2.6, 1.8 Hz, 1H), 6.32 (dd, *J* = 3.7, 1.8 Hz, 1H), 6.02 (dd, *J* = 3.7, 2.6 Hz, 1H), 3.73 (s, 3H);

^{13}C NMR (101 MHz, DMSO-D_6) δ_C 141.5 (CH), 126.5 (CH), 125.6 (C), 112.4 (CH), 107.8 (CH), 35.9 (CH_3).

HRMS (ESI^+) *m/z* calcd. for $C_6H_9N_2O$ $(M + H)^+$ 125.0709, found 125.0712.

2.2. Aryl Halide Hydroxylation

General Procedure A

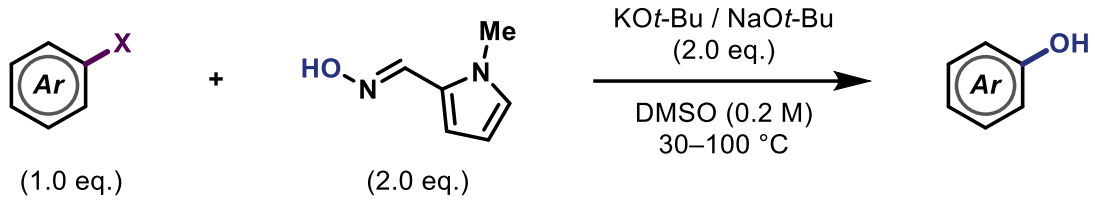

To an oven-dried screw-cap 8 mL reaction vial was charged the appropriate base (2.0 eq.), oxime **9d** (2.0 eq.), and if solid, the arene coupling partner **3** (0.30 mmol, 1.0 eq.). To the solids was sequentially added a magnetic stir bar, anhydrous DMSO (1.5 mL), and if liquid, the arene coupling partner **3**. The vial was closed and the reaction mixture was sparged with N_2 for 15 minutes, then sealed with parafilm. The reaction mixture was stirred and heated at the specified temperature in a metal heating block for the stated time. The mixture was then diluted with CH_2Cl_2 or EtOAc (20 mL), poured into a mixture of water (10 mL) and brine (5 mL), then acidified with 10% aq. HCl (~1 mL). The organic phase was collected and the aqueous phase was extracted with CH_2Cl_2 or EtOAc (3 × 20 mL). The organics were combined, dried ($MgSO_4$), and concentrated under reduced pressure. The crude product was then purified by column chromatography to afford the phenol product **8**.

4′-Hydroxyacetophenone (8a)

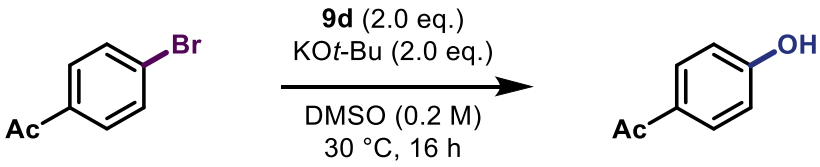

Synthesized using **General Procedure A** with potassium *tert*-butoxide (67.3 mg, 0.60 mmol, 2.0 eq.), oxime **9d** (74.5 mg, 0.60 mmol, 2.0 eq.), and 4′-bromoacetophenone **3a$_{Br}$** (59.7 mg, 0.30 mmol, 1.0 eq.) in DMSO (1.5 mL). The reaction was heated at 30 °C and stirred for 16 h. The crude product was dissolved in a minimum amount of CH_2Cl_2, dried onto silica gel, and purified by column chromatography (30% EtOAc in hexane) to afford the *title compound* **8a** (33.5 mg, 0.246 mmol, 82%) as a white solid.

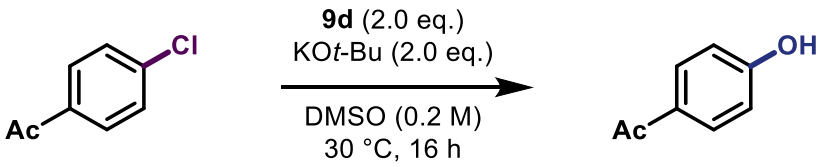

Synthesized using **General Procedure A** with potassium *tert*-butoxide (67.3 mg, 0.60 mmol, 2.0 eq.), oxime **9d** (74.5 mg, 0.60 mmol, 2.0 eq.), and 4′-chloroacetophenone **3a$_{Cl}$** (46.4 mg, 0.30 mmol, 1.0 eq.) in DMSO (1.5 mL). The reaction was heated at 30 °C and stirred for 16 h. The crude product was dissolved in a minimum amount of CH_2Cl_2, dried onto silica gel, and purified by column chromatography (30% EtOAc in hexane) to afford the *title compound* **8a** (30 mg, 0.22 mmol, 73%) as a white solid.

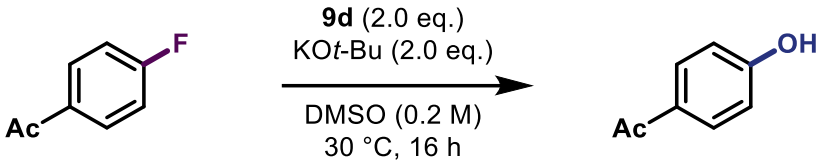

Synthesized using **General Procedure A** with potassium *tert*-butoxide (67.3 mg, 0.60 mmol, 2.0 eq.), oxime **9d** (74.5 mg, 0.60 mmol, 2.0 eq.), and 4′-fluoroacetophenone **3a$_{F}$** (41.4 mg, 0.30 mmol, 1.0 eq.) in DMSO (1.5 mL). The reaction was heated at 30 °C and stirred for 16 h. The crude product was dissolved in a minimum amount of CH_2Cl_2, dried onto silica gel, and purified by column chromatography (30% EtOAc in hexane) to afford the *title compound* **8a** (36.0 mg, 0.265 mmol, 88%) as a white solid.

R$_f$ 0.51 (50% EtOAc in hexane);

ATR-FTIR (thin film) ν_{max}/cm^{-1} 3303, 1660, 1602, 1575, 1512, 1357, 1277, 1218, 1166, 963 848, 816, 568;

^{1}H NMR (300 MHz, $CDCl_3$) δ_H 7.91 (d, *J* = 8.8 2H), 6.91 (d, *J* = 8.8 Hz, 2H), 6.37 (br s, 1H) 2.58 (s, 3H);

^{13}C NMR (101 MHz, $CDCl_3$) δ_C 198.4 (C), 161.2 (C), 131.3 (CH), 129.9 (C), 115.6 (CH), 26.5 (CH_3);

HRMS (ESI^-) *m/z* calcd. for $C_8H_7O_2$ $(M-H)^-$ 135.0452, found 135.0455.

Spectroscopic data matched those reported in the literature.[1]

4′-Hydroxybenzophenone (8b)

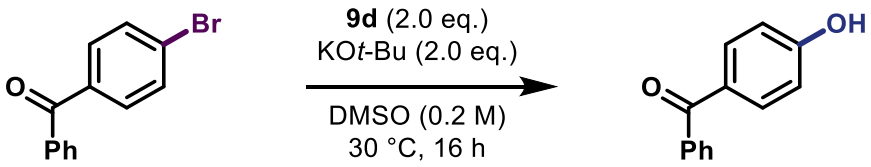

Synthesized using **General Procedure A** with potassium *tert*-butoxide (67.3 mg, 0.60 mmol, 2.0 eq.), oxime **9d** (74.5 mg, 0.60 mmol, 2.0 eq.), and 4′-bromobenzophenone **3b$_{Br}$** (78.3 mg, 0.30 mmol, 1.0 eq.) in DMSO (1.5 mL). The reaction was heated at 30 °C and stirred for 16 h. The crude product was dissolved in a minimum amount of CH_2Cl_2, dried onto silica gel, and purified by column chromatography (40% EtOAc in hexane) to afford the *title compound* **8b** (39.0 mg, 0.197 mmol, 66%) as an off-white solid.

***R*$_f$** 0.18 (40% EtOAc in hexane);

ATR-FTIR (thin film) ν_{max}/cm^{-1} 3251, 1633, 1560, 1585, 1572, 1319, 1281, 1150, 699, 606;

^{1}H NMR (400 MHz, $CDCl_3$) δ_H 7.80 (d, *J* = 8.6 Hz, 2H), 7.76 (d, *J* = 7.6 Hz, 2H), 7.57 (t, *J* = 7.6 Hz, 1H), 7.47 (dd, *J* = 7.6, 7.6 Hz, 2H), 6.92 (d, *J* = 8.6 Hz, 2H), 5.76 (br s, 1H);

^{13}C NMR (101 MHz, $CDCl_3$) δ_C 196.8 (C), 160.7 (C), 138.2 (C), 133.2 (CH), 132.3 (CH), 130.0 (CH), 129.8 (C), 128.4 (CH), 115.5 (CH);

HRMS (ESI$^+$) *m/z* calcd. for $C_{13}H_{10}NaO_2$ $(M + Na)^+$ 221.0573, found 221.0572.

Spectroscopic data matched those reported in the literature.[2]

Ethyl 4-hydroxybenzoate (8c)

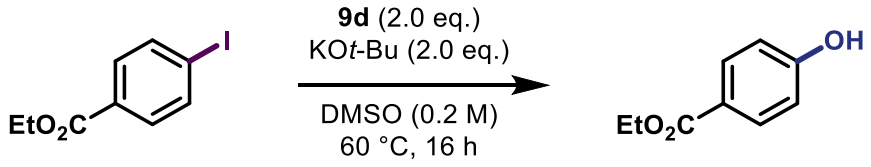

Synthesized using **General Procedure A** with potassium *tert*-butoxide (67.3 mg, 0.60 mmol, 2.0 eq.), oxime **9d** (74.5 mg, 0.60 mmol, 2.0 eq.), and ethyl 4-iodobenzoate **3c$_I$** (82.8 mg, 0.30 mmol, 1.0 eq.) in DMSO (1.5 mL). The reaction was heated at 60 °C and stirred for 16 h. The crude product was dissolved in a minimum amount of CH_2Cl_2, dried onto silica gel, and purified by column chromatography (30% EtOAc in hexane) to afford the *title compound* **8c** (32.0 mg, 0.193 mmol, 64%) as an off-white solid.

***R*$_f$** 0.65 (30% EtOAc in hexane);

ATR-FTIR (thin film) ν_{max}/cm^{-1} 3218, 1673, 1607, 1592, 1287, 1241, 1169;

^{1}H NMR (400 MHz, $CDCl_3$) δ_H 7.96 (d, *J* = 8.8 Hz, 2H), 6.88 (d, *J* = 8.8 Hz, 2H), 4.35 (q, *J* = 7.1 Hz, 2H), 1.38 (t, *J* = 7.1 Hz, 3H);

^{13}C NMR (101 MHz, $CDCl_3$) δ_C 189.1 (C), 160.0 (C), 136.0 (C), 132.0 (CH), 115.3 (CH), 61.0 (CH_2), 14.5 (CH_3);

HRMS (ESI$^-$) *m/z* calcd. for $C_9H_9O_3$ $(M - H)^-$ 165.0557, found 165.0557.

Spectroscopic data matched those reported in the literature.[1]

4-Hydroxybenzaldehyde (8d)

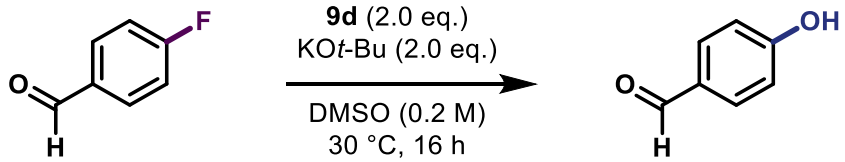

Synthesized using **General Procedure A** with potassium *tert*-butoxide (67.3 mg, 0.60 mmol, 2.0 eq.), oxime **9d** (74.5 mg, 0.60 mmol, 2.0 eq.), and 4-fluorobenzaldehyde **3d$_F$** (37.3 mg, 0.30 mmol, 1.0 eq.) in DMSO (1.5 mL). The reaction was heated at 30 °C and stirred for 16 h. The crude product was dissolved in a minimum amount of CH_2Cl_2, dried onto silica gel, and purified by column chromatography (30% EtOAc in hexane) to afford the *title compound* **8d** (30.0 mg, 0.246 mmol, 82%) as a peach-coloured solid.

***R*$_f$** 0.42 (30% EtOAc in hexane);

ATR-FTIR (thin film) ν_{max}/cm^{-1} 3254, 1675, 1601, 1583, 1216, 1157, 1009;

^{1}H NMR (400 MHz, $CDCl_3$) δ_H 9.88 (s, 1H), 7.82 (d, *J* = 8.7 Hz, 2H), 6.95 (d, *J* = 8.7 Hz, 2H), 5.58 (br s, 1H);

^{13}C NMR (101 MHz, $CDCl_3$) δ_C 191.5 (CH), 161.8 (C), 132.7 (CH), 123.0 (C), 116.16 (CH);

HRMS (ESI$^-$) *m/z* calcd. for $C_7H_5O_2$ $(M - H)^-$ 121.0295, found 121.0298.

Spectroscopic data matched those reported in the literature.[3]

2-Hydroxybenzaldehyde (8e)

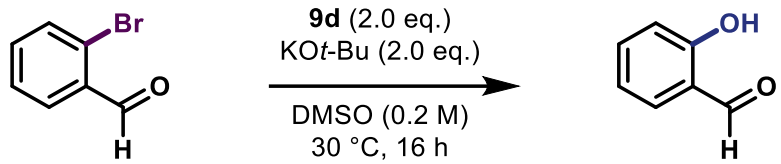

Synthesized using **General Procedure A** with potassium *tert*-butoxide (67.3 mg, 0.60 mmol, 2.0 eq.), oxime **9d** (74.5 mg, 0.60 mmol, 2.0 eq.), and 2-bromobenzaldehyde **3e$_{Br}$** (55.5 mg, 0.30 mmol, 1.0 eq.) in DMSO (1.5 mL). The reaction was heated at 30 °C and stirred for 16 h. After work-up, dibromomethane (52.1 mg, 0.30 mmol, 1.00 equiv.) was added to the reaction mixture, which was then analysed by ^{1}H NMR spectroscopy to approximate the yield of volatile phenol **8e** (66% ^{1}H NMR yield). An analytically pure sample of the volatile product was obtained by column chromatography (20% EtOAc in hexane) for characterisation data.

R$_f$ 0.75 (20% EtOAc in hexane);

ATR-FTIR (thin film) ν_{max}/cm^{-1} 3434, 2932, 1651, 1388, 1255, 1096, 660;

^{1}H NMR (400 MHz, DMSO-D$_6$) δ_H 10.71 (s, 1H), 10.26 (d, *J* = 0.6 Hz, 1H), 7.66 (dd, *J* = 7.8, 1.8, 0.6 Hz, 1H), 7.52 (ddd, *J* = 8.3, 7.2, 1.8 Hz, 1H), 7.01 – 6.98 (m, 1H), 6.98 – 6.93 (m, 1H);

^{13}C NMR (101 MHz, DMSO-D$_6$) δ_C 191.7 (CH), 160.8 (C), 136.5 (CH), 129.2 (CH), 122.3 (C), 119.5 (CH), 117.3 (CH);

HRMS (ESI$^+$) *m/z* calcd. for $C_7H_7O_2$ $(M + H)^+$ 123.0441, found 123.0441.

Spectroscopic data matched those reported in the literature.[4]

3'-Hydroxyacetophenone (8f)

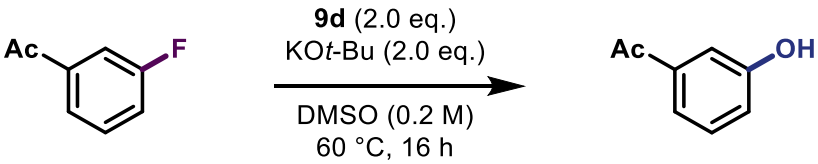

Synthesized using **General Procedure A** with potassium *tert*-butoxide (67.3 mg, 0.60 mmol, 2.0 eq.), oxime **9d** (74.5 mg, 0.60 mmol, 2.0 eq.), and 3′-fluoroacetophenone **3f$_F$** (41.4 mg, 36.8 µl, 0.30 mmol, 1.0 eq.) in DMSO (1.5 mL). The reaction was heated at 60 °C and stirred for 16 h. The crude product was dissolved in a minimum amount of CH_2Cl_2, dried onto silica

gel, and purified by column chromatography (20 – 50% EtOAc in hexane) to the *title compound* **8f** (25.0 mg, 0.184 mmol, 61%) as an off-white solid.

R_f 0.14 (20% EtOAc in hexane);

ATR-FTIR (thin film) ν_{max}/cm^{-1} 3331, 2924, 1668, 1585, 1451, 1289;

^{1}H NMR (400 MHz, $CDCl_3$) δ_H 7.55 – 7.47 (m, 2H), 7.35 (t, J = 8.0 Hz, 1H), 7.13 – 7.04 (m, 1H), 5.75 (br s, 1H), 2.60 (s, 3H);

^{13}C NMR (101 MHz, $CDCl_3$) δ_C 198.8 (C), 156.3 (C), 138.6 (C), 130.1 (CH), 121.3 (CH), 120.8 (CH), 114.8 (CH), 26.9 (CH_3);

HRMS (ESI^-) *m/z* calcd. for $C_8H_7O_2$ $(M-H)^-$ 135.0452, found 135.0449.

Spectroscopic data matched those reported in the literature.[5]

4-Hydroxybenzonitrile (8g)

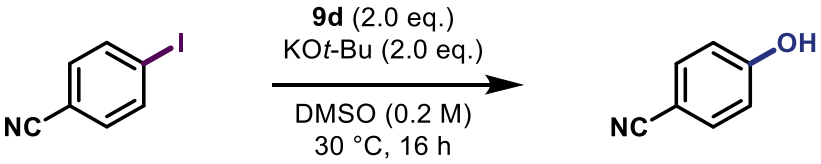

Synthesized using **General Procedure A** with potassium *tert*-butoxide (67.3 mg, 0.60 mmol, 2.0 eq.), oxime **9d** (74.5 mg, 0.60 mmol, 2.0 eq.), and 4-iodobenzonitrile **3g$_I$** (68.7 mg, 0.30 mmol, 1.0 eq.) in DMSO (1.5 mL). The reaction was heated at 30 °C and stirred for 16 h. The crude product was dissolved in a minimum amount of CH_2Cl_2, dried onto silica gel, and purified by column chromatography (40% EtOAc in hexane) to afford the *title compound* **8g** (18.0 mg, 0.151 mmol, 50%) as a brown solid.

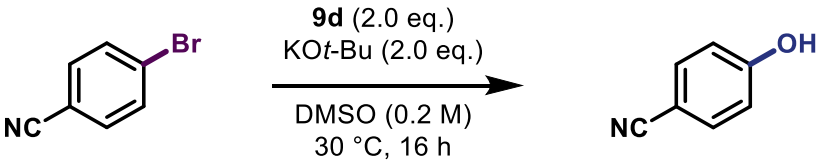

Synthesized using **General Procedure A** with potassium *tert*-butoxide (67.3 mg, 0.60 mmol, 2.0 eq.), oxime **9d** (74.5 mg, 0.60 mmol, 2.0 eq.), and 4-bromobenzonitrile **3g$_{Br}$** (54.6 mg, 0.30 mmol, 1.0 eq.) in DMSO (1.5 mL). The reaction was heated at 30 °C and stirred for 16 h. The crude product was dissolved in a minimum amount of CH_2Cl_2, dried onto silica gel, and

purified by column chromatography (40% EtOAc in hexane) to afford the *title compound* **8g** (24.0 mg, 0.202 mmol, 67%) as a brown solid.

R_f 0.61 (40% EtOAc in hexane);

ATR-FTIR (thin film) ν_{max}/cm^{-1} 3279, 2233, 1612, 1587, 1509;

^{1}H NMR (300 MHz, $CDCl_3$) δ_H 7.56 (d, J = 8.8 Hz, 1H), 6.91 (d, J = 8.8 Hz, 1H), 5.47 (br s, 1H);

^{13}C NMR (101 MHz, $CDCl_3$) δ_C 160.3 (C), 134.5 (CH), 119.4 (C), 116.6 (CH), 103.3 (C);

HRMS (ESI$^-$) *m/z* calcd. for C_7H_4NO $(M - H)^-$ 118.0298, found 118.0300.

Spectroscopic data matched those reported in the literature.[1]

3-Hydroxybenzonitrile (8h)

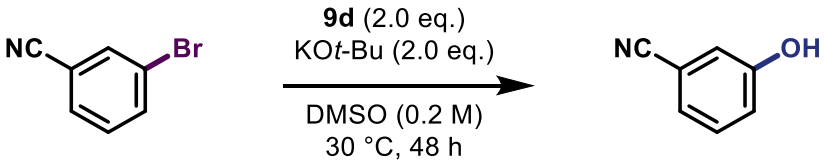

Synthesized using **General Procedure A** with potassium *tert*-butoxide (67.3 mg, 0.60 mmol, 2.0 eq.), oxime **9d** (74.5 mg, 0.60 mmol, 2.0 eq.), and 3-bromobenzonitrile **3h$_{Br}$** (54.6 mg, 0.30 mmol, 1.0 eq.) in DMSO (1.5 mL). The reaction was heated at 30 °C and stirred for 48 h. The crude product was dissolved in a minimum amount of CH_2Cl_2, dried onto silica gel, and purified by column chromatography (40% EtOAc in hexane) to afford the *title compound* **8h** (19 mg, 0.16 mmol, 53%) as an off-white solid.

R_f 0.44 (40% EtOAc in hexane);

ATR-FTIR (thin film) ν_{max}/cm^{-1} 3352, 2927, 2238, 1714, 1598, 1583;

^{1}H NMR (300 MHz, $CDCl_3$) δ_H 7.34 (dd, J = 7.9, 7.7 Hz, 1H), 7.23 (ddd, J = 7.7, 1.3, 1.3 Hz, 1H), 7.14 – 7.02 (m, 2H), 5.41 (br s, 1H);

^{13}C NMR (75 MHz, $CDCl_3$) δ_C 156.1 (C), 130.8 (CH), 124.8 (CH), 120.6 (CH), 118.9 (CH), 118.6 (C), 113.4 (C);

HRMS (ESI$^-$) *m/z* calcd. for C_7H_4NO $(M - H)^-$ 118.0298, found 118.0301.

Spectroscopic data matched those reported in the literature.[6]

4-(Methylsulfonyl)phenol (8i)

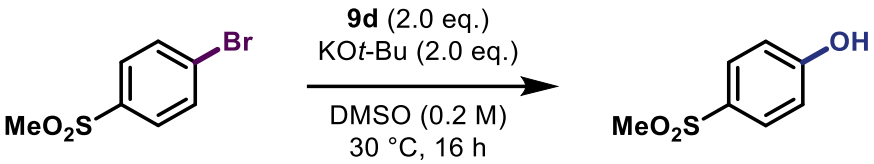

Synthesized using **General Procedure A** with potassium *tert*-butoxide (67.3 mg, 0.60 mmol, 2.0 eq.), oxime **9d** (74.5 mg, 0.60 mmol, 2.0 eq.), and 4-bromophenyl methyl sulfone **3i$_{Br}$** (70.5 mg, 0.30 mmol, 1.0 eq.) in DMSO (1.5 mL). The reaction was heated at 30 °C and stirred for 16 h. The crude product was dissolved in a minimum amount of CH_2Cl_2, dried onto silica gel, and purified by column chromatography (50% EtOAc in hexane) to afford the *title compound* **8i** (36.0 mg, 0.209 mmol, 70%) as a colourless oil.

***R*$_f$** 0.34 (50% EtOAc in hexane);

ATR-FTIR (thin film) ν_{max}/cm^{-1} 3359, 1588, 1288, 1138, 1090, 982, 838, 769, 539, 519;

^{1}H NMR (400 MHz, $CDCl_3$) δ_H 7.79 (d, *J* = 8.9 Hz, 2H), 6.97 (d, *J* = 8.9 Hz, 2H), 3.05 (s, 3H);

^{13}C NMR (101 MHz, $CDCl_3$) δ_C 161.5 (C), 131.0 (C), 129.8 (CH), 116.4 (CH), 45.0 (CH_3);

HRMS (ESI$^+$) *m/z* calcd. for $C_7H_8NaO_3S$ $(M + Na)^+$ 195.0086, found 195.0083.

Spectroscopic data matched those reported in the literature.[1]

3-(Methylsulfonyl)phenol (8j)

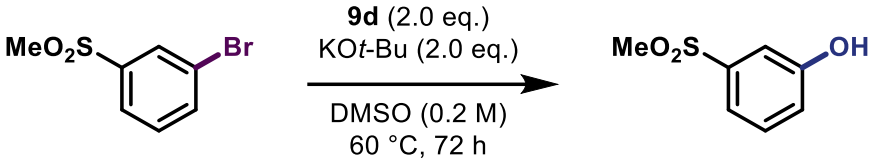

Synthesized using **General Procedure A** with potassium *tert*-butoxide (67.3 mg, 0.60 mmol, 2.0 eq.), oxime **9d** (74.5 mg, 0.60 mmol, 2.0 eq.), and 3-bromophenyl-1-methylsulfone **3j$_{Br}$** (70.5 mg, 0.30 mmol, 1.0 eq.) in DMSO (1.5 mL). The reaction was heated at 60 °C and stirred for 72 h. The crude product was dissolved in a minimum amount of CH_2Cl_2, dried onto silica gel, and purified by column chromatography (60% EtOAc in hexane) to afford the *title compound* **8j** (33.0 mg, 0.192 mmol, 64%) as a bright yellow solid.

***R*$_f$** 0.61 (60% EtOAc in hexane);

ATR-FTIR (thin film) ν_{max}/cm^{-1} 3384, 2927, 1605, 1591, 1447, 1294, 1139, 763;

^{1}H NMR (400 MHz, $CDCl_3$) δ_H 7.47 – 7.35 (m, 3H), 7.16 – 7.09 (m, 1H), 3.07 (s, 3H);

^{13}C NMR (101 MHz, $CDCl_3$) δ_C 157.2 (C), 148.9 (C), 131.0 (CH), 121.7 (CH), 118.9 (CH), 114.0 (CH), 44.5 (CH_3);

HRMS (ESI^+) *m/z* calcd. for $C_7H_8NaO_3S$ $(M + Na)^+$ 195.0086, found 195.0090.

3,5-Bis(trifluoromethyl)phenol (8k)

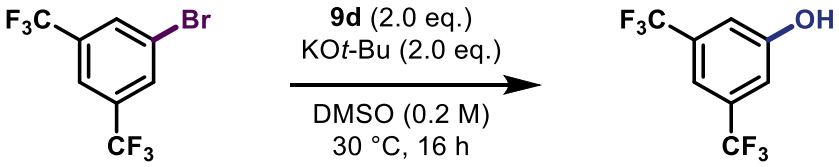

Synthesized using **General Procedure A** with potassium *tert*-butoxide (67.3 mg, 0.60 mmol, 2.0 eq.), oxime **9d** (74.5 mg, 0.60 mmol, 2.0 eq.), and 3,4-bis(trifluoromethyl)bromobenzene **3k$_{Br}$** (87.9 mg, 0.30 mmol, 1.0 eq.) in DMSO (1.5 mL). The reaction was heated at 30 °C and stirred for 16 h. The crude product was dissolved in a minimum amount of CH_2Cl_2, dried onto silica gel, and purified by column chromatography (80% CH_2Cl_2 in hexane) to afford the *title compound* **8k** (55.2 mg, 0.240 mmol, 80%) as a pale-yellow solid.

R$_f$ 0.30 (80% CH_2Cl_2 in hexane);

ATR-FTIR (thin film) ν_{max}/cm^{-1} 3276, 2922, 2852, 1710, 1614, 1464, 1391, 1279, 1176, 1136, 946, 846, 683;

^{1}H NMR (400 MHz, $CDCl_3$) δ_H 7.44 (s, 1H), 7.26 (s, 2H):

^{18}F NMR (282 MHz, $CDCl_3$) δ_F -63.2 (s, 6F);

HRMS (ESI^-) *m/z* calcd. for $C_8H_4F_6O$ $(M - H)^-$ 229.0094, found 229.0093 (−1.5 ppm error).

Spectroscopic data matched those reported in the literature.[7]

4-Hydroxybenzotrifluoride (8l)

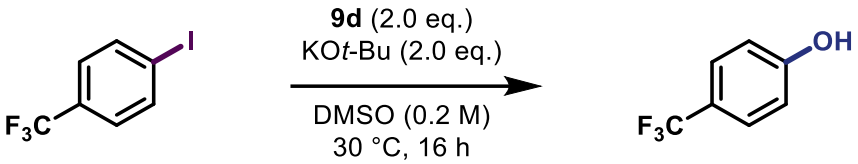

Synthesized using **General Procedure A** with potassium *tert*-butoxide (67.3 mg, 0.60 mmol, 2.0 eq.), oxime **9d** (74.5 mg, 0.60 mmol, 2.0 eq.), 4-iodobenzotrifluoride **3l$_I$** (81.6 mg, 0.30 mmol, 1.0 eq.) in DMSO (1.5 mL). The reaction was heated at 30 °C and stirred for 16 h. After work-up, 1-fluoronaphthalene (43.9 mg, 0.30 mmol, 1.00 equiv.) was added to the reaction mixture, which was then analysed by ^{19}F NMR spectroscopy to approximate the the yield of volatile phenol **8l** (57% ^{19}F NMR yield). An analytically pure sample of the volatile product was obtained by column chromatography (60% DCM in hexane) for characterisation data.

R$_f$ 0.20 (75% DCM in hexane);

ATR-FTIR (thin film) ν_{max}/cm^{-1} 3674, 2922, 2852, 1463, 1324, 1122, 1065, 840, 816, 754;

^{1}H NMR (400 MHz, $CDCl_3$) δ_H 7.50 (d, J = 8.4 Hz, 2H), 6.91 (d, J = 8.4 Hz, 2H), 5.41 (br s, 1H);

^{18}F NMR (282 MHz, $CDCl_3$) δ_F -61.5 (s, 3F);

HRMS (ESI$^-$) *m/z* calcd. for $C_7H_4F_3O$ $(M-H)^-$ 161.0220, found 161.018 (1.2 ppm error).

Spectroscopic data matched those reported in the literature.[8]

4-Nitrophenol (8m)

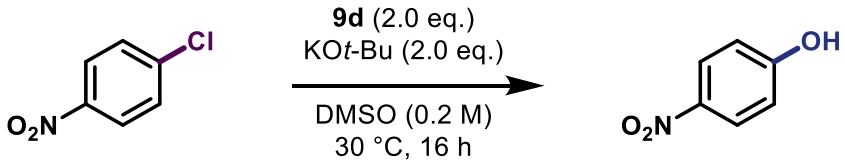

Synthesized using **General Procedure A** with potassium *tert*-butoxide (67.3 mg, 0.60 mmol, 2.0 eq.), oxime **9d** (74.5 mg, 0.60 mmol, 2.0 eq.), and chloro-4-nitrobenzene **3m$_{Cl}$** (47.3 mg, 0.30 mmol, 1.0 eq.) in DMSO (1.5 mL). The reaction was heated at 30 °C and stirred for 16 h. The crude product was dissolved in a minimum amount of CH_2Cl_2, dried onto silica gel, and

purified by column chromatography (25% EtOAc in hexane) to afford the *title compound* **8m** (31.9 mg, 0.229 mmol, 76%) as a yellow solid.

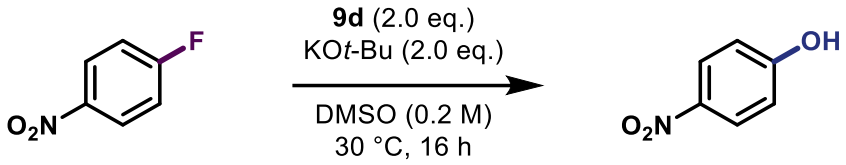

Synthesized using **General Procedure A** with potassium *tert*-butoxide (67.3 mg, 0.60 mmol, 2.0 eq.), oxime **9d** (74.5 mg, 0.60 mmol, 2.0 eq.), and 1-fluoro-4-nitrobenzene **3m$_F$** (42.3 mg, 0.30 mmol, 1.0 eq.) in DMSO (1.5 mL). The reaction was heated at 30 °C and stirred for 16 h. The crude product was dissolved in a minimum amount of CH_2Cl_2, dried onto silica gel, and purified by column chromatography (20% EtOAc in hexane) to afford the *title compound* **8m** (40.0 mg, 0.288 mmol, 96%) as a yellow solid.

***R*$_f$** 0.35 (25% EtOAc in hexane);

ATR-FTIR (thin film) ν_{max}/cm^{-1} 3130, 1591, 1513, 1498, 1334, 1256, 1110, 850;

^{1}H NMR (400 MHz, $CDCl_3$) δ_H 8.18 (d, *J* = 9.1 Hz 2H), 6.91 (d, *J* = 9.1 Hz, 2H), 5.58 (br s, 1H);

^{13}C NMR (75 MHz, $CDCl_3$) δ_C 161.9 (C), 141.6 (C), 126.4 (CH), 115.9 (CH);

HRMS (ESI$^-$) *m/z* calcd. for $C_6H_4NO_3$ $(M-H)^-$ 138.0197, found 138.0193.

Spectroscopic data matched those reported in the literature.[1]

2-Nitrophenol (8n)

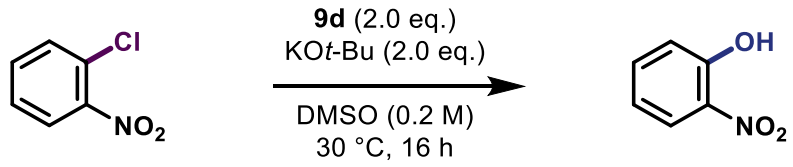

Synthesized using **General Procedure A** with potassium *tert*-butoxide (67.3 mg, 0.60 mmol, 2.0 eq.), oxime **9d** (74.5 mg, 0.60 mmol, 2.0 eq.), and 1-chloro-4-nitrobenzene **3n$_{Cl}$** (47.3 mg, 0.30 mmol, 1.0 eq.) in DMSO (1.5 mL). The reaction was heated at 30 °C and stirred for 16 h. The crude product was dissolved in a minimum amount of CH_2Cl_2, dried onto silica gel, and purified by column chromatography (20% EtOAc in hexane) to afford the *title compound* **8n** (30.5 mg, 0.219 mmol, 73%) as a yellow solid.

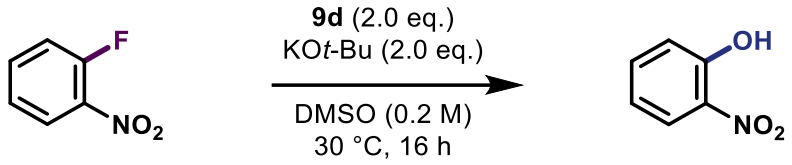

Synthesized using **General Procedure A** with potassium *tert*-butoxide (67.3 mg, 0.60 mmol, 2.0 eq.), oxime **9d** (74.5 mg, 0.60 mmol, 2.0 eq.), and 1-fluoro-2-nitrobenzene **3n$_F$** (42.3 mg, 0.30 mmol, 1.0 eq.) in DMSO (1.5 mL). The reaction was heated at 30 °C and stirred for 16 h. The crude product was dissolved in a minimum amount of CH_2Cl_2, dried onto silica gel, and purified by column chromatography (20% EtOAc in hexane) to afford the *title compound* **8n** (25.0 mg, 0.180 mmol, 60%) as a yellow solid.

R$_f$ 0.49 (20% EtOAc in hexane);

ATR-FTIR (thin film) ν_{max}/cm^{-1} 3252, 2924, 1732, 1620, 1591, 1535, 1456, 1478, 1333, 1257, 1187, 1029, 870, 747, 666;

^{1}H NMR (400 MHz, $CDCl_3$) δ_H 10.60 (s, 1H), 8.12 (dd, *J* = 8.5, 1.6 Hz, 1H), 7.59 (ddd, *J* = 8.5, 7.1, 1.6 Hz, 1H), 7.16 (dd, *J* = 8.5, 1.3 Hz, 1H), 7.00 (ddd, *J* = 8.5, 7.1, 1.3 Hz, 1H);

^{13}C NMR (101 MHz, $CDCl_3$) δ_C 155.3 (C), 137.7 (CH), 133.8 (C), 125.2 (CH), 120.4 (CH), 120.1 (CH);

HRMS (ESI^-) *m/z* calcd. for $C_6H_4NO_3$ $(M-H)^-$ 138.0197, found 138.0196.

Spectroscopic data matched those reported in the literature.[9]

1-Naphthol (8o)

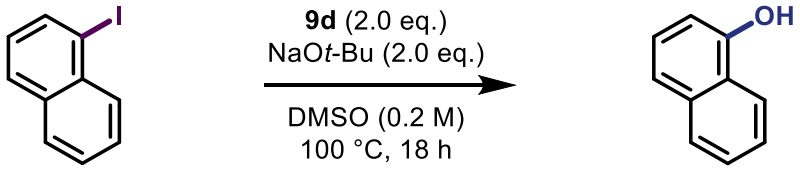

Synthesized using **General Procedure A** with sodium *tert*-butoxide (57.7 mg, 0.60 mmol, 2.0 eq.), oxime **9d** (74.5 mg, 0.60 mmol, 2.0 eq.), 1-iodonapthalene **3o$_I$** (76.2 mg, 0.30 mmol, 1.0 eq.) in DMSO (1.5 mL). The reaction was heated at 100 °C and stirred for 18 h. The crude product was dissolved in a minimum amount of CH_2Cl_2, dried onto silica gel and purified by column chromatography (10% EtOAc in hexane) to afford the *title compound* **8o** (23.2 mg, 0.161 mmol, 54%) as a beige solid.

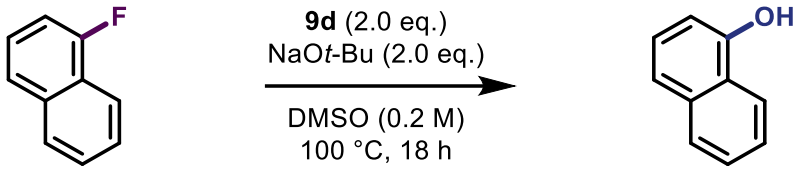

Synthesized using **General Procedure A** with sodium *tert*-butoxide (57.7 mg, 0.60 mmol, 2.0 eq.), oxime **9d** (74.5 mg, 0.60 mmol, 2.0 eq.), 1-fluoronapthalene **3o$_F$** (43.8 mg, 0.30 mmol, 1.0 eq.) in DMSO (1.5 mL). The reaction was heated at 100 °C and stirred for 18 h. The crude product was dissolved in a minimum amount of CH_2Cl_2, dried onto silica gel and purified by column chromatography (10% EtOAc in hexane) to afford the *title compound* **8o** (36.3 mg, 0.252 mmol, 84%) as a pale lilac solid.

***R*$_f$** 0.35 (20% EtOAc in hexane);

ATR-FTIR (thin film) ν_{max}/cm^{-1} 3245, 1579, 1516, 1459, 1386, 1278, 1084, 1044, 1020, 879, 795, 772, 573, 480;

^{1}H NMR (400 MHz, DMSO-d$_6$) δ_H 10.11 (br s, 1H), 8.11 (dd, *J* = 7.8, 1.7 Hz, 1H), 7.80 (dd, *J* = 7.7, 1.6 Hz, 1H), 7.49 – 7.39 (m, 2H), 7.36 – 7.25 (m, 2H), 6.86 (dd, *J* = 7.1, 1.4 Hz, 1H);

^{13}C NMR (101 MHz, DMSO-d$_6$) δ_C 153.2 (C), 134.4 (C), 127.4 (CH), 126.5 (CH), 126.1 (CH), 124.6 (CH), 122.0 (CH), 118.3 (CH), 108.0 (CH);

HRMS (ESI$^-$) *m/z* calcd. for $C_{10}H_7O$ $(M - H)^-$ 143.0502, found 143.0500.

Spectroscopic data matched those reported in the literature.[10]

4-Phenylphenol (8p)

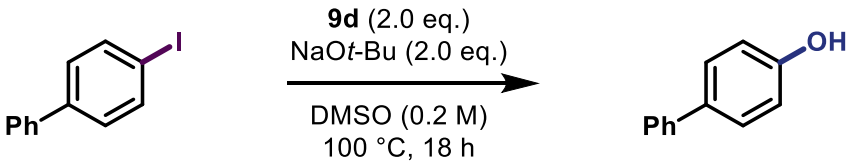

Synthesized using **General Procedure A** with sodium *tert*-butoxide (57.7 mg, 0.60 mmol, 2.0 eq.), oxime **9d** (74.5 mg, 0.60 mmol, 2.0 eq.), 4-iodobiphenyl **3p$_I$** (84.0 mg, 0.30 mmol, 1.0 eq.) in DMSO (1.5 mL). The reaction was heated at 100 °C and stirred for 18 h. The crude product was dissolved in a minimum amount of CH_2Cl_2, dried onto silica gel and purified by column chromatography (90% CH_2Cl_2 in hexane) to afford the *title compound* **8p** (17.3 mg, 0.101 mmol, 34%) as an off-white solid.

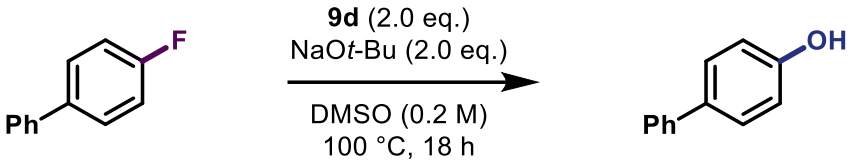

Synthesized using **General Procedure A** with sodium *tert*-butoxide (57.7 mg, 0.60 mmol, 2.0 eq.), oxime **9d** (74.5 mg, 0.60 mmol, 2.0 eq.), 4-fluorobiphenyl **3p$_F$** (51.7 mg, 0.30 mmol, 1.0 eq.) in DMSO (1.5 mL). The reaction was heated at 100 °C and stirred for 18 h. The crude product was dissolved in a minimum amount of CH_2Cl_2, dried onto silica gel and purified by column chromatography (90% CH_2Cl_2 in hexane) to afford the *title compound* **8p** (38.6 mg, 0.227 mmol, 76%) as an off-white solid.

***R**$_f$* 0.30 (80% DCM in hexane);

ATR-FTIR (thin film) ν_{max}/cm^{-1} 392, 1524, 1490, 1264, 833, 757, 688;

^{1}H NMR (300 MHz, $CDCl_3$) δ_H 7.55 (d, *J* = 7.5 Hz, 2H), 7.49 (d, *J* = 8.5 Hz, 2H), 7.42 (dd, *J* = 7.5, 7.3 Hz, 2H), 7.31 (dd, *J* = 7.3, 7.3 Hz, 1H), 6.91 (d, *J* = 8.5 Hz, 2H), 4.81 (br s, 1H);

^{13}C NMR (75 MHz, $CDCl_3$) δ_C 155.2 (C), 140.9 (C), 134.2 (C), 128.9 (CH), 128.5 (CH), 126.9 (CH), 115.8 (CH);

HRMS (ESI$^-$) *m/z* calcd. for $C_{12}H_9O$ $(M - H)^-$ 169.0659, found 169.0657.

Spectroscopic data matched those reported in the literature.[11]

2-Hydroxy-4-bromobiphenyl (8q)

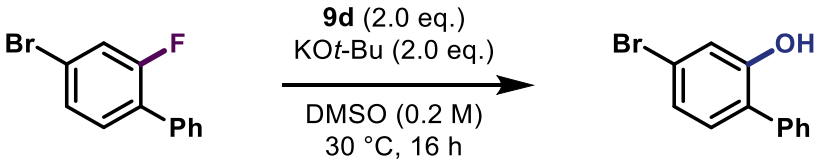

Synthesized using **General Procedure A** with potassium *tert*-butoxide (67.3 mg, 0.60 mmol, 2.0 eq.), oxime **9d** (74.5 mg, 0.60 mmol, 2.0 eq.), and 2-fluoro-4-bromobiphenyl **3q$_F$** (75.3 mg, 0.30 mmol, 1.0 eq.) in DMSO (1.5 mL). The reaction was heated at 30 °C and stirred for 16 h. The crude product was dissolved in a minimum amount of CH_2Cl_2, dried onto silica gel, and purified by column chromatography (20% EtOAc in hexane) to afford the *title compound* **8q** (58.0 mg, 0.233 mmol, 78%) as a yellow oil.

***R**$_f$* 0.50 (20% EtOAc in hexane);

ATR-FTIR (thin film) ν_{max}/cm^{-1} 3520, 1476, 878, 765, 701;

^{1}H NMR (400 MHz, $CDCl_3$) δ_H 7.55 – 7.46 (m, 2H), 7.46 – 7.37 (m, 3H), 7.17 (d, *J* = 1.8 Hz, 1H), 7.16 – 7.05 (m, 2H), 5.27 (br s, 1H);

^{13}C NMR (101 MHz, $CDCl_3$) δ_C 153.3 (C), 136.1 (C), 131.4 (CH), 129.6 (CH), 129.0 (CH), 128.4 (CH), 127.3 (C), 124.1 (CH), 122.2 (C), 119.2 (CH);

HRMS (ESI^-) *m/z* calcd. for $C_{12}H_8O^{79}Br$ $(M - H)^-$ 246.9764, found 246.9761.

4-Bromo-2-hydroxyacetophenone (8r)

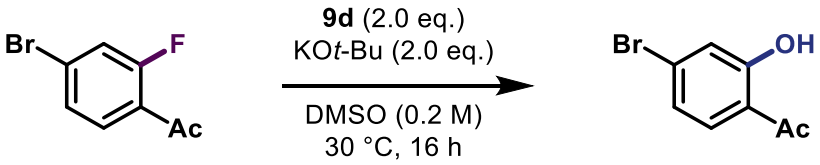

Synthesized using **General Procedure A** with potassium *tert*-butoxide (67.3 mg, 0.60 mmol, 2.0 eq.), oxime **9d** (74.5 mg, 0.60 mmol, 2.0 eq.), and 4-bromo-2-fluoroacetophenone **3r$_F$** (65.1 mg, 0.30 mmol, 1.0 eq.) in DMSO (1.5 mL). The reaction was heated at 30 °C and stirred for 16 h. The crude product was dissolved in a minimum amount of CH_2Cl_2, dried onto silica gel, and purified by column chromatography (10% EtOAc in hexane) to afford the *title compound* **8r** (36.0 mg, 0.168 mmol, 56%) as an off-white solid.

R$_f$ 0.45 (10% EtOAc in hexane);

ATR-FTIR (thin film) ν_{max}/cm^{-1} 2935, 1638, 1606, 1482, 1343, 1318, 1236, 1209, 961, 882, 787, 646;

^{1}H NMR (300 MHz, $CDCl_3$) δ_H 12.33 (s, 1H), 7.57 (d, *J* = 8.5 Hz, 1H), 7.16 (d, *J* = 1.9 Hz, 1H), 7.03 (dd, *J* = 8.5, 1.9 Hz, 1H), 2.60 (s, 3H);

^{13}C NMR (75 MHz, Chloroform-*d*) δ_C 204.0 (C), 163.0 (C), 131.7 (CH), 130.9 (C), 122.6 (CH), 121.8 (CH), 118.7 (C), 26.8 (CH_3);

HRMS (ESI^+) *m/z* calcd. for $C_8H_8^{79}BrO$ $(M + H)^+$ 214.9695, found 214.9702.

5-Hydroxy-2(trifluoromethyl) pyridine (8s)

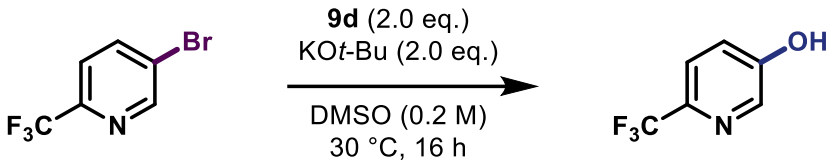

Synthesized using **General Procedure A** with potassium *tert*-butoxide (67.3 mg, 0.60 mmol, 2.0 eq.), oxime **9d** (74.5 mg, 0.60 mmol, 2.0 eq.), and 5-bromo-2(trifluoromethyl) pyridine **3s$_{Br}$** (67.8 mg, 0.30 mmol, 1.0 eq.) in DMSO (1.5 mL). The reaction was heated at 30 °C and stirred for 16 h. The crude product was dissolved in a minimum amount of CH_2Cl_2, dried onto silica gel, and purified by column chromatography (30% EtOAc in hexane) to afford the *title compound* **8s** (37.0 mg, 0.227 mmol, 76%) as a white solid.

R$_f$ 0.44 (30% EtOAc in hexane);

ATR-FTIR (thin film) ν_{max}/cm^{-1} 3359, 1588, 1288, 1138, 1090, 982, 838, 769, 539, 519;

1H NMR (400 MHz, DMSO-D_6) δ_H 10.87 (s, 1H), 8.26 (d, *J* = 2.7 Hz, 1H), 7.69 (d, *J* = 8.6 Hz, 1H), 7.34 (dd, *J* = 8.6, 2.7 Hz, 1H);

^{13}C NMR (101 MHz, DMSO-D_6) δ_C 156.5 (C), 138.6 (CH), 137.2 (q, *J* = 34.1 Hz, C), 122.8 (CH), 122.2 (q, *J* = 272.5 Hz, C), 122.0 (q, *J* = 2.8 Hz, CH);

^{18}F NMR (282 MHz, $CDCl_3$) δ_F -65.0 (s, 3F);

HRMS (ESI$^+$) *m/z* calcd. for $C_6H_5F_3NO$ $(M + H)^+$ 164.0318, found 164.0314.

Spectroscopic data matched those reported in the literature.[1]

5-Hydroxyquinoline (8t)

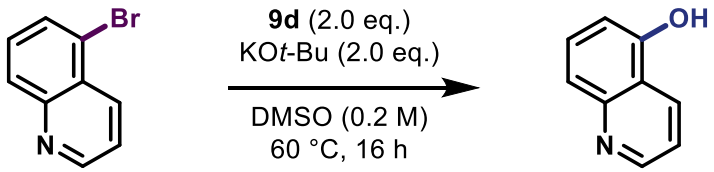

Synthesized using **General Procedure A** with potassium *tert*-butoxide (67.3 mg, 0.60 mmol, 2.0 eq.), oxime **9d** (74.5 mg, 0.60 mmol, 2.0 eq.), and 5-bromoquinoline **3t$_{Br}$** (62.4 mg, 0.30 mmol, 1.0 eq.) in DMSO (1.5 mL). The reaction was heated at 60 °C and stirred for 16 h. The crude product was dissolved in a minimum amount of CH_2Cl_2, dried onto silica gel, and

purified by column chromatography (60% EtOAc in hexane) to afford the *title compound* **8t** (19.0 mg, 0.131 mmol, 44%) as a white solid.

***R*$_f$** 0.50 (60% EtOAc in hexane);

ATR-FTIR (thin film) ν_{max}/cm^{-1} 2922, 2851, 1982, 1587, 1279, 796;

^{1}H NMR (400 MHz, DMSO-D$_6$) δ 10.49 (s, 1H), 8.84 (dd, *J* = 4.2, 1.8 Hz, 1H), 8.49 (ddd, *J* = 8.5, 1.8, 0.9 Hz, 1H), 7.54 (dd, *J* = 8.5, 7.5 Hz, 1H), 7.48 – 7.42 (m, 2H), 6.93 (dd, *J* = 7.5, 1.1 Hz, 1H);

^{13}C NMR (101 MHz, DMSO-D$_6$) δ_c 153.3 (C), 150.5 (CH), 148.9 (C), 130.6 (CH), 129.9 (CH), 120.1 (CH), 119.6 (C), 119.4, 108.4 (CH);

HRMS (ESI$^-$) *m/z* calcd. for C_9H_6NO $(M - H)^-$ 144.0455, found 144.0453.

Spectroscopic data matched those reported in the literature.[6]

6-Hydroxyquinoline (8u)

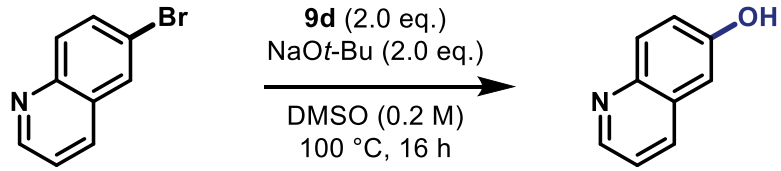

Synthesized using **General Procedure A** with sodium *tert*-butoxide (96.11 mg, 0.60 mmol, 2.0 eq.), oxime **9d** (74.5 mg, 0.60 mmol, 2.0 eq.), and 6-bromoquinoline **3u$_{Br}$** (62.4 mg, 0.30 mmol, 1.0 eq.) in DMSO (1.5 mL). The reaction was heated at 100 °C and stirred for 16 h. The crude product was dissolved in a minimum amount of CH_2Cl_2, dried onto silica gel, and purified by column chromatography (80% EtOAc in hexane) to afford the *title compound* **8u** (32.0 mg, 0.220 mmol, 73%) as a white solid.

***R*$_f$** 0.35 (80% EtOAc in hexane);

ATR-FTIR (thin film) ν_{max}/cm^{-1} 3021, 1971, 1621, 1506, 1469, 1376, 1315, 1229, 1121, 920, 831;

^{1}H NMR (400 MHz, DMSO-D$_6$) δ_H 10.05 (s, 1H), 8.65 (dd, *J* = 4.2, 1.7 Hz, 1H), 8.13 (ddd, *J* = 8.4, 1.8, 0.7 Hz, 1H), 7.87 (d, *J* = 9.0 Hz, 1H), 7.38 (dd, *J* = 8.3, 4.2 Hz, 1H), 7.32 (dd, *J* = 9.0, 2.7 Hz, 1H), 7.15 (d, *J* = 2.7 Hz, 1H);

^{13}C NMR (101 MHz, DMSO-D_6) δ_C 155.5 (C), 147.2 (CH), 143.1 (C), 134.2 (CH), 130.5 (CH), 129.4 (C), 122.0 (CH), 121.4 (CH), 108.4 (CH);

HRMS (ESI^-) *m/z* calcd. for C_9H_6NO $(M - H)^-$ 144.0455, found 144.0451.

Spectroscopic data matched those reported in the literature.[5]

6-Bromo-5-methylpyridin-3-ol (8v)

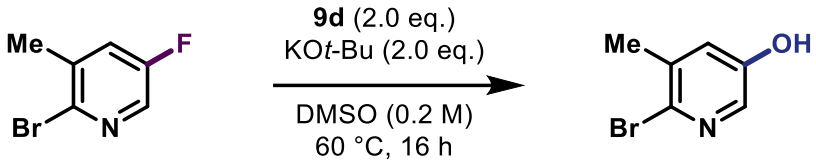

Synthesized using **General Procedure A** with potassium *tert*-butoxide (67.3 mg, 0.60 mmol, 2.0 eq.), oxime **9d** (74.5 mg, 0.60 mmol, 2.0 eq.), and 2-bromo-5-fluoro-3-methyl pyridine **3v$_F$** (57.0 mg, 0.30 mmol, 1.0 eq.) in DMSO (1.5 mL). The reaction was heated at 60 °C and stirred for 16 h. The crude product was dissolved in a minimum amount of CH_2Cl_2, dried onto silica gel, and purified by column chromatography (60% EtOAc in hexane) to afford the *title compound* **8v** (42.0 mg, 0.223 mmol, 74%) as a white solid.

R$_f$ 0.77 (60% EtOAc in hexane);

ATR-FTIR (thin film) ν_{max}/cm^{-1} 2924, 1570, 1458, 1403, 1308, 1228, 1158, 1060, 610;

^{1}H NMR (400 MHz, DMSO-D_6) δ_H 10.13 (br s, 1H), 7.76 (d, *J* = 3.0 Hz, 1H), 7.16 (d, *J* = 3.0 Hz, 1H), 2.23 (s, 3H);

^{13}C NMR (101 MHz, DMSO-D_6) δ_C 153.8 (C), 135.4 (CH), 135.0 (C), 132.2 (C), 126.2 (CH), 21.3 (CH_3);

HRMS (ESI^-) *m/z* calcd. for $C_6H_7{}^{79}BrNO$ $(M + H)^+$ 187.9706, found 187.9712.

Hydroxy-Fenofibrate derivative (8w)

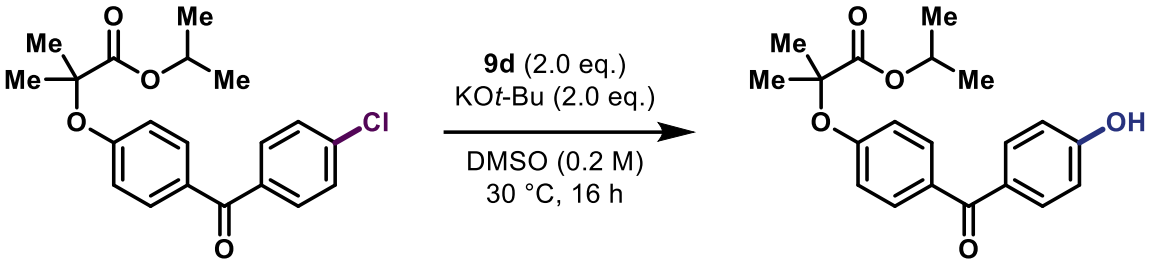

Synthesized using **General Procedure A** with potassium *tert*-butoxide (67.3 mg, 0.60 mmol, 2.0 eq.), oxime **9d** (74.5 mg, 0.60 mmol, 2.0 eq.), and Fenofibrate $\mathbf{3w_{Cl}}$ (108.2 mg, 0.30 mmol, 1.0 eq.) in DMSO (1.5 mL). The reaction was heated at 30 °C and stirred for 16 h. The crude product was dissolved in a minimum amount of CH_2Cl_2, dried onto silica gel, and purified by column chromatography (20% EtOAc in hexane) to afford the *title compound* **8w** (78.0 mg, 0.228 mmol, 76%) as an off-white solid.

$\boldsymbol{R_f}$ 0.09 (20% EtOAc in hexane);

ATR-FTIR (thin film) ν_{max}/cm^{-1} 3283, 2985, 1730, 1600, 1285, 1151, 930, 854, 771, 609;

^{1}H NMR (400 MHz, $CDCl_3$) δ_H 7.75 – 7.67 (m, 4H), 6.91 (d, J = 8.6 Hz, 2H), 6.86 (d, J = 8.9 Hz, 2H), 5.09 (p, J = 6.2 Hz, 1H), 1.66 (s, 6H), 1.21 (d, J = 6.3 Hz, 6H);

^{13}C NMR (101 MHz, $CDCl_3$) δ_C 195.4 (C), 173.6 (C), 160.4 (C), 159.4 (C), 132.8 (CH), 132.0 (CH), 131.2 (C), 130.2 (C), 117.4 (CH), 115.3 (CH), 79.5 (C), 69.6 (CH), 25.5 (CH_3), 21.6 (CH_3);

HRMS (ESI^-) *m/z* calcd. for $C_{20}H_{22}NaO_5$ $(M + Na)^+$ 365.1359, found 365.1361.

Spectroscopic data matched those reported in the literature.[12]

Hydroxy-Iloperidone derivative (8x)

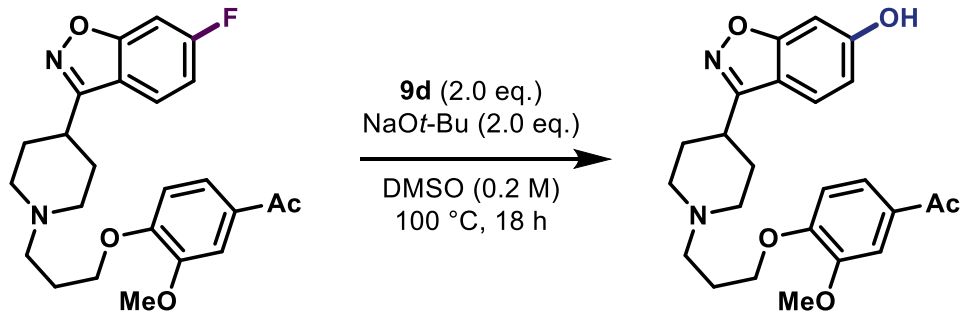

Synthesized using **General Procedure A** with sodium *tert*-butoxide (46.1 mg, 0.48 mmol, 2.0 eq.), oxime **9d** (59.6 mg, 0.48 mmol, 2.0 eq.), Iloperidone **3x$_F$** (104.3 mg, 0.24 mmol, 1.0 eq.) in DMSO (1.2 mL). The reaction was heated at 100 °C and stirred for 18 h. The crude product was dissolved in a minimum amount of CH_2Cl_2, dried onto silica gel and purified by column chromatography (3% MeOH in DCM) to afford the *title compound* **8x** (84.9 mg, 0.200 mmol, 83%) as a pale-yellow solid.

R$_f$ 0.30 (10% MeOH in DCM);

ATR-FTIR (thin film) ν_{max}/cm^{-1} 2943, 1671, 1595, 1510, 1418, 1270, 1221, 1148, 1031, 827, 735;

^{1}H NMR (400 MHz, DMSO-d$_6$) δ_H 10.36 (br s, 1H), 7.68 (d, *J* = 8.7 Hz, 1H), 7.61 (dd, *J* = 8.5, 2.0 Hz, 1H), 7.44 (d, *J* = 2.0 Hz, 1H), 7.07 (d, *J* = 8.5 Hz, 1H), 6.92 (d, *J* = 2.0 Hz, 1H), 6.83 (dd, *J* = 8.7, 2.0 Hz, 1H), 4.11 (t, *J* = 6.4 Hz, 2H), 3.82 (s, 3H), 3.10 – 2.96 (m, 3H), 2.58 – 2.50 (m, 5H), 2.18 (t, *J* = 11.5 Hz, 2H), 2.03 – 1.79 (m, 6H);

^{13}C NMR (101 MHz, DMSO-d$_6$) δ_C 196.4 (C), 164.3 (C), 160.8 (C), 160.2 (C), 152.4 (C), 148.7 (C), 129.8 (C), 123.2 (CH), 122.6 (CH), 113.8 (CH), 112.7 (CH), 111.7 (C), 110.4 (CH), 94.7 (CH), 66.8 (CH_2), 55.6 (CH_3), 54.5 (CH_2), 53.0 (CH_2), 33.4 (CH), 30.0 (CH_2), 26.4 (CH_3), 26.0 (CH_2);

HRMS (ESI$^+$) *m/z* calcd. for $C_{24}H_{29}N_2O_5$ $(M + H)^+$ 425.2071, found 425.2073.

Hydroxy-Etoricoxib derivative (8y)

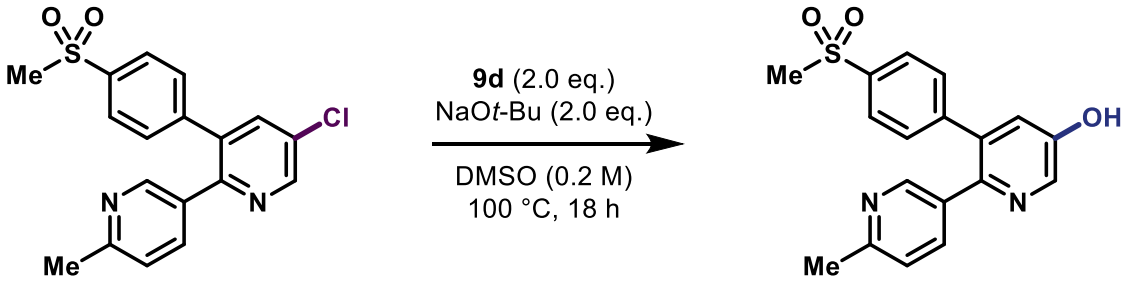

Synthesized using **General Procedure A** with sodium *tert*-butoxide (9.6 mg, 0.14 mmol, 2.0 eq.), oxime **9d** (17.4 mg, 0.14 mmol, 2.0 eq.), and Etoricoxib $\mathbf{3y_{Cl}}$ (25.0 mg, 0.07 mmol, 1.0 eq.) in DMSO (0.4 mL). The reaction was heated at 100 °C and stirred for 18 h. The crude product was dissolved in a minimum amount of CH_2Cl_2, dried onto silica gel, and purified by column chromatography (5% MeOH in DCM) to afford the *title compound* **8y** (13 mg, 0.04 mmol, 55%) as a white solid.

R_f 0.35 (5% MeOH in DCM);

ATR-FTIR (thin film) ν_{max}/cm^{-1} 2925, 2854, 1598, 1441, 1310, 1225, 1151, 779, 732, 544;

^{1}H NMR (500 MHz, DMSO-d_6) δ_H 10.37 (s, 1H), 8.32 (d, *J* = 2.7 Hz, 1H), 8.23 (dd, *J* = 2.4, 0.8 Hz, 1H), 7.88 (d, *J* = 8.6 Hz, 2H), 7.50 – 7.44 (m, 3H), 7.21 (d, *J* = 2.7 Hz, 1H), 7.13 (d, *J* = 8.0 Hz, 1H) 3.24 (s, 3H), 2.41 (s, 3H);

^{13}C NMR (126 MHz, DMSO-d_6) δ_C 156.4 (C), 153.0 (C), 149.3 (CH), 144.5 (C), 144.4 (C), 139.8 (C), 137.8 (CH), 137.0 (CH), 134.9 (C), 132.3 (C), 130.3 (CH), 127.1 (CH), 124.2 (CH), 122.2 (CH), 43.3 (CH_3), 23.7 (CH_3);

HRMS (ESI^-) *m/z* calcd. for $C_{18}H_{17}N_2O_3S$ $(M + H)^+$ 341.0954, found 341.0955.

Hydroxy-Blonanserin derivative (8z)

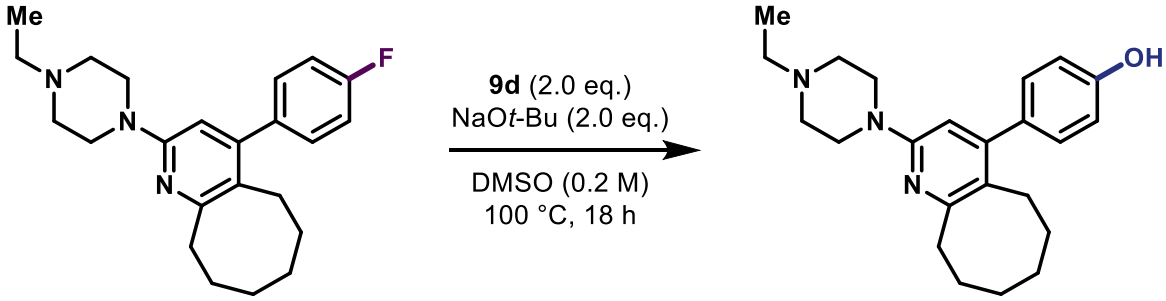

Synthesized using **General Procedure A** with sodium *tert*-butoxide (11.5 mg, 0.12 mmol, 2.0 eq.), oxime **9d** (14.9 mg, 0.12 mmol, 2.0 eq.), Blonanserin **3z$_F$** (20.6 mg, 0.06 mmol, 1.0 eq.) in DMSO (0.3 mL). The reaction was heated at 100 °C and stirred for 18 h. The crude product was dissolved in a minimum amount of CH_2Cl_2, dried onto silica gel and purified by column chromatography (5% MeOH in DCM) to afford the *title compound* **8z** (10.2 mg, 0.0279 mmol, 47%) as a pale-yellow solid.

R$_f$ 0.35 (15% MeOH in DCM);

ATR-FTIR (thin film) ν_{max}/cm^{-1} 2922, 2850, 1588, 1543, 1514, 1448, 1270, 1243, 1168, 998, 832;

^{1}H NMR (400 MHz, DMSO-d$_6$) δ_H 9.53 (br s, 1H), 7.05 (d, *J* = 8.5 Hz, 2H), 6.80 (d, *J* = 8.5 Hz, 2H), 6.34 (s, 1H), 3.62 – 3.34 (m, 5H), 2.85 – 2.72 (m, 2H), 2.63 – 2.50 (m, 4H), 1.72 – 1.61 (m, 2H), 1.42 – 1.19 (m, 9H), 1.05 (t, *J* = 7.1 Hz, 3H);

^{13}C NMR (126 MHz, DMSO-d$_6$) δ_C 158.6 (C), 156.7 (C), 156.6 (C), 151.1 (C), 131.4 (C), 129.4 (CH), 121.9 (C), 114.8 (CH), 105.9 (CH), 52.2 (CH_2), 51.7 (CH_2), 44.8 (CH_2), 34.9 (CH_2), 31.1 (CH_2), 30.3 (CH_2), 26.0 (CH_2), 25.8 (CH_2), 25.4 (CH_2), 11.9 (CH_3);

HRMS (ESI$^+$) *m/z* calcd. for $C_{23}H_{32}N_3O$ $(M + H)^+$ 366.2540, found 366.2544.

2.3. Large-Scale Hydroxylation

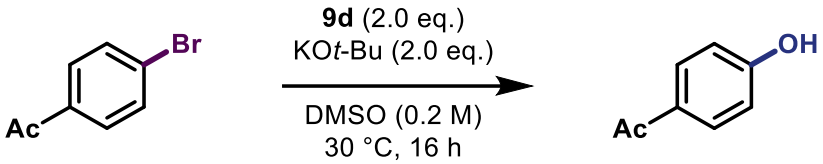

To an oven-dried 100 mL round bottom flask was charged potassium *tert*-butoxide (1.35 g, 12.0 mmol, 2.0 eq.), oxime **9d** (1.49 g, 12.0 mmol, 2.0 eq.), and 4′-bromoacetophenone **3a$_{Br}$** (1.19 g, 6.00 mmol, 1.0 eq.). The flask was sealed with a septum and anhydrous DMSO (30 mL) was added. The reaction mixture was sparged with N_2 for 30 minutes, then heated at 30 °C (oil bath) and stirred for 16 h under nitrogen. The mixture was then diluted with CH_2Cl_2 (60 mL) and poured into water (60 mL). The organic phase was collected and the aqueous phase was extracted with CH_2Cl_2 (2 × 60 mL). The organics were discarded and the aqueous phase was acidified with 10% aq. HCl until pH ~3. The aqueous phase was then extracted with CH_2Cl_2 (4 × 60 mL). The organics were combined, dried ($MgSO_4$), and concentrated under reduced pressure. The crude product was dissolved in a minimum amount of CH_2Cl_2 and purified by column chromatography (20% EtOAc in hexane, then 35% EtOAc in hexane) to afford the *title compound* **8a** (682 mg, 4.99 mmol, 83%) as a pale-yellow solid.

Spectroscopic data matched those reported in the literature.[1]

3. Table of Screened Oximes

The reactivity of the following oximes was examined in this study (Table S1), of which pyrrole oxime **9d** proved optimal for the desired transformation.

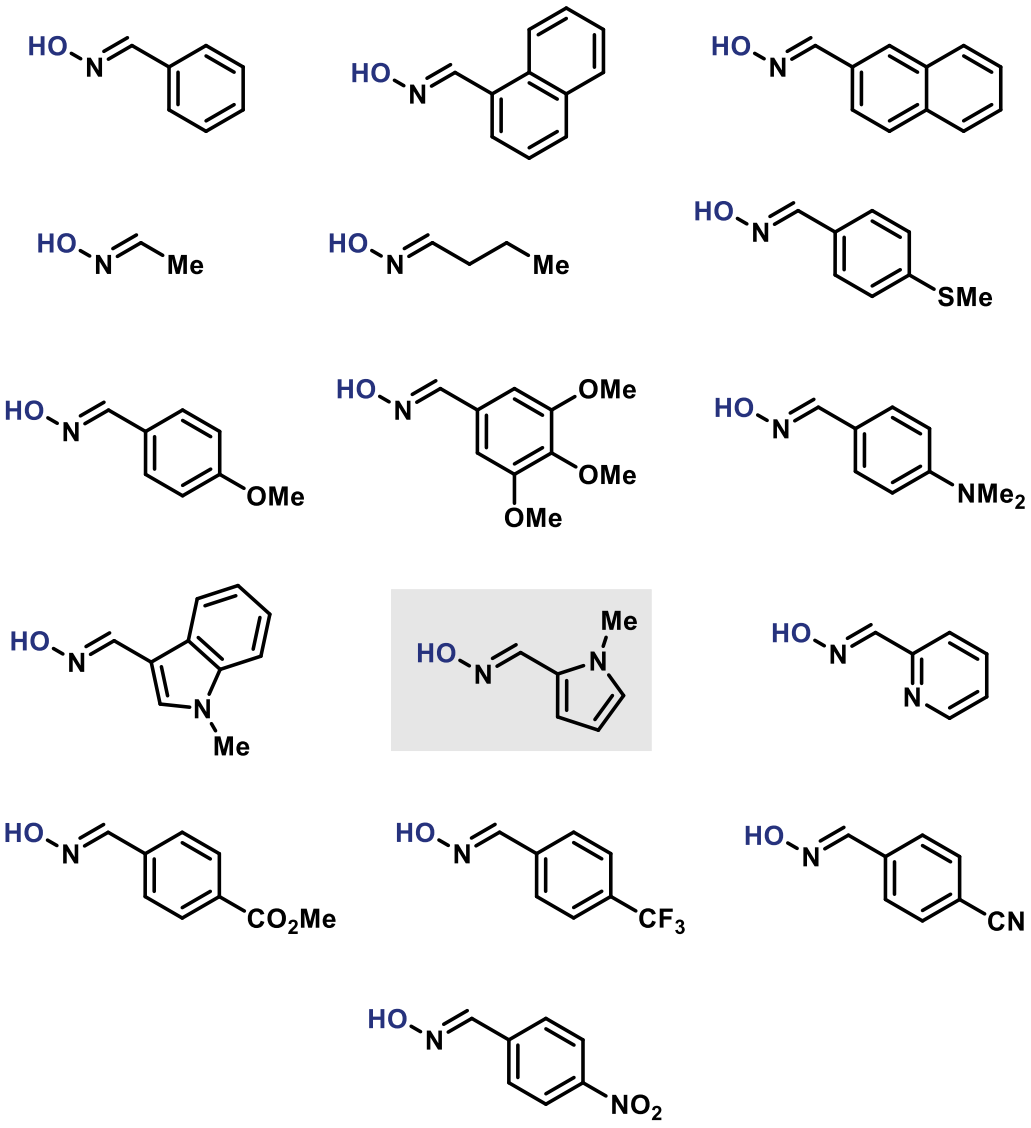

Table S1. Oximes examined in this study.

4. Evidence Against Trace-Metal Catalysis

To exclude possible trace-metal catalysis, all reactions described in this manuscript were conducted using a newly purchased batch of magnetic stirrer bars, which were never used in a metal-catalysed reaction.

In addition, reactivity was not limited by the batch of base used. Indeed, different batches of high purity KO*t*-Bu (as a solid or as a solution in THF) could be used to reproduce the model reaction (Table S2, entries 1 and 2). Excellent conversion was also observed when using KHMDS (1.0 M in THF) as the base, which demonstrates that KO*t*-Bu is not essential to the reaction (entry 3). Despite the potential superior reaction performance of KHMDS, this base was not used further in an effort to develop a milder reaction protocol.

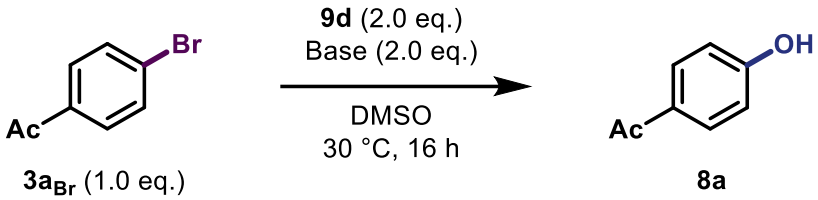

3a$_{Br}$ (1.0 eq.) **8a**

Entry[a]	Conditions	Conversion[b]
1	KO*t*-Bu, DMSO (0.5 mL)	85%
2	KO*t*-Bu (1.0 M in THF), DMSO (1.0 mL)	85%
3	KHMDS (1.0 M in THF), DMSO (0.5 mL)	>95%

Table S2. [a] Reactions performed with 0.1 mmol of aryl bromide **3a$_{Br}$** and 0.2 mmol oxime **9d** with the stated based (0.2 mmol) in DMSO under nitrogen. [b] Determined using the ^{1}H NMR spectrum of the unpurified reaction mixture, ratio of starting material to product.

5. Experimental Evidence for a Radical Mechanism

5.1. Hydrodehalogenation

During the optimisation of the coupling reaction between bromide **3a$_{Br}$** and oxime **9d**, we observed varying levels of acetophenone (**10**) formation by ^{1}H NMR spectroscopic analysis of the crude reaction mixture. Formation of this hydrodehalogenated by-product was especially prominent under photochemical conditions (due to a presumed higher concentration of radical intermediates) and in the presence of THF (which may serve as a H-atom donor for an aryl radical); an exemplar reaction and ^{1}H NMR spectrum (in $CDCl_3$) is shown in Scheme S1.

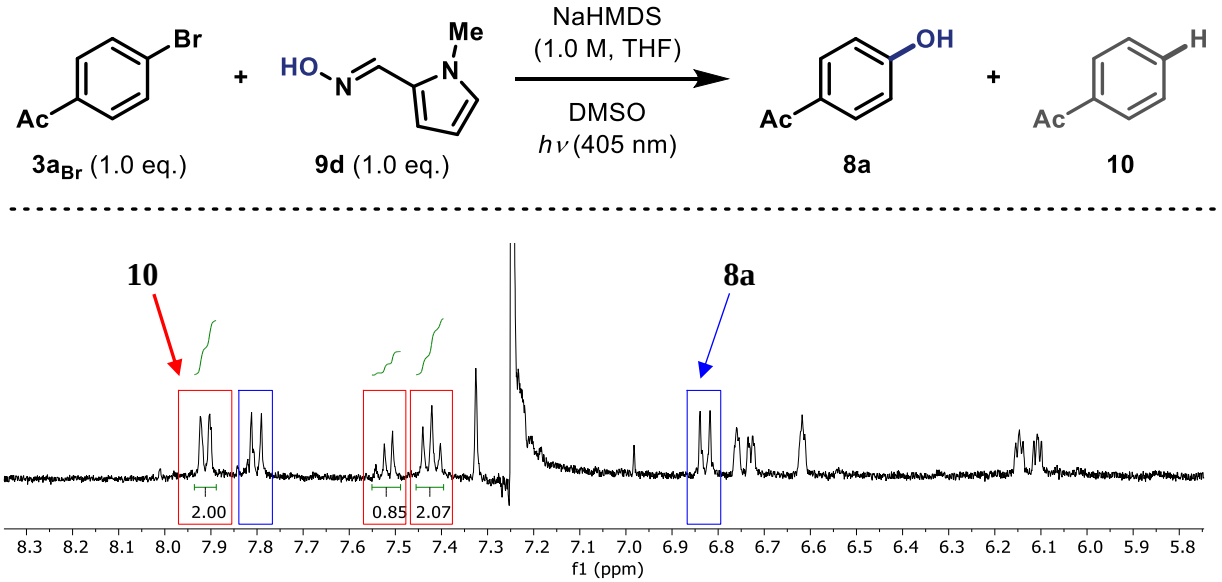

Scheme S1. Detection of acetophenone by ^{1}H NMR spectroscopic analysis of the crude reaction mixture (aliquot diluted in $CDCl_3$).

5.2. EPR Spectroscopy with Radical Scavengers

Radical scavengers (Galvinoxyl, DPPH and TEMPO) were shown was to inhibit the coupling of aryl bromide **3a$_{Br}$** and oxime **9d**, but no direct trapped (radical–radical coupling) products were detected by high-resolution mass spectrometry. Instead of radical–radical coupling, we propose that these scavengers terminate radical chains by acting as electron acceptors (radical-anion scavengers, see Scheme S2).

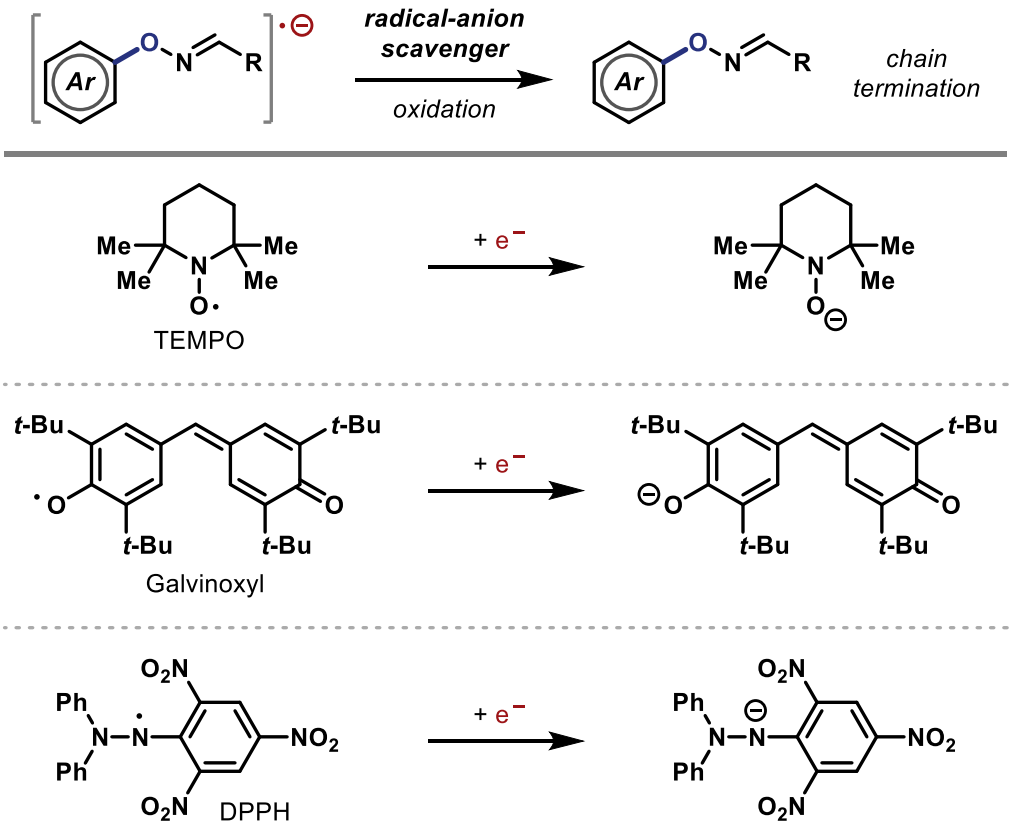

Scheme S2. Proposed chain termination by electron transfer.

To probe this theory, we monitored the consumption of the TEMPO free radical over time by EPR spectroscopy. First, we monitored the intensity of the EPR spectrum of TEMPO (1 mol%) in the presence of the oxime anion over time – no change in signal intensity was observed, indicating that there is no reaction between the oxime anion and TEMPO (Scheme S3).

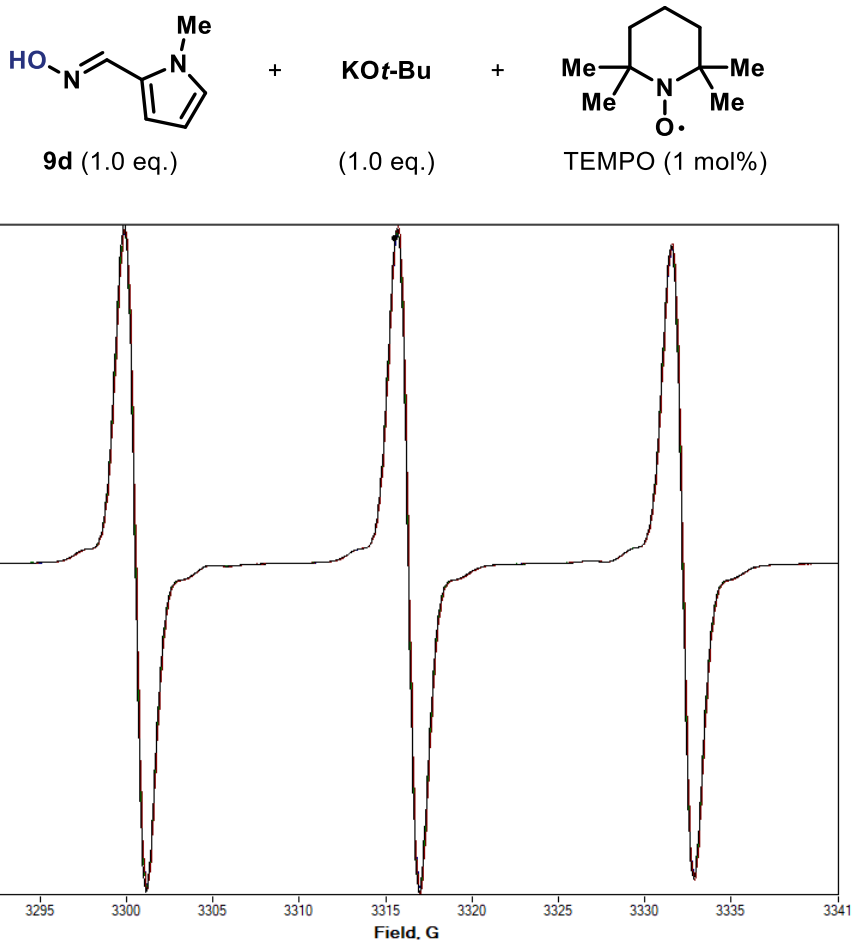

Scheme S3. Overlaid EPR spectra of TEMPO (1 mol%) in the presence of the oxime anion (in DMSO). Measurements taken after 5, 15, 53 and 914 mins (no change observed).

Next, we monitored the intensity of the EPR spectrum of TEMPO (1 mol%) in the presence of both the oxime anion and aryl bromide **3a**$_{\mathbf{Br}}$. A clear decrease in signal intensity was observed over 11 h, clearly demonstrating that the TEMPO radical is consumed under these reaction conditions and that a radical mechanism is operative (see Scheme S4 and Figure S1).

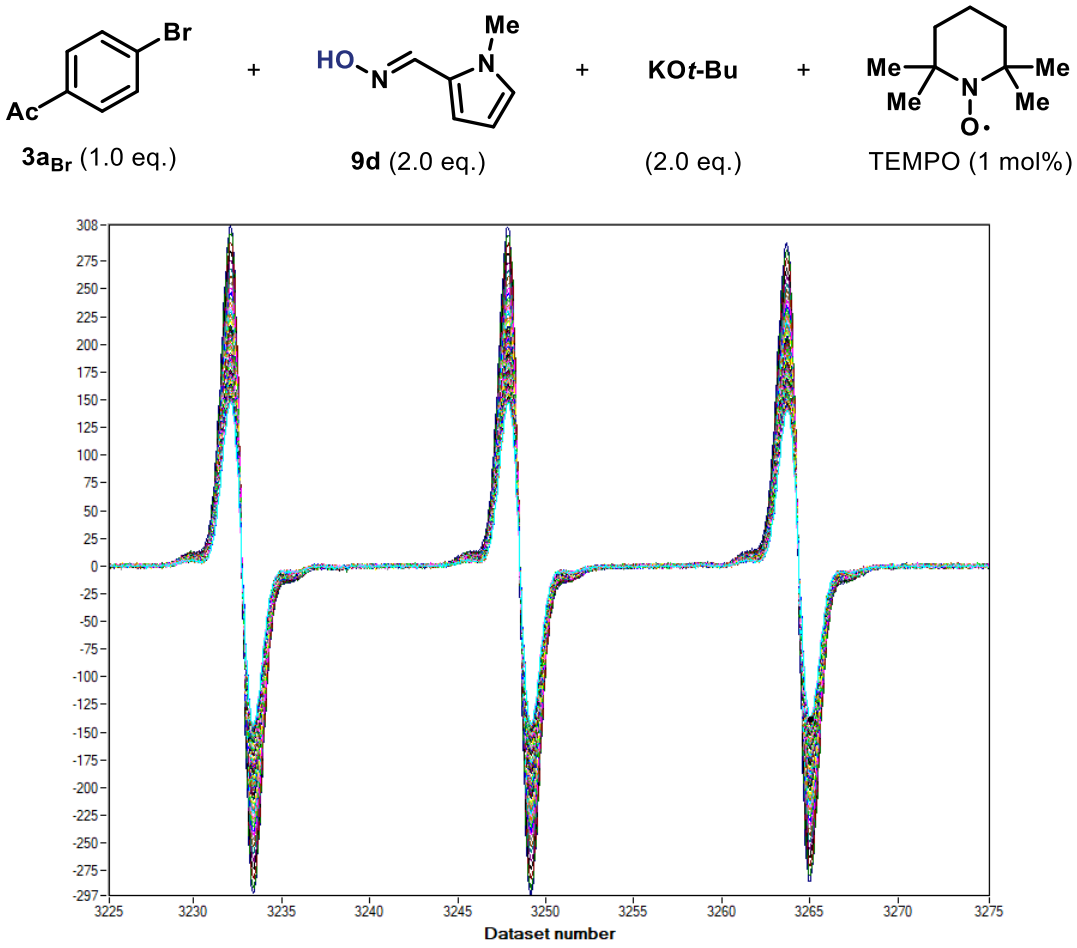

Scheme S4. Overlaid EPR spectra of TEMPO (1 mol%) in the presence of both the oxime anion and aryl bromide **3a$_{Br}$** (in DMSO). Measurements were taken every 5.63 min over 11 h.

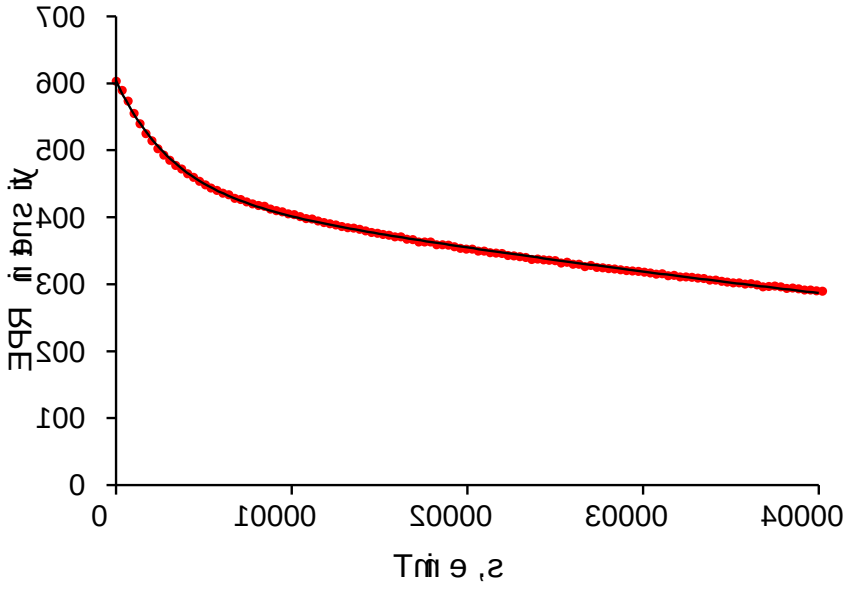

Figure S1. Change in EPR intensity of TEMPO over time fits well with a bi-exponential decay.

5.3. Dihalogenated Arene Substitution Patterns

In analogy to the experiments conducted by Bunnett and Creary on the substitution of dihalogenated substrates with thiophenoxide ion (see J. F. Bunnett, X. Creary, *J. Org. Chem.* **1974**, *39*, 3612–3614) we examined the reactivity of 4-chloroiodobenzene **SI1** and 3-chloroiodobenzene **SI4** with oxime **9d** and NaO*t*-Bu at 100 °C. Interestingly, we observed good levels of conversions in both cases, but both reactions afforded inseparable mixtures of monosubstituted products (**SI2**/**3** and **SI5**/**6**), with substitution of the iodide substituent slightly favoured (Scheme S5). This low level of selectivity is presumably due to the high temperatures employed and potentially competing polar (S_NAr, chloride favoured) and open-shell ($S_{RN}1$, iodide favoured) substitution pathways.

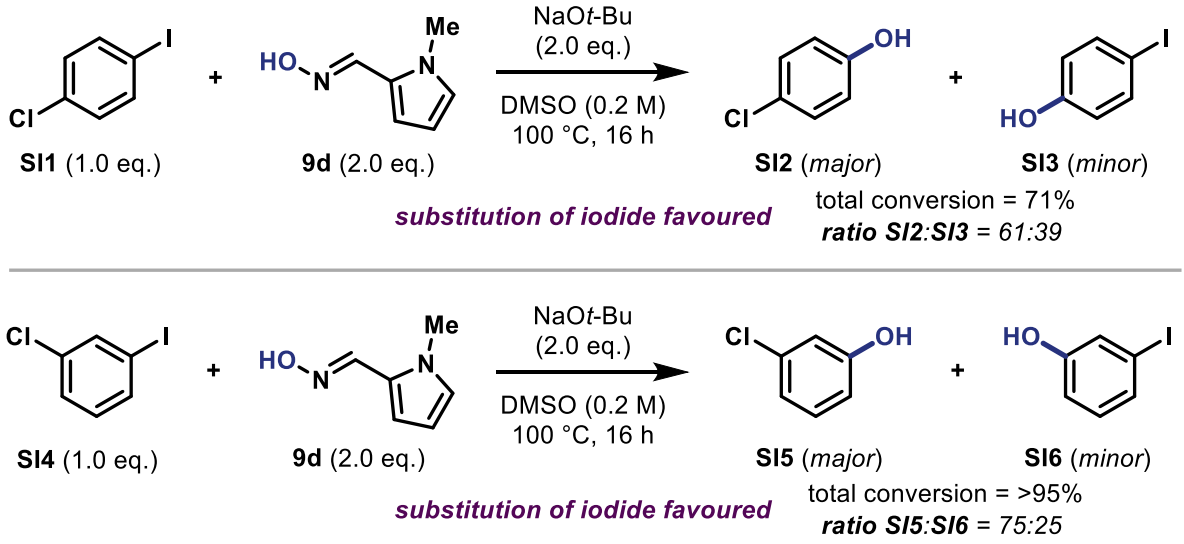

Scheme S5. Reactivity of dehalogenated substrates (total conversion and ratios determined by ^{1}H NMR spectroscopic analysis of the crude reaction mixture).

However, unlike the thiophenoxide ion used by Bunnett and Creary, which favours disubstitution, we propose that monosubstitution is likely observed in our system due to the stabilising effects of the oxime π-system. Here, the spin density of the coupled radical-anion intermediate will be based primarily in the lower in energy oxime π-system, not the arene (as with thiophenoxide). Therefore, there is limited opportunity for the π*–σ* orbital mixing needed to the promote fragmentation of the Ar–Cl bond (Scheme S6). Indeed, the spin density of the oxime coupled radical-anion (**A**) can be easily visualised using DFT, which shows that almost all of the spin density is based in the oxime π-system.

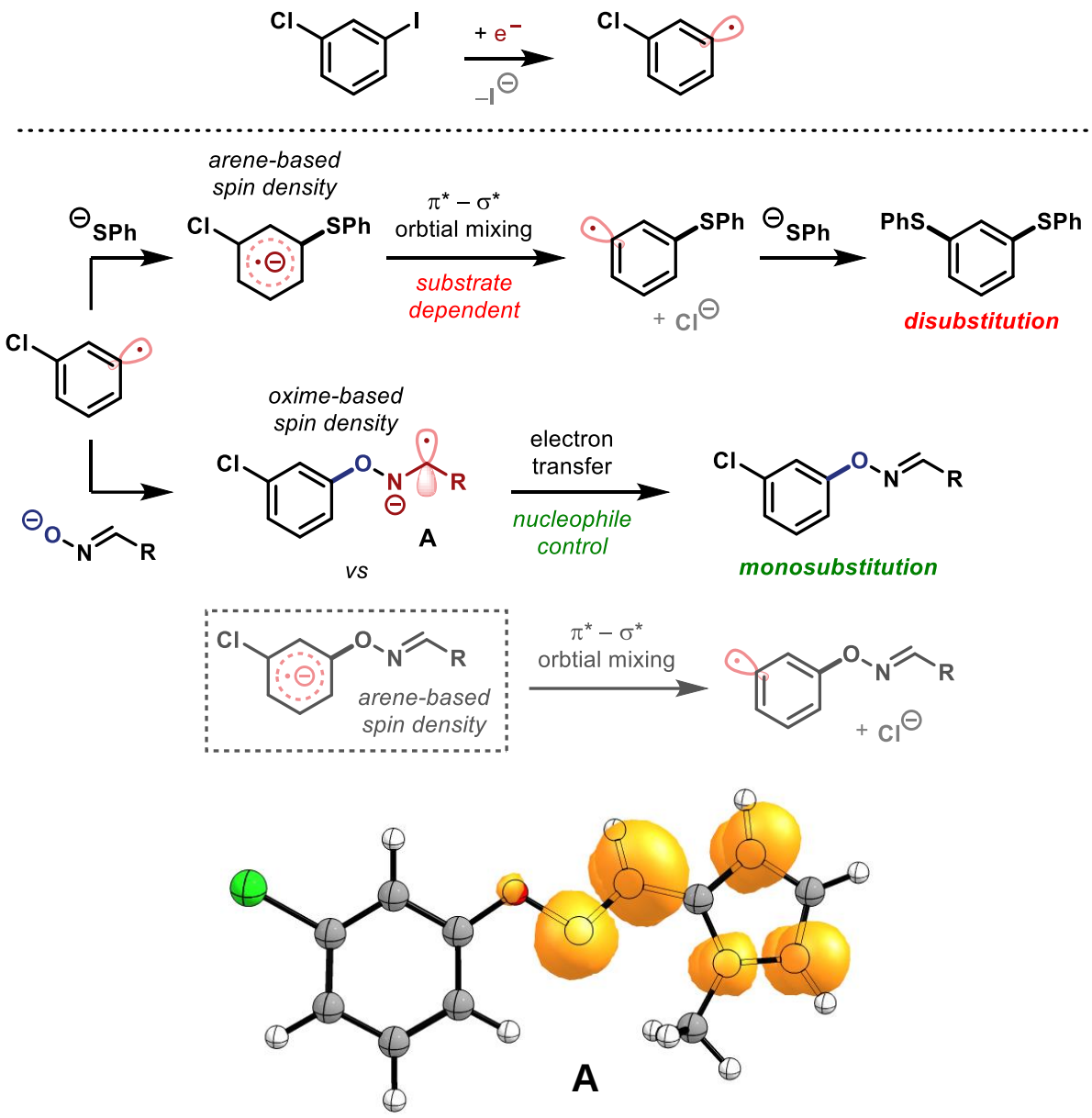

Scheme S6. Mechanistic rationale for monosubstitution including a plot of the total spin density for the coupled radical-anion intermediate **A** (isosurface contour values set at 0.002 a.u.). Calculation performed using ωB97X-D3(BJ) ma-def2-SVP CPCM(DMSO).

6. UV/Vis Spectroscopy & Photochemistry

A series of UV/Vis absorption studies were performed to clarify if a charge-transfer-complex (CTC) between oxime **9d** and 4′-bromoacetophenone **3a$_{Br}$** was formed in the presence of KO*t*-Bu. An overview of the most relevant absorption spectra are shown in Figure S2, in which a new redshifted absorption band was clearly observed upon mixing oxime **9d** and 4′-bromoacetophenone in the presence of KO*t*-Bu (typical of a CTC). However, 4′-bromoacetophenone also formed a new redshifted absorption band in the presence of KO*t*-Bu with a maximum at 490 nm (potentially due to enolate formation). To minimise the contribution of this secondary absorption band, further analysis was conducted by measuring the absorbance at 425 nm.

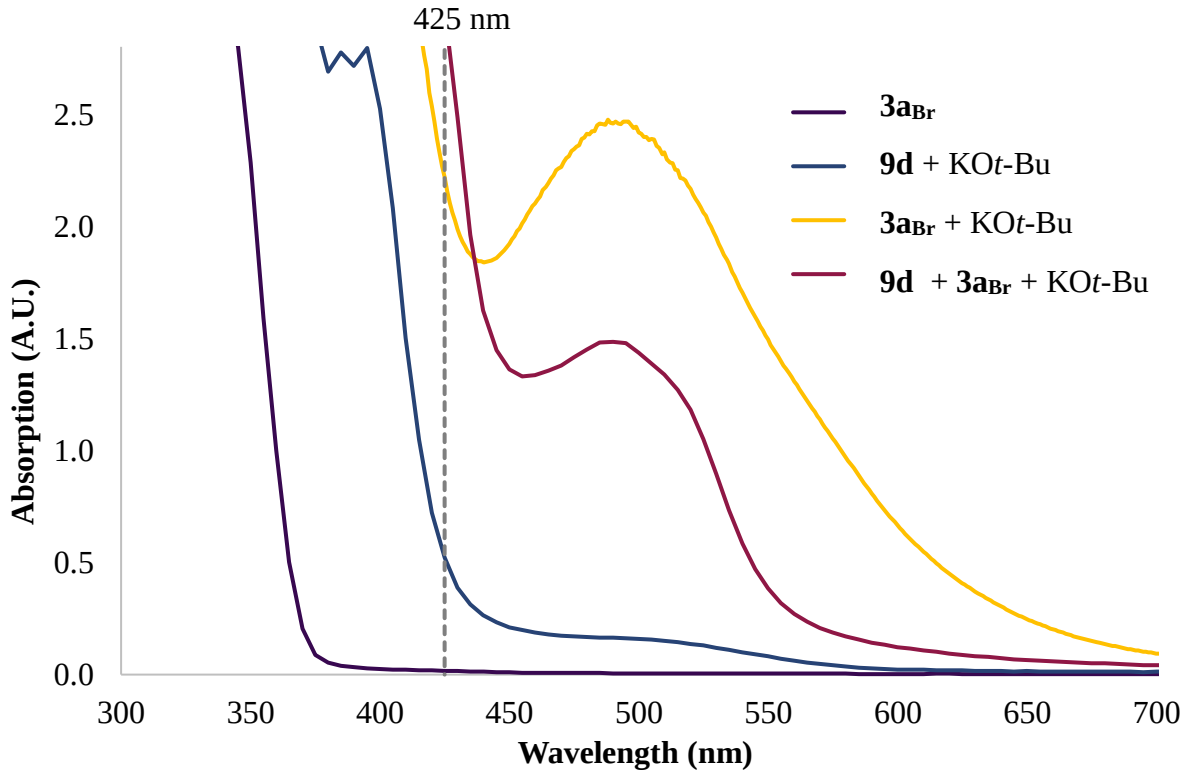

Figure S2. Absorption spectra of oxime **9d**, 4′-bromoacetophenone **3a$_{Br}$** and their combination with KO*t*-Bu (0.1 M in DMSO).

The interaction between the oxime anion and 4′-bromoacetophenone was then investigated by the method of continuous variation (Job's plot).[13] Two stock solutions of 4′-bromoacetophenone in DMSO (0.1 M), and oxime **9d** + KO*t*-Bu (1:1) in DMSO (0.1 M) were prepared. The molar fraction of 4′-bromoacetophenone and the (pre-prepared) oxime anion was

then varied, keeping solution concentration at a constant value of c_{tot} = 0.1 M in DMSO, and changes in absorption were measured at 425 nm (Figure S3).

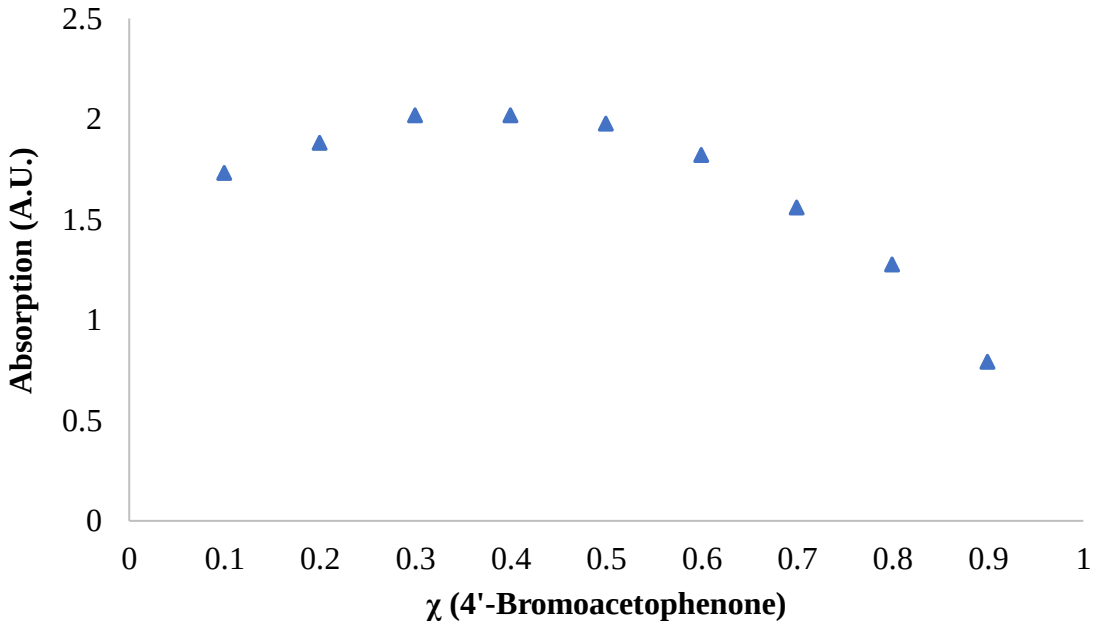

Figure S3. Job plot showing the absorption (λ = 425 nm) of a solution of 4′-bromoacetophenone and the oxime anion.

To correct for the background absorption of the oxime anion at 425 nm, its absorption coefficient was determined by measuring the absorbance of oxime **9d** and KO*t*-Bu (1:1) at varying concentrations (Figure S4). Applying this correction to the original Job plot reveals a maximum at χ = 0.5, which indicates a CTC is formed with a 1:1 stoichiometry (Figure S5).

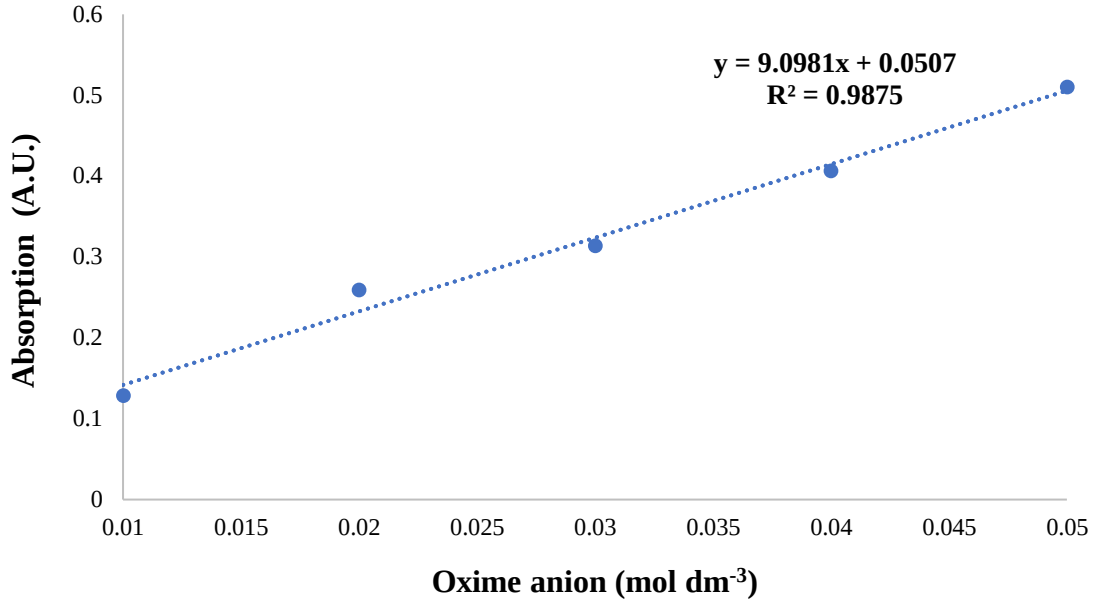

Figure S4. Graph showing the absorption (λ = 425 nm) of solutions of oxime **9d** and KO*t*-Bu as a function of concentration in DMSO.

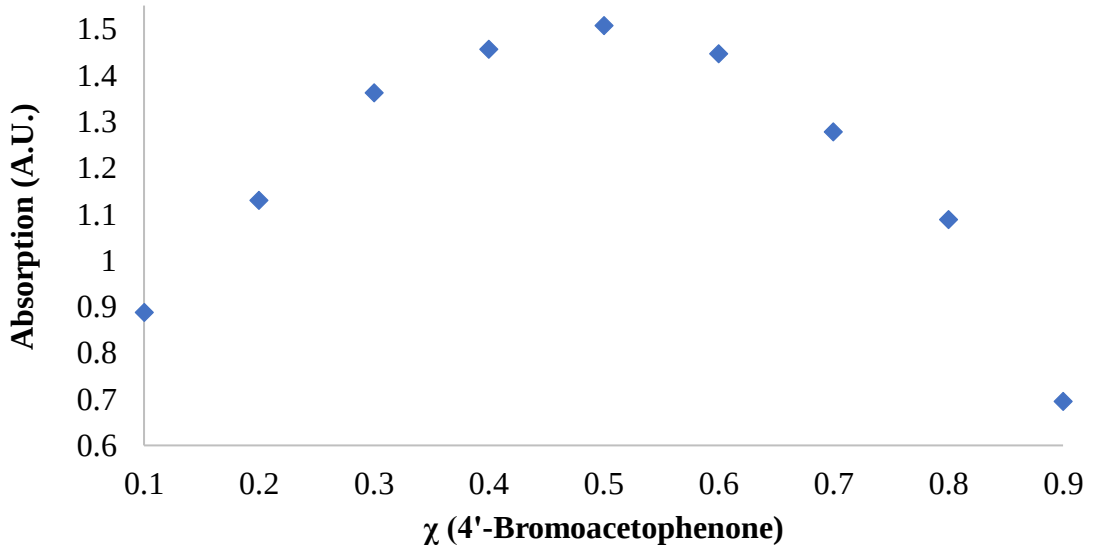

Figure S5. Job plot showing the absorption (λ = 425 nm) of a solution of 4′-bromoacetophenone and the oxime anion with a correction for the contribution of the oxime anion.

To further probe the plausibility of CTC formation, the reactivity of the reaction mixture under irradiation with different wavelengths of light was investigated (Table S3). The formation of phenol **8a** was greatly accelerated under irradiation with blue LEDs (λ_{max} = 450 nm, entry 1), which corresponds to the suspected CT band at ~425 nm. Conversely, the yield of phenol **8a** was unaffected by irradiation with green LEDs (λ_{max} = 525 nm, entry 2), which demonstrates that photoexcitation of the absorption band at ~490 nm (formed from the reaction of 4′-bromoacetophenone with KO*t*-Bu) does not influence the rate of reaction.

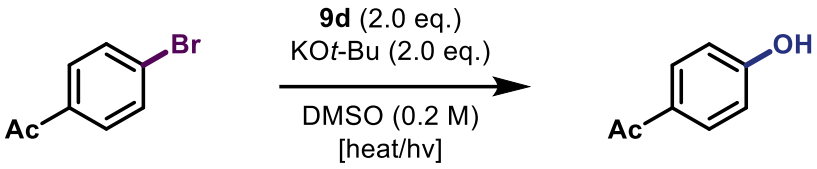

3a$_{Br}$ (1.0 eq.) **8a**

Entry[a]	Temp./hv	Time	Yield[b] **8a**
1	450 nm	1 h	65%
2	525 nm	1 h	39%
3	30 °C, darkness	1 h	38%
4	30 °C, ambient light	1 h	44%

Table S3. Photochemical reactivity studies. [a] Reactions performed with 0.1 mmol of aryl bromide **3a$_{Br}$** and 0.2 mmol oxime **9d** with the KO*t*-Bu (0.2 mmol) in DMSO (0.5 mL) under nitrogen. [b] Determined by ^{1}H NMR spectroscopy against an internal standard (dibromomethane).

7. Computational Studies

All calculations were carried out using the ORCA 4.2.0 software package.[14] This work was performed on the Viking Cluster, which is a high-performance computer facility provided by the University of York. We are grateful for computational support from the University of York High Performance Computing service, Viking and the Research Computing team.

7.1. Charge-Transfer Complex Characterisation

To further investigate the plausibility of CTC formation between oxime anion **1d** and 4′-bromoacetophenone **3a$_{Br}$**, the geometry of a ground state complex was optimised using the ωB97X-D3(BJ) range-separated hybrid functional[15] with Truhlar's minimally augmented Karlsruhe ma-def2-SVP double-zeta basis set[16] and the CPCM solvation model (DMSO).[17] The obtained geometry was confirmed to be a local minimum by frequency analysis at the same level. The optimized structure is given below in .xyz format and visualized using ChemCraft.[18] This ground state geometry was analysed by time-dependent density functional theory (TD-DFT) at the CAM-B3LYP ma-def2-TZVP level using the CPCM solvation model (DMSO). The first 5 excited states are reported below and the key contributing molecular orbitals (90 & 91) are depicted using ChemCraft (Figure S6). The lowest energy excited state was determined to be composed of a charge-transfer excitation between the CTC HOMO (MO 90) and LUMO(MO 91). These orbitals represent a mixing of the π orbitals of the oxime anion HOMO and the LUMO of 4′-bromoacetophenone. We tenatively propose that the vibrational distortion of this CTC facilitates a slow thermal dissociative ET into the C–Br σ* orbital to directly form an aryl radical.

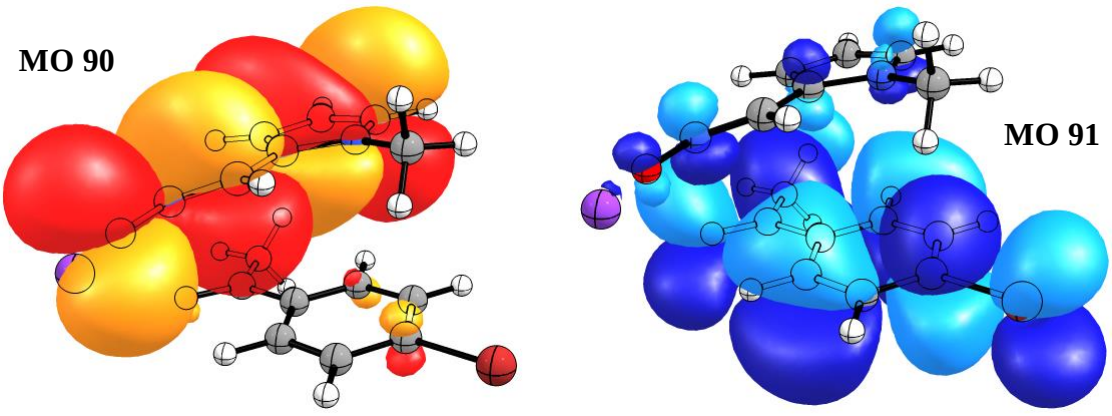

Figure S6. Calculated molecular orbitals 90 & 91 representing the HOMO and the LUMO of the CTC (isosurface contour values set at 0.012 a.u.).

Charge-Transfer Complex (*DMSO*)

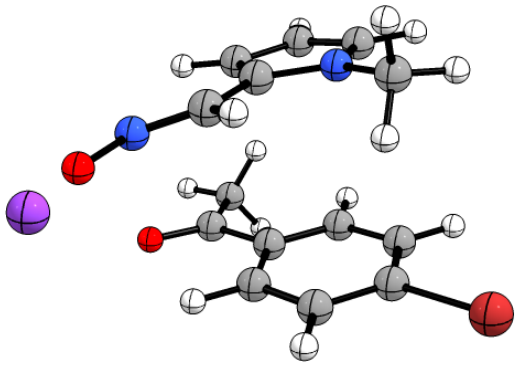

ωB97X-D3(BJ) ma-def2-SVP CPCM(DMSO)

Charge: 0; Multiplicity: 1; # of imaginary frequencies: 0

E = −3975.30423595 Eh; H_{298} = −3975.02588270 Eh; G_{298} = − 3975.09695728 Eh

C	-1.26549948167862	4.52806117040196	-0.96937983613770
C	-1.99301676529415	3.72876790807530	-1.83220588513532
C	-3.34672275752478	3.75174423318341	-1.38184562308056
C	-3.39816979460573	4.56718463309981	-0.25548049347320
C	-4.51787320798138	4.91146914260166	0.62407212348221
N	-5.63992574331945	4.28550975259557	0.52671849874173
H	-4.39015545894504	5.68968917962594	1.39238641744803
O	-6.62099147608385	4.60575178511126	1.36188556553243
C	-3.00947628530257	2.97409837195769	3.39486087434762
C	-3.68528922097009	2.23502603818282	2.42847843816791
C	-1.63296973650499	3.16533597318383	3.25339898555528
C	-0.92691793063400	2.63243527992743	2.17560691230008
C	-1.61784080405447	1.88961400302127	1.21900755927735
C	-2.99953047574044	1.68659652561942	1.33529862570984
H	-3.54633753786816	3.40429973275800	4.24306226833824
H	0.14753801453786	2.80054276443407	2.07610158768738
H	-1.06240176618537	1.48385233903864	0.37237370749428
Br	-0.70537819794049	4.18798644662915	4.54828835359712
N	-2.12164337232582	5.03272609180167	-0.01961792020741
H	-0.20552705676382	4.78058790322192	-0.94892350572368
H	-4.19917593827404	3.22741030893821	-1.81319200349843
H	-1.59258345198493	3.18251780201553	-2.68739864606680
C	-1.73062052731858	5.94523479145289	1.04225558248507
H	-2.12598166833485	6.95683686716910	0.86126969198635

H	-0.63493291877765	5.99291792405469	1.07876224486733
H	-2.09576493203086	5.58752870023553	2.01393160923716
C	-3.76676468793679	0.90642846983424	0.31272975385065
O	-4.98498810150639	0.80577990319827	0.39996212496645
C	-3.01445442465142	0.22837923636625	-0.80124042691417
H	-2.43946076481741	0.96853253919528	-1.37626970577084
H	-3.72182712764571	-0.28794986601809	-1.46225752045881
H	-2.29929708520578	-0.49724361311844	-0.38275470337929
H	-4.76265955735232	2.08418909061686	2.51655112544623
K	-7.25993975897774	2.19259857158862	0.43753421932741

TD-DFT: CAM-B3LYP ma-def2-TZVP CPCM(DMSO)

ABSORPTION SPECTRUM VIA TRANSITION ELECTRIC DIPOLE MOMENTS

State	Energy (cm-1)	Wavelength (nm)	fosc	T2 (au**2)	TX (au)	TY (au)	TZ (au)
1	20671.5	483.8	0.000000000	0.00000	-0.00000	-0.00000	-0.00000
2	21269.6	470.2	0.000000001	0.00000	-0.00004	-0.00006	-0.00009
3	**20835.5**	**479.9**	**0.027526074**	**0.43493**	**-0.37027**	**0.45919**	**-0.29491**
4	24316.3	411.2	0.000000000	0.00000	0.00001	-0.00003	-0.00005
5	27630.7	361.9	0.000394339	0.00470	-0.06586	-0.01900	-0.00035

TD-DFT/TDA EXCITED STATES

STATE 1: E= 0.094186 au 2.563 eV 20671.5 cm**-1

90a -> 91a : 0.050706 (c= -0.22518052)

90a -> 93a : 0.041949 (c= 0.20481422)

90a -> 94a : 0.010672 (c= 0.10330325)

90a -> 95a : 0.035168 (c= -0.18753100)
90a -> 96a : 0.036586 (c= 0.19127419)
90a -> 98a : 0.185924 (c= -0.43118963)
90a -> 99a : 0.016515 (c= -0.12850953)
90a -> 102a : 0.025364 (c= 0.15925967)
90a -> 104a : 0.015355 (c= -0.12391711)
90b -> 91b : 0.050706 (c= 0.22518052)
90b -> 93b : 0.041949 (c= -0.20481421)
90b -> 94b : 0.010672 (c= -0.10330325)
90b -> 95b : 0.035168 (c= 0.18753101)
90b -> 96b : 0.036586 (c= -0.19127416)
90b -> 98b : 0.185924 (c= 0.43118962)
90b -> 99b : 0.016515 (c= 0.12850951)
90b -> 102b : 0.025364 (c= -0.15925966)
90b -> 104b : 0.015355 (c= 0.12391710)

STATE 2: E= 0.096911 au 2.637 eV 21269.6 cm**-1
90a -> 91a : 0.429248 (c= 0.65517051)
90a -> 98a : 0.022794 (c= -0.15097565)
90b -> 91b : 0.429249 (c= -0.65517094)
90b -> 98b : 0.022792 (c= 0.15097029)

STATE 3: E= 0.094934 au 2.583 eV 20835.5 cm-1**
90a -> 91a : 0.494130 (c= 0.70294368)
90b -> 91b : 0.494130 (c= 0.70294392)

STATE 4: E= 0.110793 au 3.015 eV 24316.3 cm**-1
89a -> 91a : 0.045538 (c= -0.21339541)
89a -> 93a : 0.036591 (c= 0.19128706)
89a -> 94a : 0.010924 (c= 0.10451980)
89a -> 95a : 0.035174 (c= -0.18754735)
89a -> 96a : 0.038776 (c= 0.19691507)
89a -> 98a : 0.184569 (c= -0.42961527)

89a -> 99a : 0.015540 (c= -0.12465763)
89a -> 102a : 0.027123 (c= 0.16469153)
89a -> 104a : 0.015510 (c= -0.12453967)
89a -> 105a : 0.011344 (c= 0.10650797)
89b -> 91b : 0.045537 (c= 0.21339488)
89b -> 93b : 0.036591 (c= -0.19128673)
89b -> 94b : 0.010924 (c= -0.10452003)
89b -> 95b : 0.035174 (c= 0.18754721)
89b -> 96b : 0.038775 (c= -0.19691468)
89b -> 98b : 0.184568 (c= 0.42961410)
89b -> 99b : 0.015540 (c= 0.12465800)
89b -> 102b : 0.027123 (c= -0.16469099)
89b -> 104b : 0.015510 (c= 0.12453922)
89b -> 105b : 0.011344 (c= -0.10650794)

STATE 5: E= 0.125895 au 3.426 eV 27630.7 cm**-1
89a -> 91a : 0.157922 (c= -0.39739396)
89a -> 93a : 0.029486 (c= 0.17171344)
89a -> 95a : 0.029852 (c= -0.17277617)
89a -> 96a : 0.034662 (c= 0.18617831)
89a -> 98a : 0.145085 (c= -0.38090079)
89a -> 99a : 0.011203 (c= -0.10584373)
89a -> 102a : 0.019275 (c= 0.13883279)
89a -> 104a : 0.010979 (c= -0.10478173)
89b -> 91b : 0.157944 (c= -0.39742133)
89b -> 93b : 0.029495 (c= 0.17174146)
89b -> 95b : 0.029849 (c= -0.17276942)
89b -> 96b : 0.034658 (c= 0.18616702)
89b -> 98b : 0.145074 (c= -0.38088546)
89b -> 99b : 0.011202 (c= -0.10584027)
89b -> 102b : 0.019272 (c= 0.13882484)
89b -> 104b : 0.010978 (c= -0.10477831)

7.2. Radical–Anion Coupling

The proposed radical–anion coupling step was studied using density functional theory. We evaluated the B3LYP-D3(BJ), M06-2X-D3(0) and ωB97X-D3(BJ) functionals with the ma-def2-TZVP basis set using the CPCM solvation model (DMSO). The obtained geometries were confirmed to be either a local minimum or a transition state (TS) by frequency analysis at the same level. Higher energy conformers were taken into account, but were not used further. The optimized structures are given below in .xyz format and visualized using ChemCraft.[18]

We found out that these functionals all gave similar energies for the activation barrier and overall driving force (Table S4). However, the more modern ωB97X-D3(BJ) functional was selected for all subsequent studies to aid comparison with a polar S_NAr pathway.

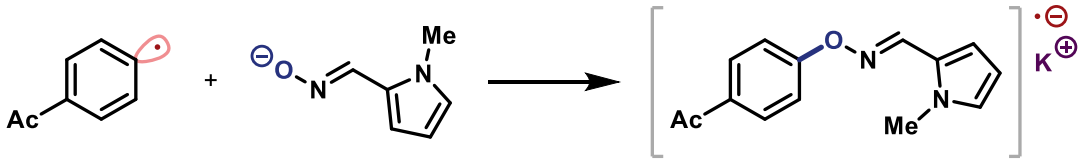

Functional	$\Delta H^{‡}$	ΔH	$\Delta G^{‡}$	ΔG
B3LYP-D3(BJ)	−1.7	−30.4	15.6	−16.9
M06-2X-D3(0)	2.1	−32.8	16.2	−19.0
ωB97X-D3(BJ)	0.4	−31.6	15.0	−17.2

Table S4. Method evaluation. All energies in kcal/mol.

The activation barrier to radical–anion coupling appeared to be almost entirely entropic in nature ($\Delta H^{‡}$ = 0.4 kcal/mol). Interestingly, a potential two-centre three-electron (2c,3e) σ bonded species was identified in the gas phase (Figure S7), which could significantly accelerate the rate of radical–anion coupling if this weak interaction is present in solution (unfortunatley dielectric continuum solvation models are known to obscure such weak radical-anion interactions).[19] Rendering a plot of the total spin density clearly indicated that the spin density is shared between the C and O atoms, which is consistent with a 2c,3e σ bonded species.

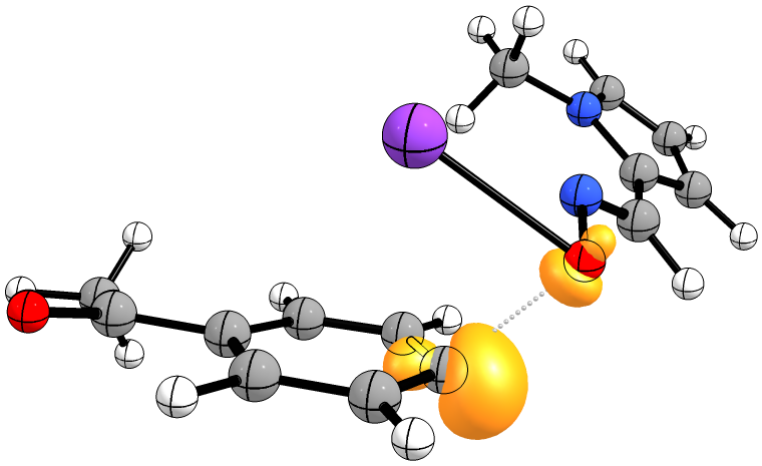

Figure S7. Proposed 2c,3e σ bonded species rendered with a plot of the total spin density (isosurface contour values set at 0.02 a.u.).

In addition to weak attractive interactions, when accounting for concentration effects,[20] the large excess of the oxime anion relative to the coupled radical-anion intermediate will likely lower the activation barrier further as the reaction quotient (Q) can be used to modify the calculated Gibbs free energy according to the following equations:

$$Q = \frac{[Products]}{[Reactants]}$$

$$\Delta G_{298} = \Delta G^{o}_{298} + RTln(Q)$$

For example, assuming that the oxime anion reactant is 2000/1000/500 times higher in concentration than the short-lived radical-anion product at 30 °C (T = 303.15 K), the radical–anion coupling activation energy may potentially be lowered by 3.7–4.6 kcal/mol.

$$(Q = 0.0005) \qquad RTln(Q) = -4.6 \text{ kcal/mol}$$

$$(Q = 0.001) \qquad RTln(Q) = -4.2 \text{ kcal/mol}$$

$$(Q = 0.002) \qquad RTln(Q) = -3.7 \text{ kcal/mol}$$

Acetophenone aryl radical (*DMSO*)

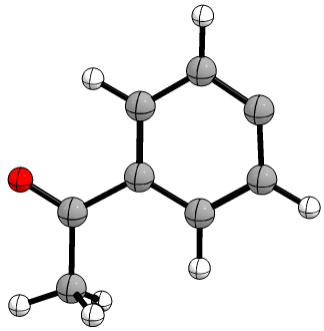

ωB97X-D3(BJ) ma-def2-TZVP CPCM(DMSO)

Charge: 0; Multiplicity: 2; # of imaginary frequencies: 0

E = −384.51707608 Eh; H_{298} = −384.38253872 Eh; G_{298} = −384.42387316 Eh

C	-6.08197612739829	-2.10562084356793	0.30593937407063
C	-5.11878584280913	-2.98621797019229	-0.12390276228758
C	-7.30898992309480	-2.42977109531170	0.82525951827712
C	-7.59696396749376	-3.79238649144600	0.92198912365651
C	-6.66488792609019	-4.74481459223671	0.50415159211085
C	-5.43234045424413	-4.33868918828746	-0.01595343782274
H	-8.02666303334878	-1.68375645722931	1.14751864420454
H	-8.55503356826571	-4.09648293455692	1.32633866380645
H	-4.72000117801864	-5.09025192704560	-0.33605404258825
H	-4.16547206005032	-2.66209420668317	-0.52611734989447
C	-6.95487359594591	-6.21104674419257	0.59970970439894
O	-6.12977098909847	-7.02953916999113	0.22940423477099
C	-8.28187458704541	-6.64979775713809	1.16005524371238
H	-9.09830275184979	-6.24407503444481	0.55737430906925
H	-8.40457349285013	-6.27294303344949	2.17850918753743
H	-8.33154050239633	-7.73729255422674	1.16184799697795

Oxime anion (*DMSO*)

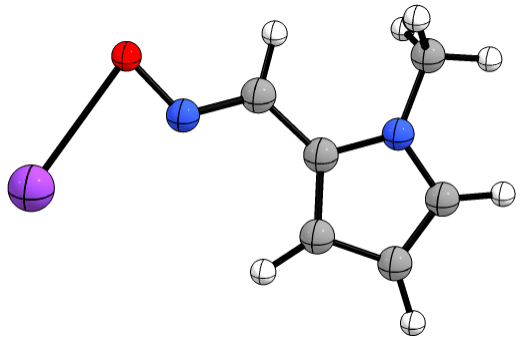

ωB97X-D3(BJ) ma-def2-TZVP CPCM(DMSO)

Charge: 0; Multiplicity: 1; # of imaginary frequencies: 0

E = −1017.83477709 Eh; H_{298} = −1017.69825471 Eh; G_{298} = −1017.74694153 Eh

C	-3.44908472820003	0.54560912082644	0.13296850359426
C	-3.95535237932681	-0.67908872814470	-0.23734941136020
N	-2.95127252491845	-1.60679089858852	-0.14091474717069
H	-4.94256169736150	-0.97263648493489	-0.56214229628529
C	-1.79729167322340	-0.99400047438713	0.28973695836111
C	-2.08106719357606	0.34960861188817	0.46673344033383
H	-3.99852998507241	1.47610711684272	0.15847904359631
C	-3.10512623074905	-3.02003902489969	-0.44467976198448
H	-4.13615812037380	-3.19479682953998	-0.74834236984846
H	-2.88714330217035	-3.63077333987057	0.43340653698300
H	-2.44183086097676	-3.31608930295606	-1.25944050664644
C	-0.56224942845480	-1.75093763045117	0.48033848874891
N	0.48832997223159	-1.18848960617928	0.95695559334311
H	-0.53353091020120	-2.80801574656447	0.20916181692526
O	1.58785503567463	-1.93445604098296	1.09191656190177
H	-1.37413476541289	1.09686385971421	0.79639572600743
K	2.40497284611128	0.41397475522789	1.86917862050056

Radical–anion coupling Transition State (*DMSO*)

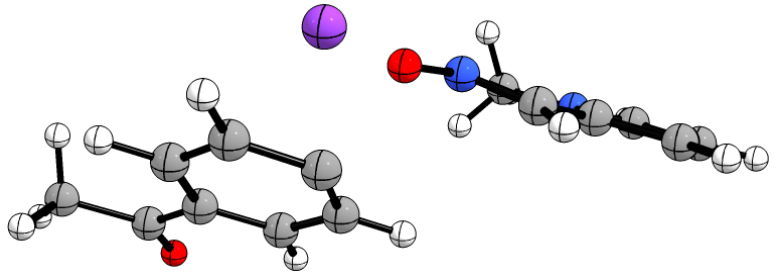

ωB97X-D3(BJ) ma-def2-TZVP CPCM(DMSO)

Charge: 0; Multiplicity: 2; # of imaginary frequencies: 1

E = −1402.35228876 Eh; H_{298} = −1402.08013187 Eh; G_{298} = −1402.14684957 Eh

C	-2.34461944151794	-2.40141030633205	-0.26769031134891
C	-3.02699890705182	-3.29169245801400	0.53202698603013
N	-2.21837131770355	-4.36079230563639	0.79660693705054
H	-4.02932545211540	-3.25601134576952	0.93300073086482
C	-1.00510317563976	-4.17128498039433	0.16936627636115
C	-1.06349894397231	-2.96051812054016	-0.50070125439190
H	-2.72652526518421	-1.46206358663003	-0.64039038016094
C	-2.63428444259517	-5.50849913232915	1.58732365347301
H	-3.68579054361449	-5.37976419615248	1.84044615675956
H	-2.04776972523867	-5.57865518206657	2.50400201648164
H	-2.51244209059400	-6.42705916750582	1.01229449872754
C	0.12514411056381	-5.08256073258310	0.19754356143268
N	0.18340514643216	-6.11832128961925	0.94594372380145
H	0.95971066940759	-4.83735131306913	-0.46231056817387
O	1.31605849125749	-6.86764797869248	0.81531819901714
H	-0.25887798563515	-2.53833260634860	-1.08656319117310
K	-0.26363392395584	-8.24886181672935	2.48272848735533
C	0.95100727043158	-8.37709552419573	-0.35123226504109
C	1.60222249701539	-9.50536167096125	0.16891036800915
C	-0.39666390695251	-8.46584049788717	-0.73250157958474

C	-1.06598781336288	-9.67383946612067	-0.62185867012318
C	-0.42536288354356	-10.81602712352429	-0.10963620265856
C	0.92280607813386	-10.70897593969562	0.27808015203209
H	2.64072512512841	-9.44634235394493	0.48296901896523
H	-2.10027669620566	-9.75476729450198	-0.94003816506479
H	-0.91799001775581	-7.59906708318241	-1.12662443087608
H	1.44800758265783	-11.57470131291889	0.66739978703935
C	-1.17541039298529	-12.08471267930111	-0.00086865362696
O	-2.35394935869274	-12.15961579340934	-0.33508242302414
C	-0.46495375286848	-13.30489482492762	0.53597583529913
H	0.40804938594808	-13.53972376889456	-0.07787219191875
H	-1.15100738714090	-14.15063587403729	0.53513627229778
H	-0.11196193265006	-13.12147627408459	1.55390862616930

Radical-anion intermediate (*DMSO*)

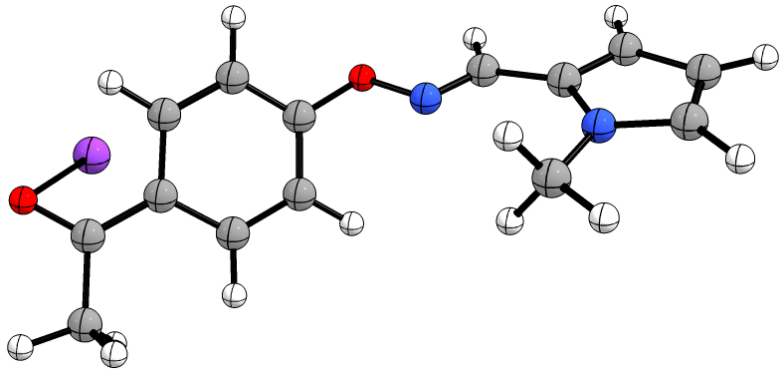

ωB97X-D3(BJ) ma-def2-TZVP CPCM(DMSO)

Charge: 0; Multiplicity: 2; # of imaginary frequencies: 0

E = −1402.40510818 Eh; H_{298} = −1402.13109604 Eh; G_{298} = −1402.19826433 Eh

C	-2.02313535139824	-1.69332975749344	0.79443737619020
C	-2.98948237863799	-2.63222440537717	0.49733421499394
N	-2.40786679878817	-3.86181599046902	0.41949563726962
H	-4.05185482135923	-2.52281529009797	0.33577954387265
C	-1.05810867320012	-3.73114408317170	0.66580198692958

C	-0.79759343053064	-2.39106029302965	0.90220442662664
H	-2.18640314609108	-0.63298252070045	0.91935621269303
C	-3.13434197703290	-5.08891500766137	0.12624087293179
H	-4.18703196734280	-4.83542751237053	0.00996154104273
H	-3.01784697326087	-5.80407206301636	0.93998603407313
H	-2.76368645077013	-5.54168762600489	-0.79306890158126
C	-0.07771437576457	-4.79669368625712	0.68065995142454
N	-0.35451264710808	-6.01653512985326	0.43347969388324
H	0.94401717126949	-4.49864554060187	0.91881498673885
O	0.80647052125273	-6.80167501542916	0.50347497621072
H	0.17675144476022	-1.97972945476288	1.12606055558737
K	2.67491559621497	-12.29334295666106	1.27794309935233
C	0.50792852194865	-8.15944936480407	0.45228592075338
C	-0.52393063697985	-8.72228477838751	1.21417970216861
C	1.31188615676434	-8.97179072570740	-0.34134527086380
C	1.10488540719998	-10.33951908747028	-0.37229649700480
C	0.06803781751789	-10.95978058677557	0.39605341472230
C	-0.74451828948043	-10.08138280697263	1.18227825081288
H	-1.14841869918440	-8.07986251762762	1.82484458512901
H	-1.54875660451530	-10.49023750615219	1.78312040224719
H	1.71747371926356	-10.95514976751547	-1.02268493379128
H	2.09647425897491	-8.51916779903896	-0.94025815171470
C	-0.11762800147302	-12.36939832896785	0.38006977320852
O	0.70252798526799	-13.15549201518959	-0.24394424456493
C	-1.26686344154096	-12.98752168751967	1.14864282086887
H	-2.22481108134313	-12.50746553409127	0.92379913603094
H	-1.11790015046161	-12.91133379214411	2.23313770094509
H	-1.33870820417119	-14.04542186867762	0.89070518281361

2c,3e σ Bonded species (*gas*)

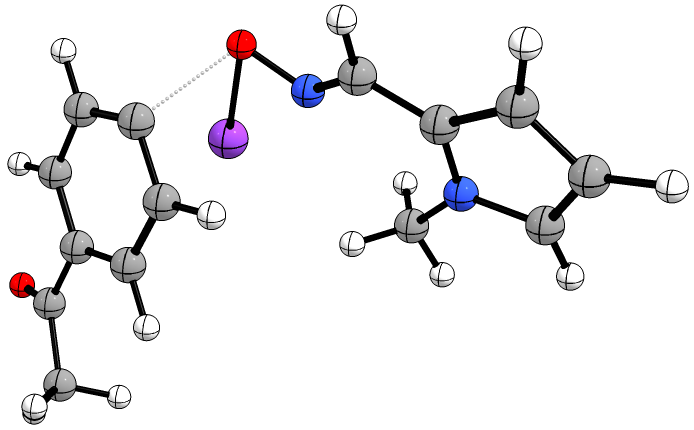

ωB97X-D3(BJ) ma-def2-TZVP

Charge: 0; Multiplicity: 2; # of imaginary frequencies: 0

E = −1402.30900077 Eh; H_{298} = −1402.03526042 Eh; G_{298} = −1402.10326951 Eh

C	-2.626861	-2.607745	-0.307685
C	-3.126163	-3.475894	0.630550
N	-2.190095	-4.448281	0.874588
H	-4.073767	-3.488023	1.147909
C	-1.078016	-4.210012	0.093019
C	-1.332476	-3.072849	-0.650163
H	-3.134343	-1.739936	-0.700936
C	-2.395673	-5.547696	1.791677
H	-3.416338	-5.488527	2.171402
H	-1.695260	-5.492518	2.627606
H	-2.255599	-6.502324	1.280240
C	0.129179	-5.017916	0.049253
N	0.372482	-5.995964	0.841341
H	0.867505	-4.753552	-0.708860
O	1.533912	-6.644029	0.636418
H	-0.645905	-2.632698	-1.358446
K	0.442957	-8.111704	2.323626
C	1.016693	-8.435124	-0.545783

C	1.735931	-9.504305	-0.022551
C	-0.351946	-8.515115	-0.751281
C	-1.018958	-9.694042	-0.419246
C	-0.326600	-10.772779	0.144565
C	1.061049	-10.666873	0.328084
H	2.809493	-9.426983	0.123036
H	-2.088153	-9.764240	-0.593628
H	-0.902051	-7.672781	-1.158569
H	1.589756	-11.517902	0.745138
C	-1.009356	-12.034732	0.559498
O	-0.429947	-12.868290	1.226739
C	-2.445925	-12.254010	0.132661
H	-3.100435	-11.509993	0.595330
H	-2.757117	-13.249145	0.445348
H	-2.548481	-12.153731	-0.950496

7.3. Redox Potential Estimation

The redox potential of *O*-aryl oxime interemdiate **7a** was estimated according to a method based on the work of Nicewicz and co-workers:[21] Geometries of the redox couple were optimized at the B3LYP-D3(BJ) ma-def2-TZVP level using the CPCM continuum solvation model (Acetonitrile). The obtained geometries were confirmed to be local minima by frequency analysis at the same level. Higher energy conformers were taken into account, but were not used further. The optimized structures are given below in .xyz format and visualized using ChemCraft.

From the calculated Gibbs free energies of the redox couple at 298 K, the redox potential was calculated and referenced to saturated calomel electrode (SCE) by subtraction of its absolute potential in acetonitrile (E_{ref} = 4.422 V).[22]

$$G_{298}(radical\ anion) = -801.59776309\ \text{Eh}$$

$$G_{298}(neutral) = -801.51384082\ \text{Eh}$$

$$E_{1/2} = -\frac{G_{298}(radical\ anion) - G_{298}(neutral)}{F} - E_{ref} = -2.14\ \text{V (vs SCE in MeCN)}$$

_O_-Aryl oxime intermediate (*DMSO*)

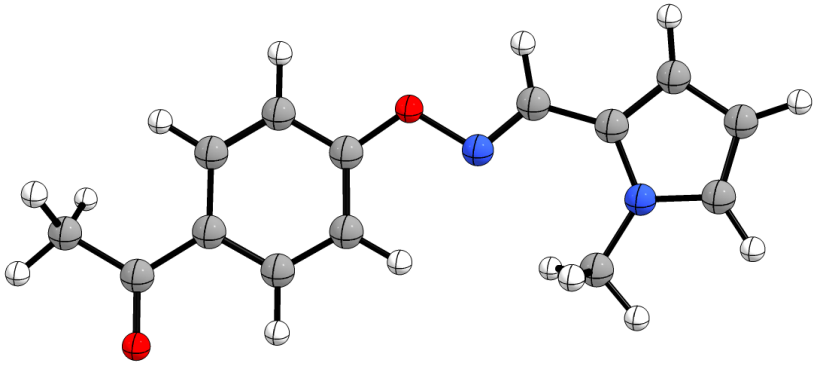

B3LYP-D3(BJ) ma-def2-TZVP CPCM(DMSO)

Charge: 0; Multiplicity: 1; # of imaginary frequencies: 0

E = −801.72362550 Eh; H_{298} = −801.45289633 Eh; G_{298} = −801.51384082 Eh

C	3.53382163695200	-2.58947091252254	1.63092009908746
C	3.83416444192416	-3.66619990536047	2.44861975942891
N	3.16970595896441	-4.76630140253163	2.00198569081877
H	4.47198670853950	-3.72983287859898	3.31478201051116
C	2.42854987614240	-4.41593242570850	0.88664743764704
C	2.64778778023464	-3.06037588826062	0.64571025545263
H	3.91499630391590	-1.58765520578936	1.74211805601442
C	3.25063440762830	-6.08032529560107	2.62285910145163
H	3.92380751076857	-6.01080617213901	3.47377346057234
H	3.63318430943468	-6.81329064062119	1.91464071472881
H	2.26758913287154	-6.40323612821064	2.96159784336280
C	1.58699175695006	-5.27438898085382	0.11266464200044
N	1.40512819893241	-6.51886047324347	0.36591234118370
H	1.08781382714511	-4.80627230496006	-0.73418790826193
O	0.51659755859452	-7.06088732228670	-0.59937361219857
H	2.20294078357295	-2.49907982221736	-0.16068664407285
C	0.24261416408660	-8.38087487559712	-0.41789757918642
C	0.76268223672812	-9.15826107511090	0.62003221180690
C	-0.62207010748441	-8.94218149008659	-1.36087787757690
C	-0.96473331083069	-10.27739018408689	-1.26497416438717
C	-0.45698849277451	-11.07972405212240	-0.23321281434651
C	0.40724314791216	-10.49325299781747	0.69868802925932

H	1.42886884427246	-8.71829475337069	1.34423875962537
H	-1.63471840157781	-10.69332189940917	-2.00409583826938
H	-1.01352141409713	-8.32212209617531	-2.15645284996580
H	0.80424791000797	-11.10386399363476	1.49836245714018
C	-0.80627819285069	-12.51249745668432	-0.10470002163128
O	-0.35166153539440	-13.19456033234129	0.80835664822168
C	-1.73623771126064	-13.12713001672707	-1.12071748736229
H	-2.69696098611273	-12.60781407028021	-1.12660745496006
H	-1.89215850263242	-14.17604814034478	-0.87961924959433
H	-1.31623284056304	-13.04277080730551	-2.12543101650007

_O_-Aryl oxime intermediate radical anion (_DMSO_)

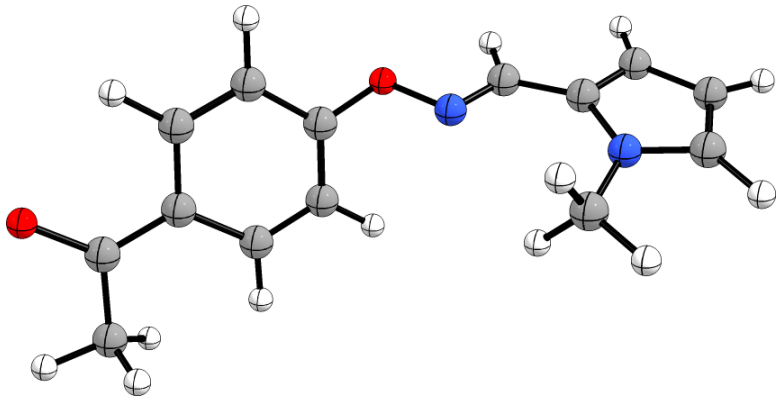

B3LYP-D3(BJ) ma-def2-TZVP CPCM(DMSO)

Charge: −1; Multiplicity: 2; # of imaginary frequencies: 0

E = −801.80269737 Eh; H_{298} = −801.53554491 Eh; G_{298} = −801.59776309 Eh

C	3.77950073914877	-2.70211837295770	1.58628130942947
C	3.47686052471939	-3.55150777733782	2.63461956200888
N	2.77818506856929	-4.62037892190292	2.15461524424603
H	3.70683175978383	-3.47924140577447	3.68484976675132
C	2.62129216286897	-4.47520157231499	0.78808664196892
C	3.24181478555611	-3.28346690269625	0.42039635522488
H	4.32498525724226	-1.77559918880032	1.66196853881106
C	2.30015857642076	-5.71939008003158	2.97953140220722
H	2.62022252605355	-5.53741990516302	4.00280019586858

H	2.71120064523609	-6.66519361381920	2.63128660351125
H	1.21371733269198	-5.78146418045962	2.94298291866030
C	1.94809366809369	-5.37908918820161	-0.10015827385558
N	1.35674276032553	-6.45355072117058	0.27461284059239
H	1.95997413913660	-5.09859500808441	-1.15295273866833
O	0.78039107611073	-7.10716007462890	-0.84220870900407
H	3.28711466348105	-2.89775033673120	-0.58586618749553
C	0.39787465034087	-8.41109793199936	-0.54997622498056
C	1.22457427361902	-9.29411441301483	0.15573840909806
C	-0.83258175649634	-8.85442176086530	-1.04430984982980
C	-1.23224401987237	-10.16143923105713	-0.84879750247827
C	-0.42321483968112	-11.09689260432235	-0.12681839835590
C	0.82404222790431	-10.59816679616609	0.36693584907637
H	2.17426855576141	-8.94377361202676	0.53912837091314
H	-2.18425067100017	-10.49617327732931	-1.23859308742079
H	-1.46465519936794	-8.15923319594177	-1.58565858671849
H	1.48315179974595	-11.25580154635550	0.91825290652195
C	-0.85368774626865	-12.43948987042000	0.07259224958816
O	-1.97512338582110	-12.88071249883738	-0.38499164653395
C	0.03492221760489	-13.39613088694227	0.84485229594305
H	1.00727864848060	-13.54312394951001	0.35988700373952
H	-0.45951941396304	-14.36492552206892	0.91629403214234
H	0.24507897357491	-13.04210565306723	1.86066870903825

7.4. Polar Nucleophilic Aromatic Substitution (S_NAr)

A potential polar S_NAr pathway was also studied using density functional theory. Based on the excellent performance of the ωB97X-D3(0) functional in the study of Murphy, Tuttle and co-workers,[23] the more moden ωB97X-D3(BJ) variant was selected to aid comparison with the proposed $S_{RN}1$ pathway. Geometries were optimised at the ωB97X-D3(BJ) ma-def2-SVP/TZVP level using the CPCM continuum solvation model (DMSO). The obtained geometries were confirmed to be either a local minimum or a transition state (TS) by frequency analysis at the same level. Higher energy conformers were taken into account, but were not used further. The optimized structures are given below in .xyz format and visualized using ChemCraft.

A direct S_NAr pathway was considered very unlikely to proceed at 30 °C due to the significant activation barrier calculated for the addition of the oxime anion ($\Delta G^{\ddagger}$ = 32.4 kcal/mol).

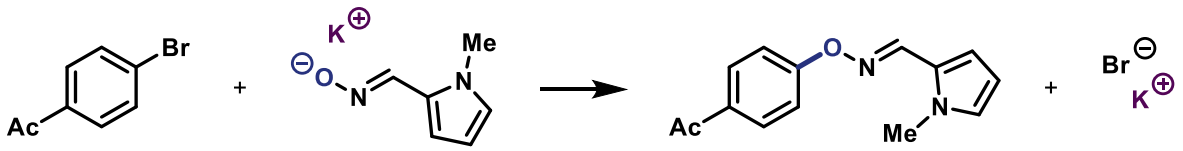

ΔG = −36.0 kcal/mol
$\Delta G^{\ddagger}$ = 32.4 kcal/mol

In addition, even when accounting for a CTC as an intermediate,[24] the calculated activation barrier for subsitution ($\Delta G^{\ddagger}$ = 25.7 kcal/mol) is still challenging to overcome at 30 °C.

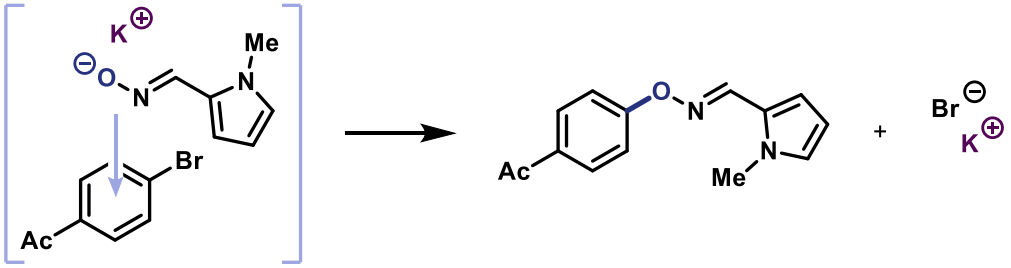

ΔG = −42.7 kcal/mol
$\Delta G^{\ddagger}$ = 25.7 kcal/mol

In support of our additive inhibition studies, an S_NAr pathway for the corresponding fluoride (4′-fluorooacetophenone, **3a**$_F$) was also considered relatively unlikely to proceed at 30 °C due to the activation barrier calculated for the addition of the oxime anion ($\Delta G^{\ddagger}$ = 29.8 kcal/mol).

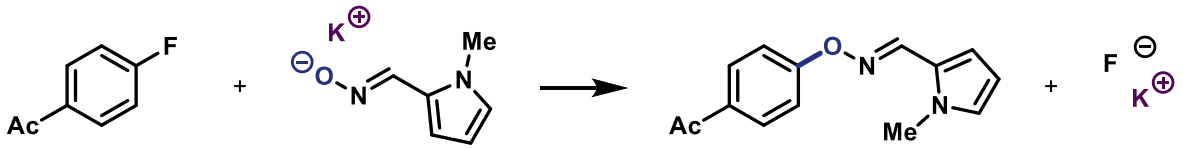

ΔG = −16.2 kcal/mol
$\Delta G^{\ddagger}$ = 29.8 kcal/mol

4′-Bromoacetophenone (*DMSO*)

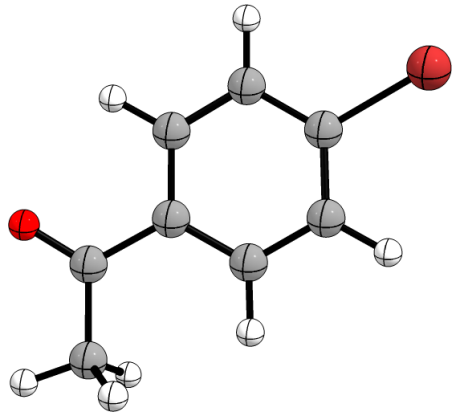

ωB97X-D3(BJ) ma-def2-TZVP CPCM(DMSO)

Charge: 0; Multiplicity: 1; # of imaginary frequencies: 0

E = −2958.67996208 Eh; H_{298} = −2958.54094136 Eh; G_{298} = −2958.58617014 Eh

C	2.66117498915067	-8.00989039365332	-0.31852037355424
Br	1.26446950944194	-7.05646496315193	-1.16501720817347
C	2.65453508331049	-9.39570866479896	-0.35913314263459
C	3.68371922515456	-10.08898973293485	0.26448847867376
C	4.70579466998286	-9.40379524160709	0.92003298441951
C	4.68705927294263	-8.00847091059471	0.94520470405386
C	3.66731362601981	-7.30269007199148	0.32777283282734
H	1.86087727722490	-9.92816083641269	-0.86808462604480
H	3.67558061139778	-11.17131787814374	0.23078658962016
C	5.82822487880769	-10.12656683502140	1.60045563929427
O	6.70871916740554	-9.50133160662971	2.16610501122278
C	5.84089048222424	-11.63119526205309	1.56634926595919
H	5.86384881721741	-11.98419623225301	0.53223400532735
H	4.93290520495857	-12.02582536210041	2.02935374117199
H	6.71582819912175	-11.99790876978273	2.10024321551198
H	5.48174921915121	-7.47710457531347	1.45463591101873
H	3.65265976648789	-6.22003266355727	0.34705297130618

Oxime anion (*DMSO*)

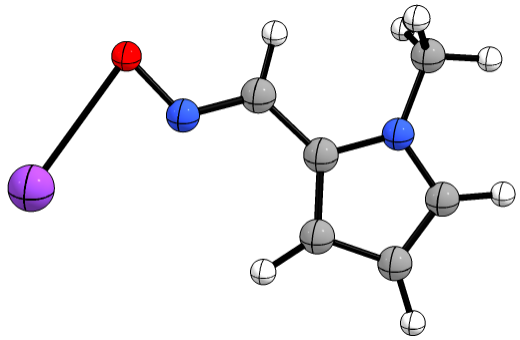

ωB97X-D3(BJ) ma-def2-TZVP CPCM(DMSO)

Charge: 0; Multiplicity: 1; # of imaginary frequencies: 0

E = −1017.83477709 Eh; H_{298} = −1017.69825471 Eh; G_{298} = −1017.74694153 Eh

Aryl Bromide S_NAr Transition State (*DMSO*)

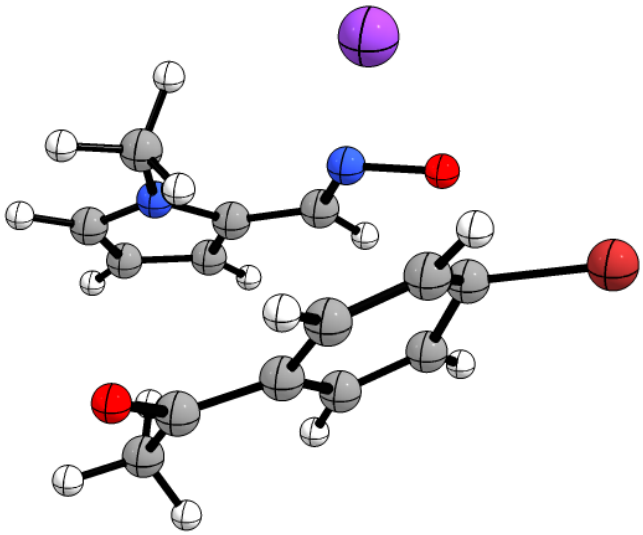

ωB97X-D3(BJ) ma-def2-TZVP CPCM(DMSO)

Charge: 0; Multiplicity: 1; # of imaginary frequencies: 1

E = −3976.49047548 Eh; H_{298} = −3976.21402665 Eh; G_{298} = −3976.28140525 Eh

C	-3.17902878650837	3.42322144354075	-2.77124226199656
C	-1.91680768138742	3.97827037586177	-2.80829218075553
C	-1.70553621237375	4.59210885133370	-1.55138147027152
C	-2.84561817538682	4.39472895595183	-0.78959918265990

C	-3.02310032730016	4.78869911148958	0.59299735138537
N	-4.11142373756584	4.61036264630878	1.24252454234007
H	-2.15849298784626	5.24198421340461	1.07498790513304
O	-4.00744897408127	4.89741989147888	2.58718358845216
C	-4.42224123616548	2.40103799904938	3.21537379253955
C	-4.29154499622333	1.46442655748160	2.22754715800671
C	-3.41044573687346	3.41230319719092	3.37710577859395
C	-2.13428463649102	3.12981373748533	2.79619808196556
C	-2.03153808606016	2.17902663649558	1.81291801258798
C	-3.11685548891089	1.35856111668672	1.44550629153724
H	-5.30338269069983	2.43007212786881	3.84766919525426
H	-1.28207412156319	3.73878399058664	3.07203526869892
H	-1.07462324296878	2.06483463511586	1.31538223783428
Br	-3.36199356658262	4.22078064887282	5.14455277873732
N	-3.73906915150174	3.67103853229112	-1.55314904104349
H	-3.72706351699830	2.86835288403297	-3.51852489054960
H	-0.82105831983527	5.11512583106041	-1.21522977011339
H	-1.23191395183063	3.94033803442556	-3.64272290762604
C	-5.07302284912113	3.22683861198419	-1.17703003480846
H	-5.02536009146574	2.61579817800998	-0.27694749205295
H	-5.47291820589383	2.63399763185153	-1.99843097036128
H	-5.72521668782799	4.08365829147274	-1.00239388787317
C	-3.06788551616320	0.46075296705554	0.30589384060728
O	-4.02119129465426	-0.26412655956625	-0.00433732670205
C	-1.82660009756439	0.45727730404455	-0.56274338874712
H	-1.69092516199345	1.44180442362935	-1.02026173329557
H	-1.93806975706086	-0.29173459178328	-1.34602562382201
H	-0.93213051314964	0.23832151564190	0.02460736201812
H	-5.10319303551063	0.76705065503416	2.04426396848348
K	-6.59449116444021	4.20727015461196	2.01506900850334

_O_-Aryl oxime product (_DMSO_)

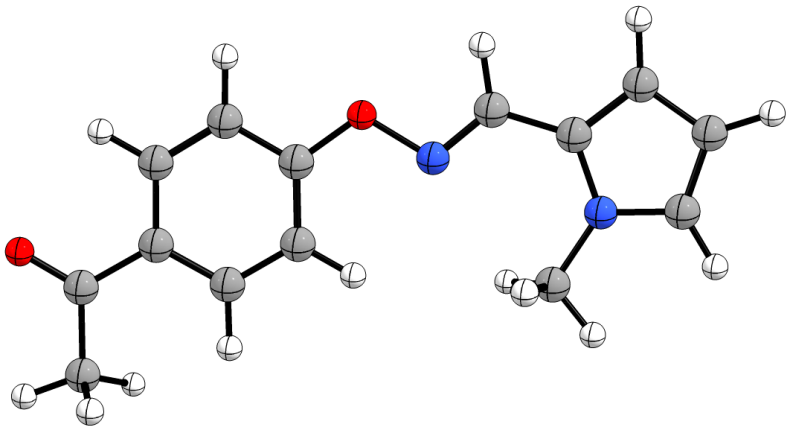

ωB97X-D3(BJ) ma-def2-TZVP CPCM(DMSO)

Charge: 0; Multiplicity: 1; # of imaginary frequencies: 0

E = −802.44322701 Eh; H_{298} = −802.16916153 Eh; G_{298} = −802.22937414 Eh

C	3.51991627782058	-2.57760660615772	1.63667865059655
C	3.72904258211952	-3.63386779644251	2.50164236377525
N	3.08033315600602	-4.73281167282442	2.03074030607402
H	4.29282835215021	-3.68843366734254	3.42133546651470
C	2.44275563039961	-4.39989824508491	0.85388485288125
C	2.70386236531031	-3.06383387919090	0.59163481732790
H	3.91153199996008	-1.57764722146249	1.75080151525375
C	3.08341116172560	-6.02936792410478	2.69348991394294
H	3.68289895843029	-5.94188025121324	3.59821608321226
H	3.51469397970180	-6.78895613840651	2.04178929856254
H	2.06780353955371	-6.32511988605518	2.95588283321951
C	1.64255326847221	-5.27684219969330	0.03251884341858
N	1.42989933730810	-6.50339963421452	0.31243327604208
H	1.21442787261319	-4.83031869731275	-0.86521413802628
O	0.61688829500157	-7.07395565681080	-0.68262053510802
H	2.33574638548204	-2.51812539100196	-0.26580023750118
C	0.33219071422776	-8.38984795819429	-0.46215563224803
C	0.78510684490748	-9.11754108935043	0.63405433077086

C	-0.47144741555158	-8.98938119546548	-1.43600648195732
C	-0.81797950117283	-10.31808029533627	-1.30666634152315
C	-0.37561732651367	-11.07304914683589	-0.21388430867265
C	0.42468930994658	-10.45398979184907	0.74501206339616
H	1.40526107816762	-8.64948728975696	1.38406155117723
H	-1.44039830282194	-10.79016688863954	-2.05747513052749
H	-0.81116422026372	-8.39959884915072	-2.27978783938917
H	0.78298574768680	-11.01104299085827	1.60234853058075
C	-0.76943235736967	-12.50454981317006	-0.10772438865207
O	-1.47190671940740	-13.02430558331992	-0.96246772076863
C	-0.28428810239949	-13.30161733404986	1.07623630996316
H	0.80817916894640	-13.31215008116599	1.10284882758167
H	-0.65931075472112	-14.32119196777180	1.00339940871944
H	-0.63246132571605	-12.84666485776674	2.00684351136339

Potassium bromide (*DMSO*)


ωB97X-D3(BJ) ma-def2-TZVP CPCM(DMSO)

Charge: 0; Multiplicity: 1; # of imaginary frequencies: 0

E = −3174.13646548 Eh; H_{298} = −3174.13218004 Eh; G_{298} = −3174.16109689 Eh

K	3.07827004026620	-8.29263697405635	-0.06573364165943
Br	0.82603995973380	-6.75240302594365	-1.42893635834056

Charge-Transfer Complex (*DMSO*)

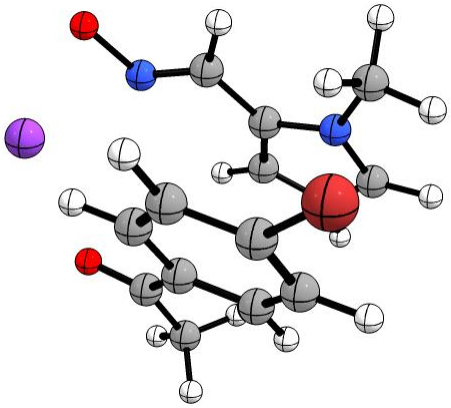

Geometry: ωB97X-D3(BJ) ma-def2-SVP CPCM(DMSO)

Charge: 0; Multiplicity: 1; # of imaginary frequencies: 0

$G_{correction}$ = 0.20727867 Eh

Single-point calculation: ωB97X-D3(BJ) ma-def2-TZVP CPCM(DMSO)

E = −3976.529708085059 Eh

$E + G_{correction} = G_{298}$ = −3976.32242941505 Eh

4′-Fluoroacetophenone (*DMSO*)

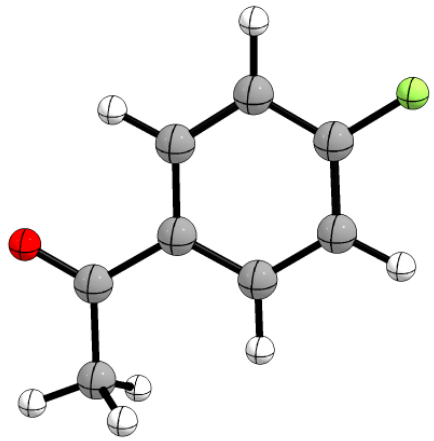

ωB97X-D3(BJ) ma-def2-TZVP CPCM(DMSO)

Charge: 0; Multiplicity: 1; # of imaginary frequencies: 0

E = −484.49852848 Eh; H_{298} = −484.35830174 Eh; G_{298} = −484.40113738 Eh

C 2.64785976390140 -8.00484198140970 -0.32654405287930

F	1.64904566317991	-7.32534482441695	-0.93138257950028
C	2.63015980733207	-9.38627427426855	-0.37439887699811
C	3.66084420580254	-10.07516441084246	0.24997292327806
C	4.68285360785226	-9.38727609970999	0.90558934516127
C	4.66233774154617	-7.99067187788962	0.93007857011621
C	3.64302188897558	-7.28480012240838	0.31330358029051
H	1.82879497629504	-9.90363922737554	-0.88777012182647
H	3.65595366837750	-11.15748089112745	0.21802119436370
C	5.80391566024088	-10.10662278583263	1.58494289389604
O	6.68578597133381	-9.48216351841162	2.15150780210690
C	5.81854411658830	-11.61201080820616	1.55339070472849
H	5.84312039346131	-11.96744375314615	0.52018669226791
H	4.91135177385791	-12.00785735505340	2.01681287741604
H	6.69381407827759	-11.97632404229525	2.08847902493872
H	5.45714023271153	-7.45978712023135	1.43963556272163
H	3.61079645026620	-6.20193690737471	0.32212445991869

Aryl Fluoride S_NAr Transition State (*DMSO*)

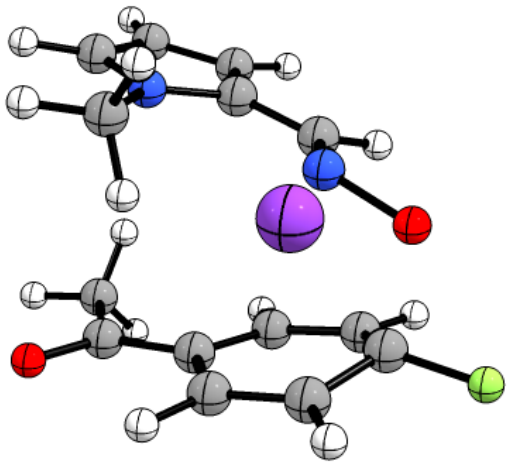

Geometry: ωB97X-D3(BJ) ma-def2-SVP CPCM(DMSO)

Charge: 0; Multiplicity: 1; # of imaginary frequencies: 1

$G_{correction}$ = 0.21256112 Eh

Single-point calculation: ωB97X-D3(BJ) ma-def2-TZVP CPCM(DMSO)

E = −1502.31308053097Eh

$E + G_{correction} = G_{298}$ = −1502.10051941097 Eh

C	-3.74522419448586	-1.62937411297507	-2.98854643729204
C	-2.36700553432501	-1.62612577972044	-2.84065382812636
C	-2.04250621874266	-0.47464880595014	-2.07437870096901
C	-3.23273002535094	0.18691014991279	-1.78343567589434
C	-3.37062560220466	1.37051530050951	-0.94737349629378
N	-4.49094459888107	1.96193857422866	-0.73280715457076
H	-2.45041495171921	1.73432751723459	-0.47082531272835
O	-4.44372298756998	2.93542951674011	0.22765247471854
N	-4.26717485607165	-0.53912570700943	-2.34743665445505
H	-4.40201360321615	-2.33053912454451	-3.50333032148774
H	-1.05334348726410	-0.15066891819376	-1.74784634483284
H	-1.67857105024189	-2.37209942857378	-3.23842456168617
C	-5.68981375443094	-0.22912507147762	-2.31205430018273
H	-6.03285980834717	-0.14224186539145	-1.27339542577279
H	-6.22963792476454	-1.04661634890673	-2.80604257562300
H	-5.89407964818118	0.71004604383155	-2.84588346298379
K	-6.97171292375736	2.83414707491295	-0.82330946204347
H	-3.55699338369193	-2.47083902057696	-0.15012073342592
C	-4.17789261611690	-2.89393160236614	0.65646685191842
C	-6.01186207424216	1.60580309766433	1.83447976829710
C	-4.67150933886017	2.13618896345384	1.82467537158265
C	-6.21372546430698	0.27571194371780	1.54674354629241
C	-3.60119356541989	1.19227203168159	1.95245412633136
C	-5.12875959139743	-0.63025114006868	1.38533169331971

C	-3.83040028459483	-0.13690033055419	1.66461547372697
C	-5.36882300121307	-1.99144240457299	0.91791999014802
O	-6.51041882597826	-2.41398304009859	0.68499574348353
F	-4.50957622685991	3.31804415975450	2.50394628215010
H	-4.53327991214306	-3.88800860441265	0.35447809049941
H	-6.84581099105505	2.29528728484280	2.00231554136607
H	-7.23422324018925	-0.10821406740864	1.45010370423950
H	-2.59730700291221	1.56605587869906	2.16990108256959
H	-2.97401772073915	-0.81624062165560	1.65799429301948
H	-3.54243059072531	-2.99055954272672	1.54962241470528

Potassium Fluoride (*DMSO*)


ωB97X-D3(BJ) ma-def2-TZVP CPCM(DMSO)

Charge: 0; Multiplicity: 1; # of imaginary frequencies: 0

E = −699.92254523 Eh; H_{298} = −699.91818475 Eh; G_{298} = −699.94451748 Eh

K	2.85364384920425	-8.13901600087745	-0.20169687209054
F	1.05066615079574	-6.90602399912254	-1.29297312790946

8. X-Ray Crystallography

Oxford Diffraction SuperNova

Diffraction data were collected at 110 K on an Oxford Diffraction SuperNova diffractometer with Cu-K_α radiation (λ = 1.54184 Å) using an EOS CCD camera. The crystal was cooled with an Oxford Instruments Cryojet. Diffractometer control, data collection, initial unit cell determination, frame integration and unit-cell refinement were carried out with CrysAlisPro.[25] Face-indexed absorption corrections were applied using spherical harmonics, implemented in SCALE3 ABSPACK[26] scaling algorithm within CrysAlisPro. OLEX2[27] was used for overall structure solution, refinement and preparation of computer graphics and publication data. Within OLEX2, the algorithm used for structure solution was ShelXT (dual-space).[28] Refinement by full-matrix least-squares used the ShelXL[29] algorithm within OLEX2.[27] All non-hydrogen atoms were refined anisotropically. Hydrogen atoms were located by difference map and allowed to refine.

8.1. (*E*)-1-methyl-1H-pyrrole-2-carboxaldehyde oxime (9d)

CCDC: 2102632

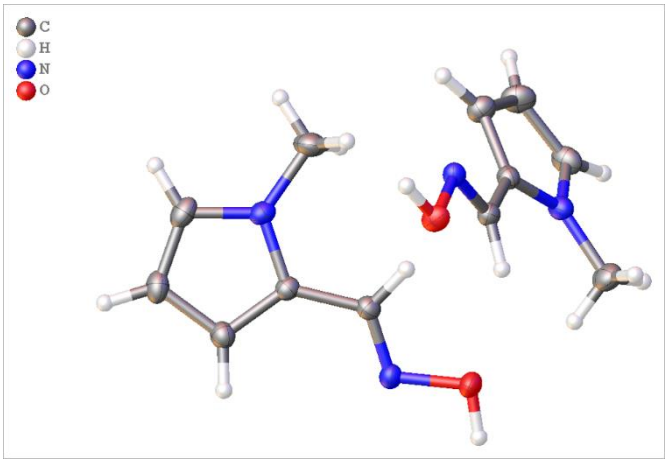

Table S5. Crystal data and structure refinement for mjj2001.

Identification code	mjj2001
Empirical formula	$C_6H_8N_2O$
Formula weight	124.14
Temperature/K	111(3)

Crystal system	orthorhombic
Space group	Pbcn
a/Å	18.1149(5)
b/Å	7.9429(2)
c/Å	18.0218(5)
α/°	90
β/°	90
γ/°	90
Volume/Å^3	2593.05(12)
Z	16
ρ_{calc}g/cm^3	1.272
μ/mm^{-1}	0.090
F(000)	1056.0
Crystal size/mm^3	0.404 × 0.103 × 0.025
Radiation	Mo Kα (λ = 0.71073)
2Θ range for data collection/°	6.378 to 60.156
Index ranges	-25 ≤ h ≤ 24, -10 ≤ k ≤ 11, -25 ≤ l ≤ 21
Reflections collected	15188
Independent reflections	3802 [R_{int} = 0.0393, R_{sigma} = 0.0361]
Data/restraints/parameters	3802/0/227
Goodness-of-fit on F^2	1.063
Final R indexes [I>=2σ (I)]	R_1 = 0.0470, wR_2 = 0.1156
Final R indexes [all data]	R_1 = 0.0643, wR_2 = 0.1261
Largest diff. peak/hole / e Å^{-3}	0.30/-0.29

8.2. Hydroxy-Blonanserin derivative (8z)

CCDC: 2102633

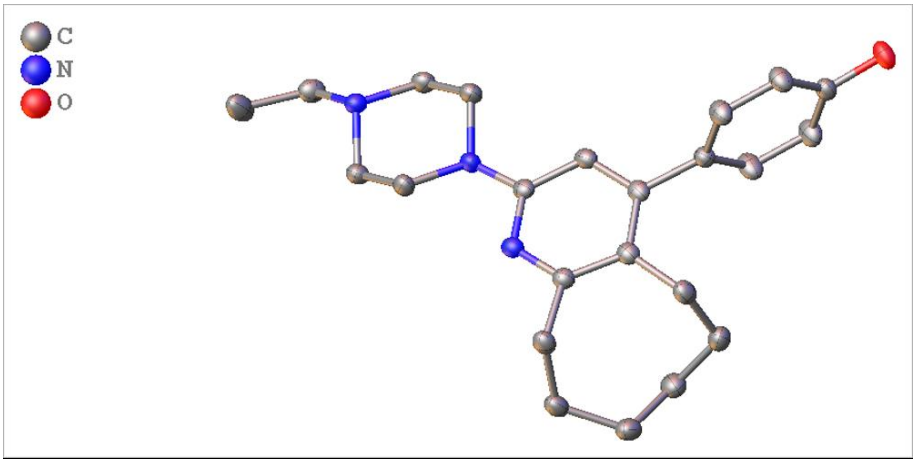

Table S6. Crystal data and structure refinement for mjj21001.

Identification code	mjj21001
Empirical formula	$C_{23}H_{31}N_3O$
Formula weight	365.51
Temperature/K	109.9(6)
Crystal system	monoclinic
Space group	$P2_1/n$
a/Å	9.5000(3)
b/Å	11.7569(3)
c/Å	18.0932(5)
α/°	90
β/°	101.562(3)
γ/°	90
Volume/Å^3	1979.83(10)
Z	4
ρ_{calc}g/cm^3	1.226

μ/mm^{-1}	0.588
F(000)	792.0
Crystal size/mm^3	0.276 × 0.128 × 0.095
Radiation	Cu Kα (λ = 1.54184)
2Θ range for data collection/°	9.026 to 134.152
Index ranges	$-11 \leq h \leq 8$, $-12 \leq k \leq 14$, $-16 \leq l \leq 21$
Reflections collected	7406
Independent reflections	3538 [R_{int} = 0.0187, R_{sigma} = 0.0227]
Data/restraints/parameters	3538/0/369
Goodness-of-fit on F^2	1.021
Final R indexes [I>=2σ (I)]	R_1 = 0.0353, wR_2 = 0.0874
Final R indexes [all data]	R_1 = 0.0422, wR_2 = 0.0928
Largest diff. peak/hole / e $Å^{-3}$	0.17/-0.18

9. References

[1] Fier, P. S.; Maloney, K. M., *Org. Lett.* **2016**, *18*, 2244–2247.

[2] Huang, H.; Lambert, T. H., *Angew. Chem. Int. Ed.* **2021**, *60*, 11163–11167.

[3] You, S.; Zhang, R.; Cai, M., *Synthesis* **2021**, *53*, 1962–1970.

[4] Kadwa, E.; Friedrich, H.; Bala, M., *Synlett* **2019**, *30*, 44–48.

[5] Xia, S.; Gan, L.; Wang, K.; Li, Z.; Ma, D., *J. Am. Chem. Soc.* **2016**, *138*, 13493–13496.

[6] Yang, L.; Huang, Z.; Li, G.; Zhang, W.; Cao, R.; Wang, C.; Xiao, J.; Xue, D., *Angew. Chem. Int. Ed.* **2018**, *57*, 1968–1972.

[7] Zhao, D.; Wu, N.; Zhang, S.; Xi, P.; Su, X.; Lan, J.; You, J., *Angew. Chem. Int. Ed.* **2009**, *48*, 8729–8732.

[8] Zhu, C.; Wang, R.; Falck, J. R., *Org. Lett.* **2012**, *14*, 3494–3497.

[9] Zou, Y.-Q.; Chen, J.-R.; Liu, X.-P.; Lu, L.-Q.; Davis, R. L.; Jørgensen, K. A.; Xiao, W.-J., *Angew. Chem. Int. Ed.* **2012**, *51*, 784–788.

[10] Cheung, C. W.; Buchwald, S. L., *J. Org. Chem.* **2014**, *79*, 5351–5358.

[11] Schimler, S.; Sanford, M., *Synlett* **2016**, *27*, 2279–2284.

[12] Schimler, S. D.; Cismesia, M. A.; Hanley, P. S.; Froese, R. D. J.; Jansma, M. J.; Bland, D. C.; Sanford, M. S., *J. Am. Chem. Soc.* **2017**, *139*, 1452–1455.

[13] Benesi, H. A.; Hildebrand, J. H., *J. Am. Chem. Soc.* **1949**, *71*, 2703–2707.

[14] Neese, F., *Comput. Mol. Sci.* **2012**, *2*, 73.

[15] Najibi, A.; Goerigk, L., *J. Chem. Theory Comput.* **2018**, *14*, 5725–5738.

[16] Zheng, J.; Xu, X.; Truhlar, D. G., *Theor. Chem. Acc.* **2011**, *128*, 295–305.

[17] (a) Barone, V.; Cossi, M., *J. Phys. Chem. A* **1998**, *102*, 1995–2001. (b) Cossi, M.; Rega, N.; Scalmani, G.; Barone, V., *J. Comput. Chem.* **2003**, *24*, 669–681.

[18] ChemCraft 1.8, https://www.chemcraftprog.com.

[19] Cardinale, A.; Isse, A. A.; Gennaro, A.; Robert, M.; Savéant, J.-M., *J. Am. Chem. Soc.* **2002**, *124*, 13533–13539.

[20] Ryu, H.; Park, J.; Kim, H. K.; Park, J. Y.; Kim, S.-T.; Baik, M.-H., *Organometallics* **2018**, *37*, 3228–3239.

[21] Roth, H.; Romero, N.; Nicewicz, D., *Synlett* **2015**, *27*, 714–723.

[22] Isse, A. A.; Gennaro, A., *J. Phys. Chem. B* **2010**, *114*, 7894–7899.

[23] Rohrbach, S.; Murphy, J. A.; Tuttle, T., *J. Am. Chem. Soc.* **2020**, *142*, 14871–14876.

[24] Senaweera, S.; Weaver, J. D., *Chem. Commun.* **2017**, *53*, 7545–7548.

[25] CrysAlisPro, Oxford Diffraction Ltd.

[26] Empirical absorption correction using spherical harmonics, implemented in SCALE3 ABSPACK scaling algorithm within CrysAlisPro software, Oxford Diffraction Ltd.

[27] "Olex2" crystallography software, *J. Appl. Cryst.* **2009**, *42*, 339–341.

[28] SHELXT – Integrated space-group and crystal-structure determination G. M. Sheldrick, *Acta Cryst.* **2015**, iA71, 3–8.

[29] "Crystal structure refinement with SHELXL" G.M. Sheldrick, *Acta Cryst.* **2015**, *C71*, 3–8.

10. NMR Spectral Data

^{1}H NMR of (*E*)-1-methyl-1H-pyrrole-2-carboxaldehyde oxime (9d)

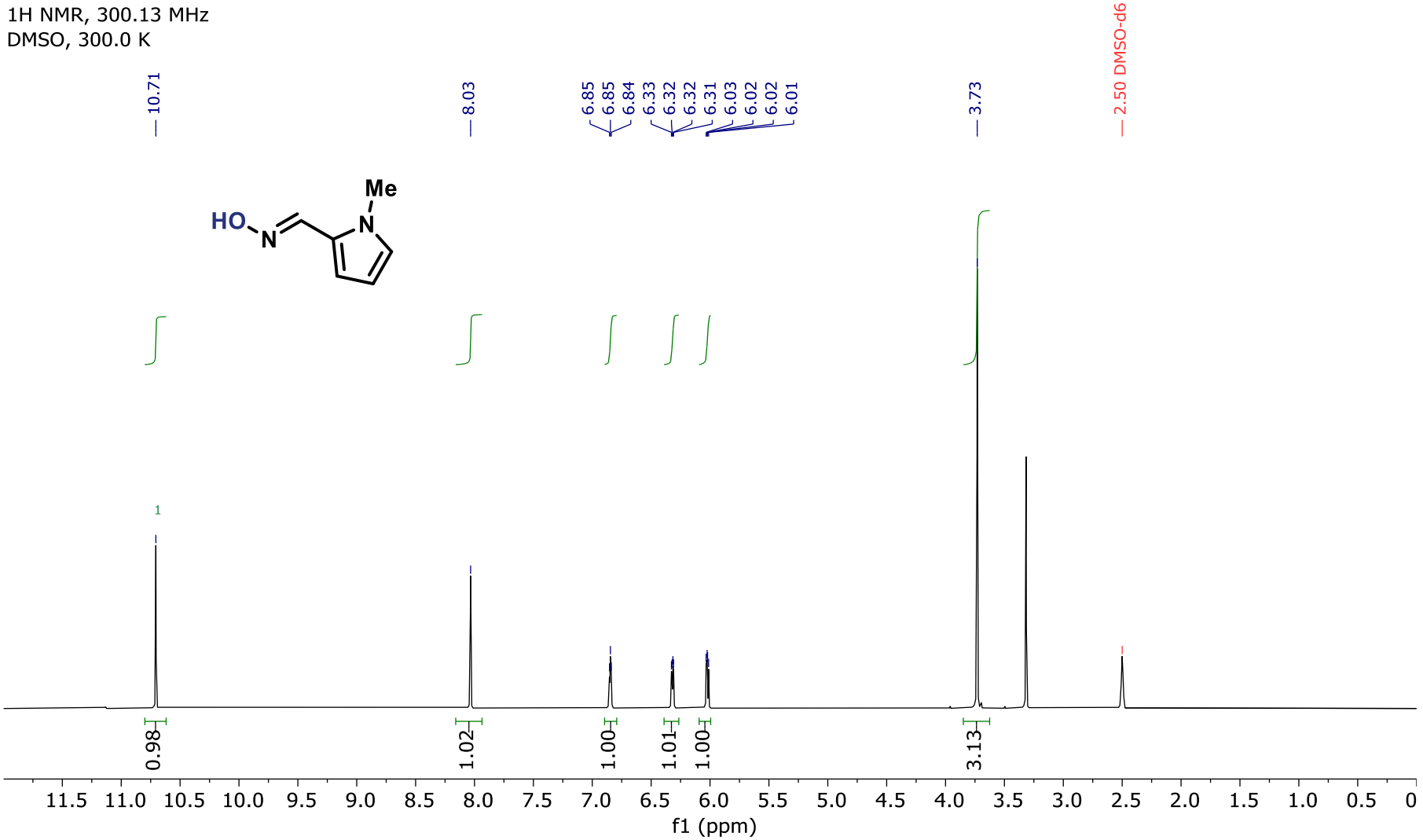

^{13}C NMR of (*E*)-1-methyl-1H-pyrrole-2-carboxaldehyde oxime (9d)

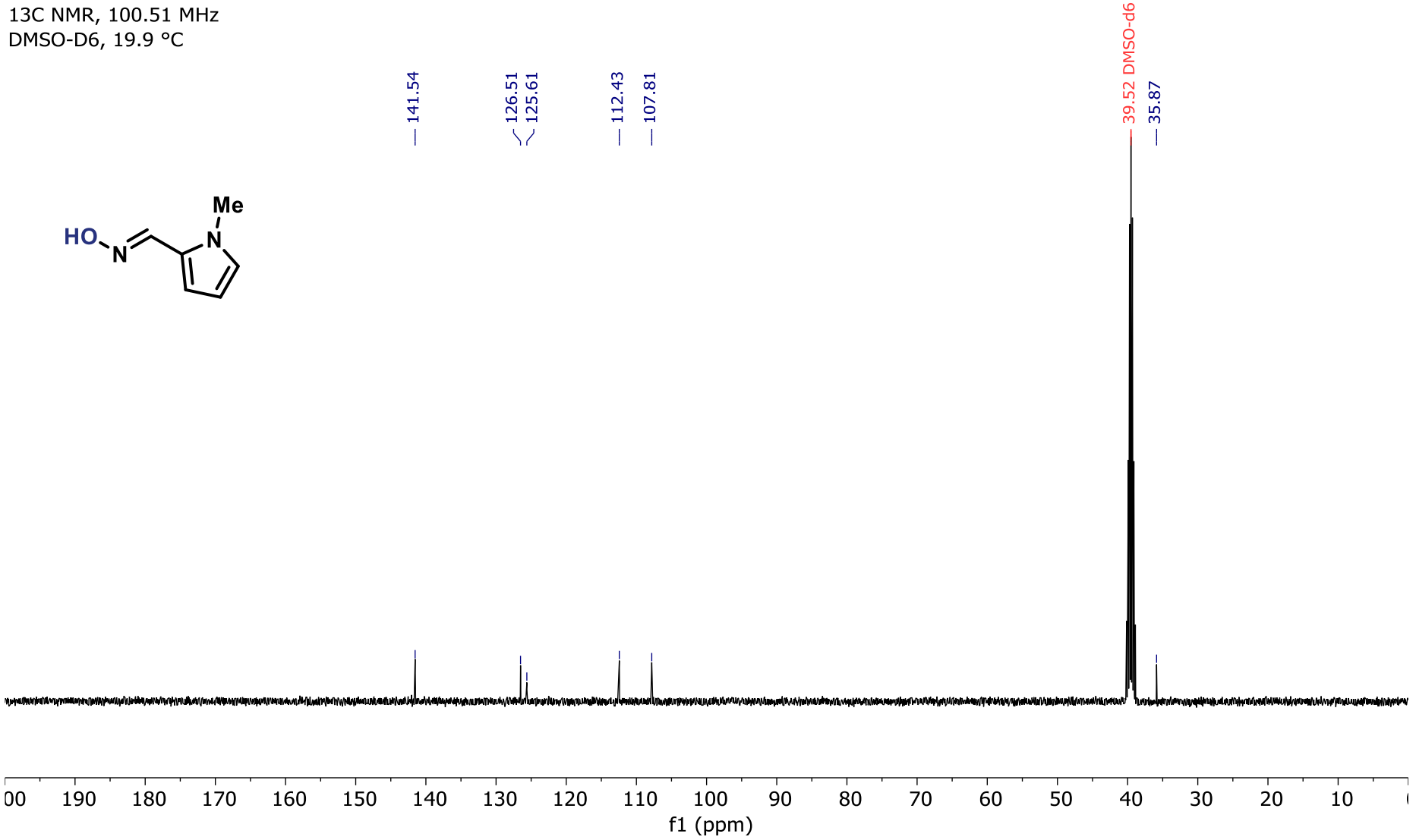

^{1}H NMR of 4′-hydroxyacetophenone (8a)

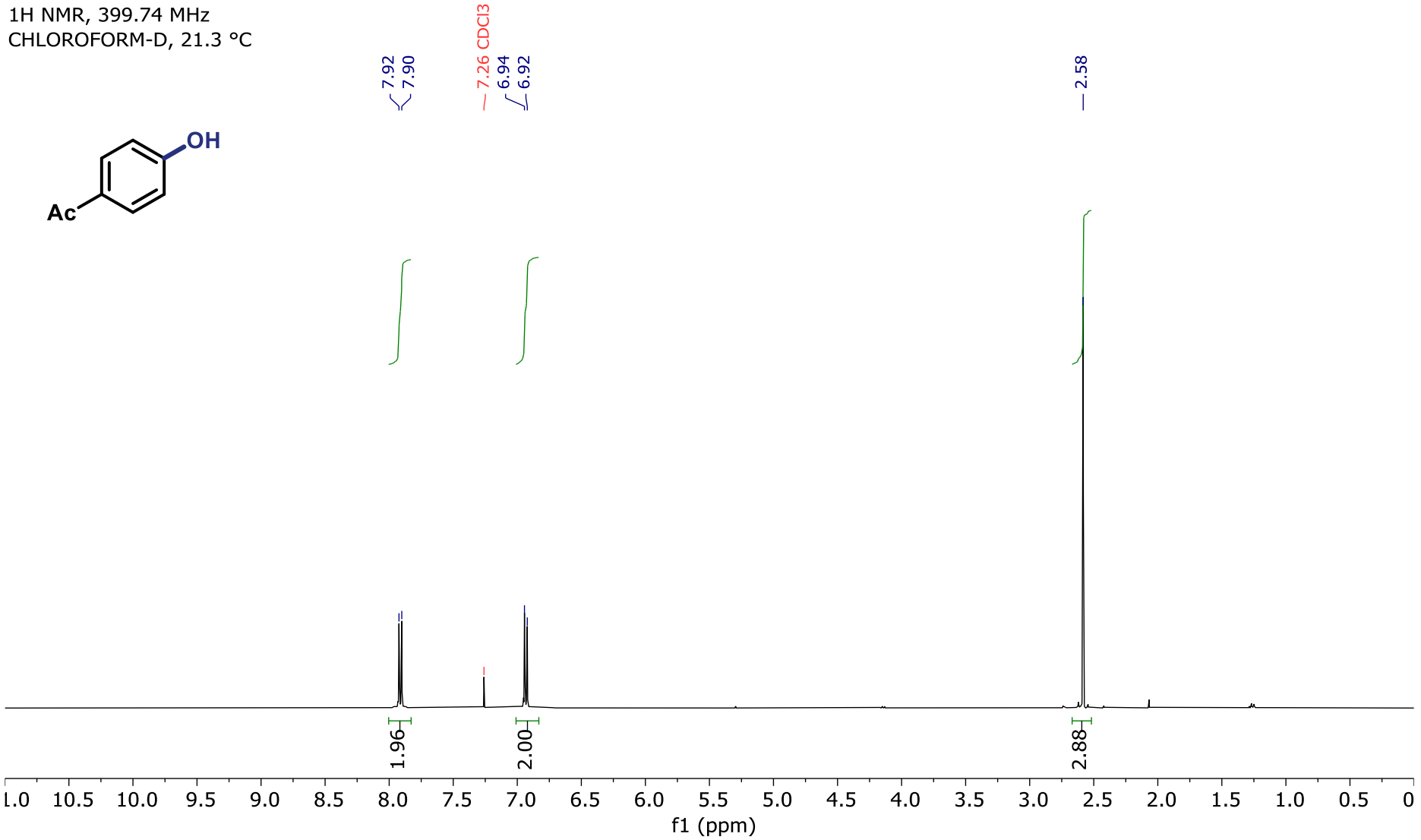

^{13}C NMR of 4′-hydroxyacetophenone (8a)

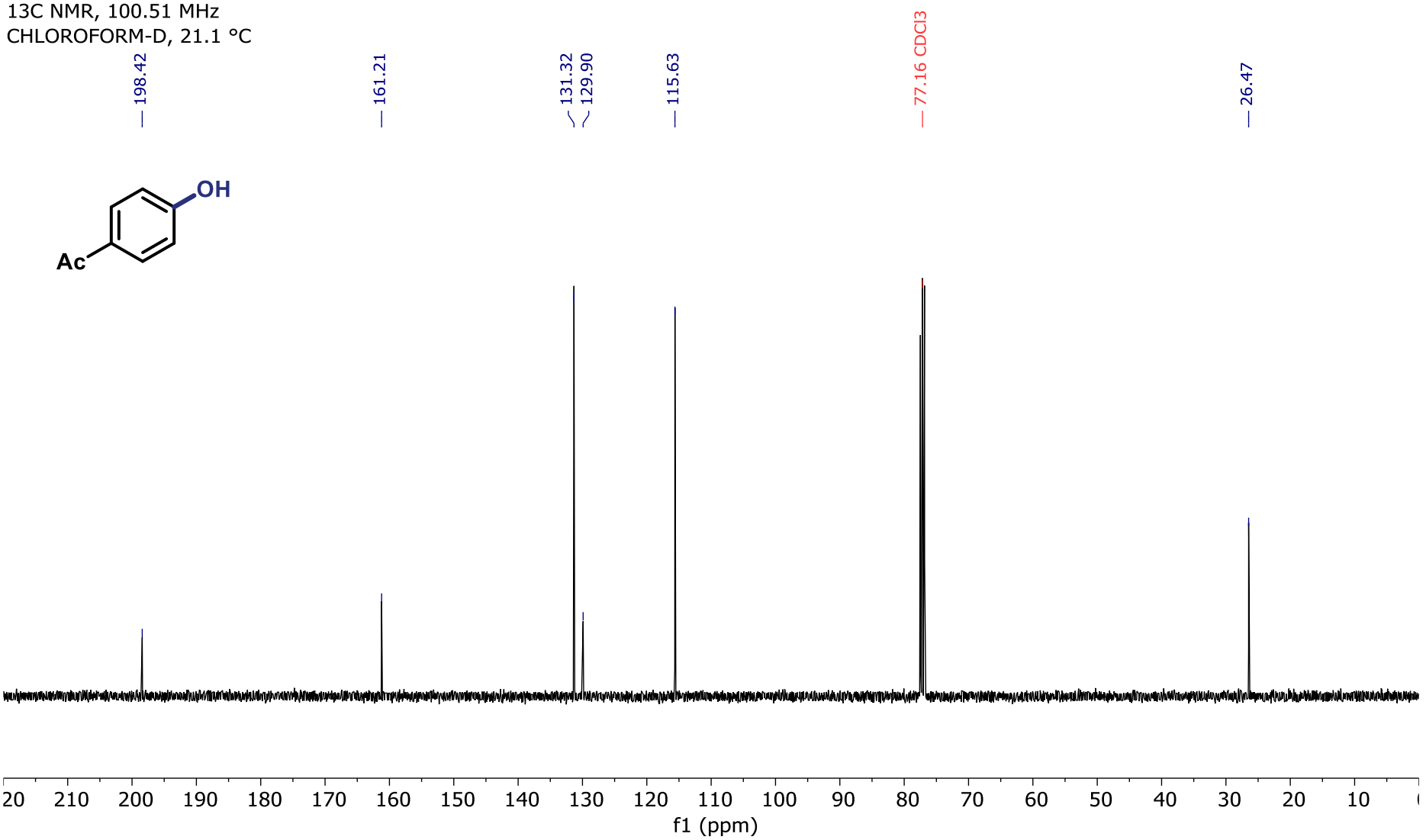

^{1}H NMR of 4′-hydroxybenzophenone (8b)

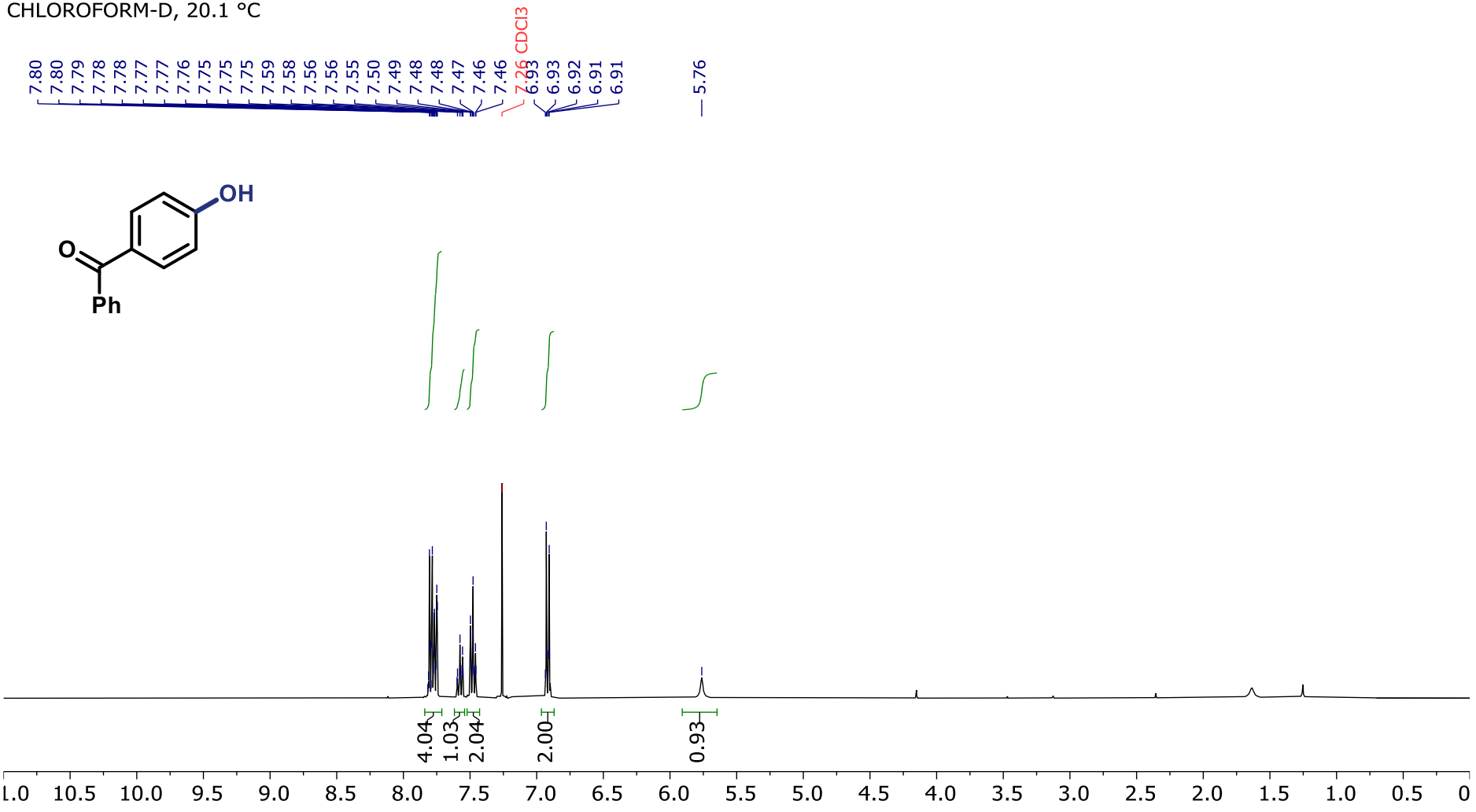

^{13}C NMR of 4′-hydroxybenzophenone (8b)

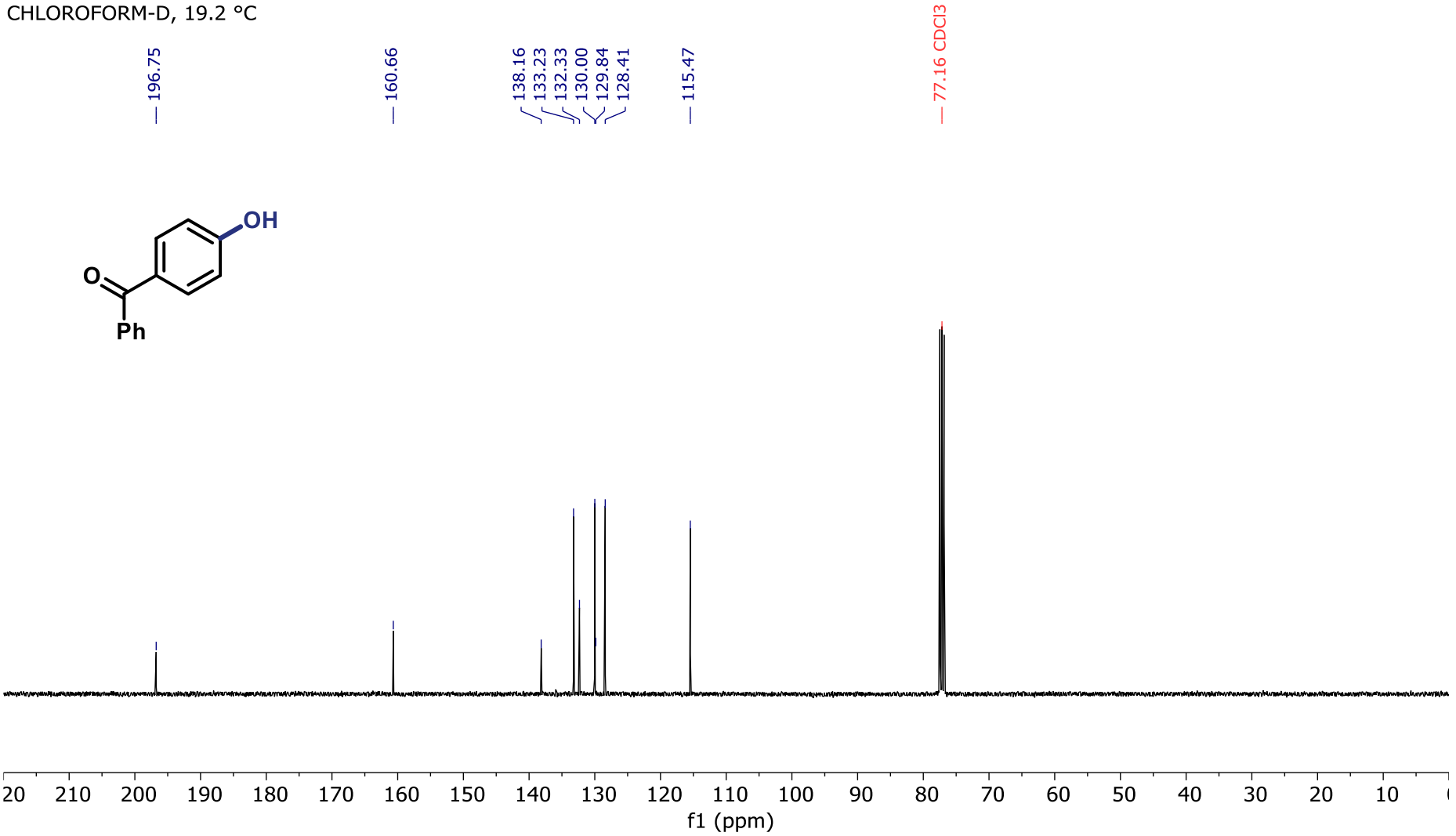

^{1}H NMR of ethyl 4-hydroxybenzoate (8c)

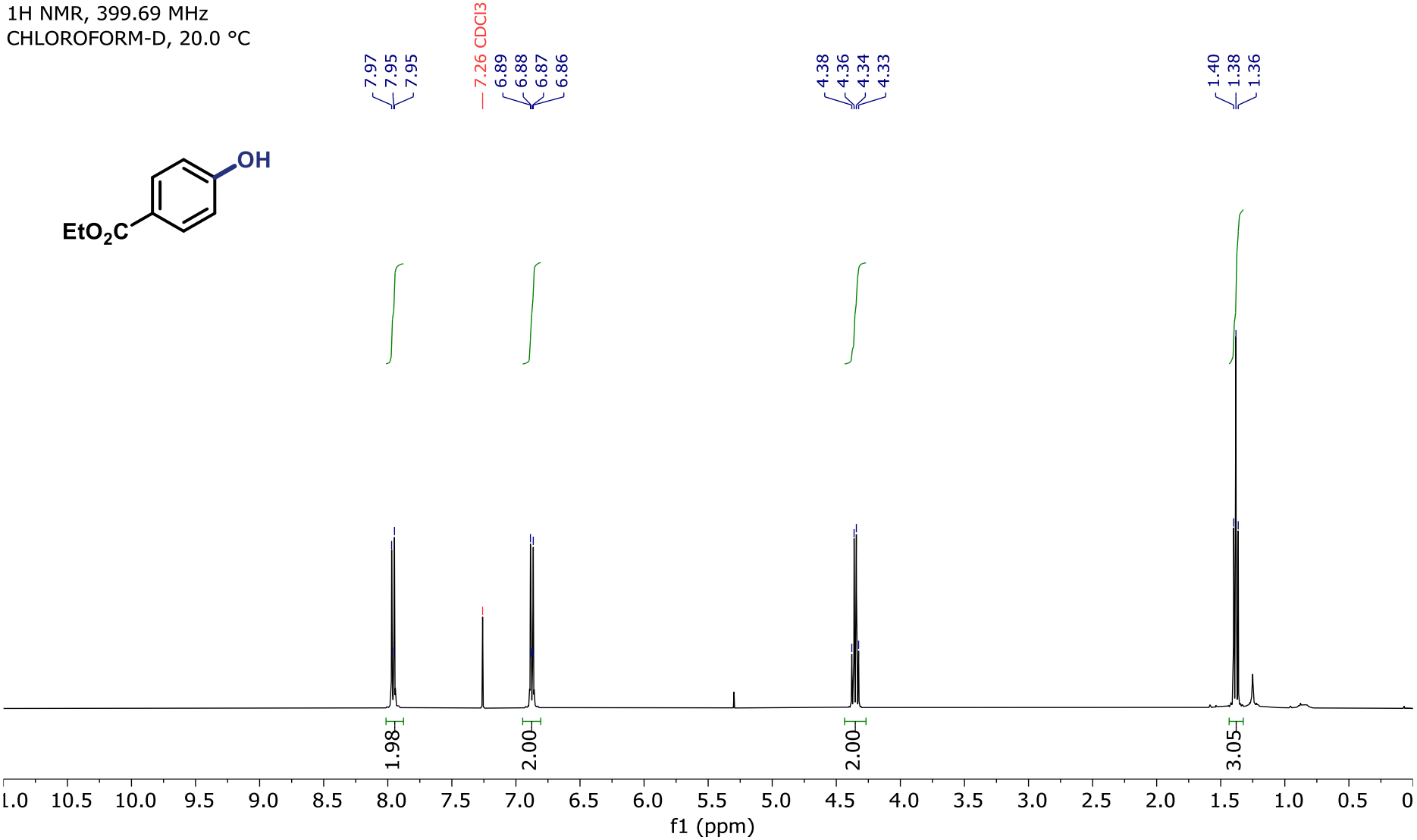

^{13}C NMR of ethyl 4-hydroxybenzoate (8c)

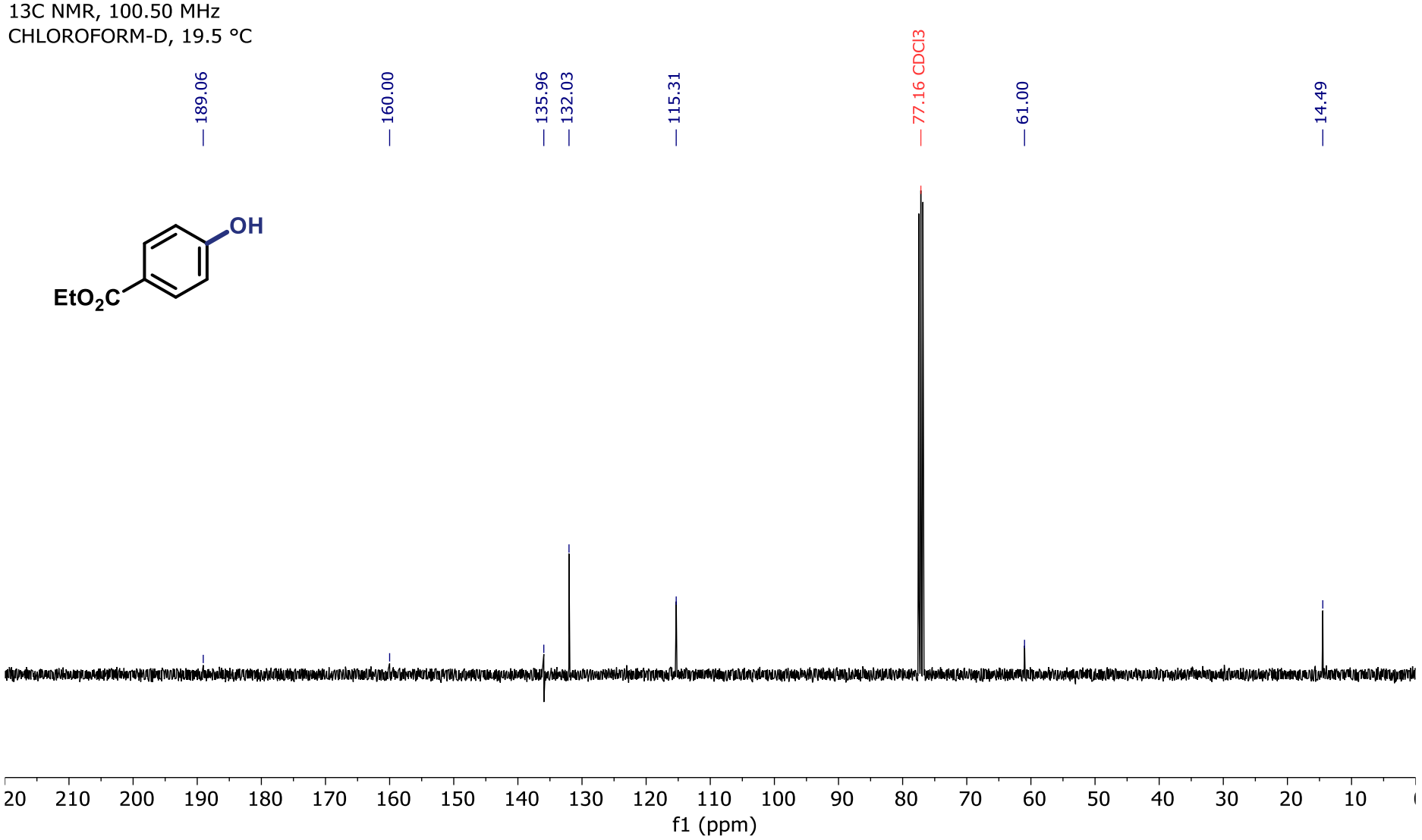

^{1}H NMR of 4-hydroxybenzaldehyde (8d)

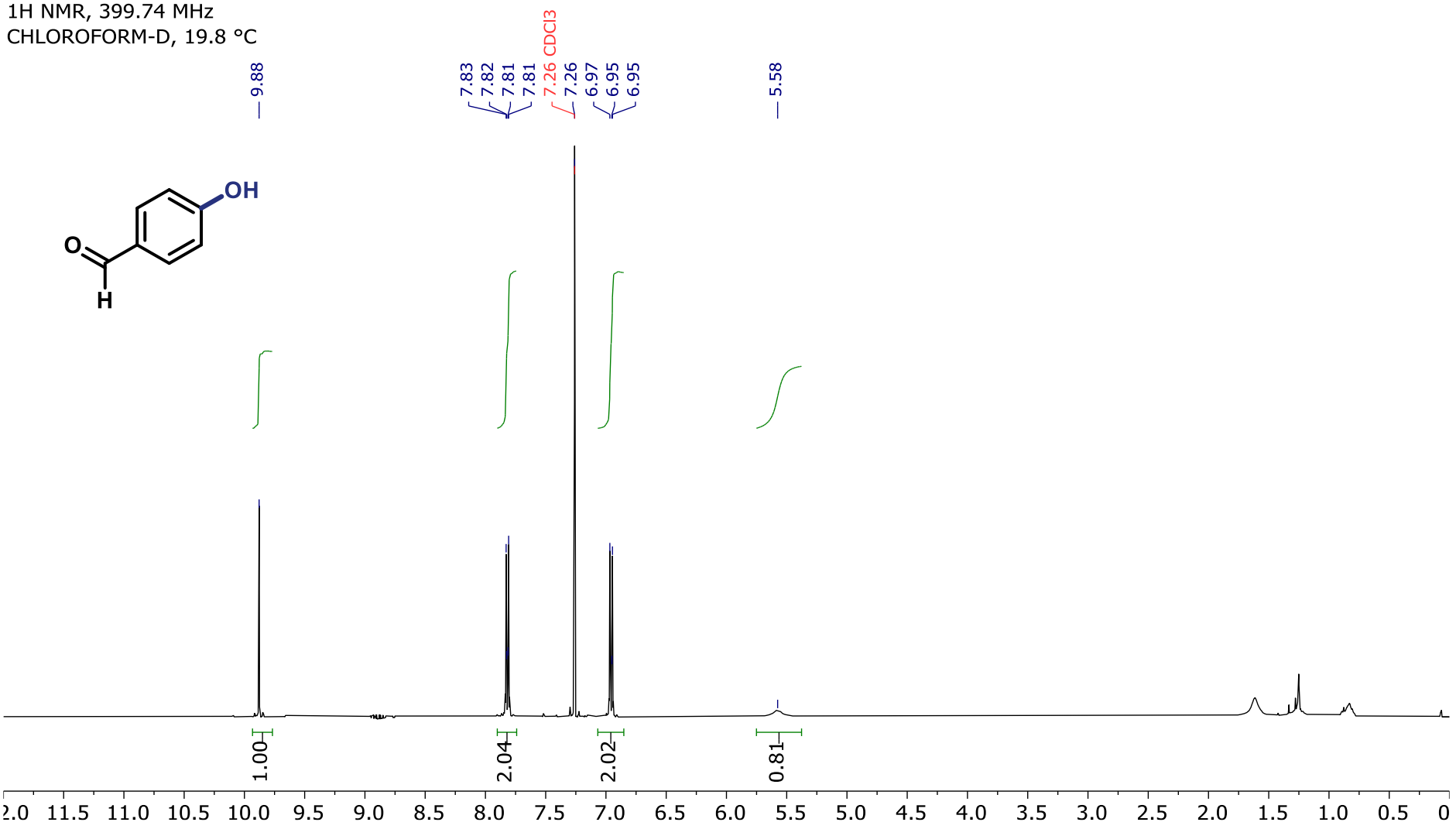

^{13}C NMR of 4-hydroxybenzaldehyde (8d)

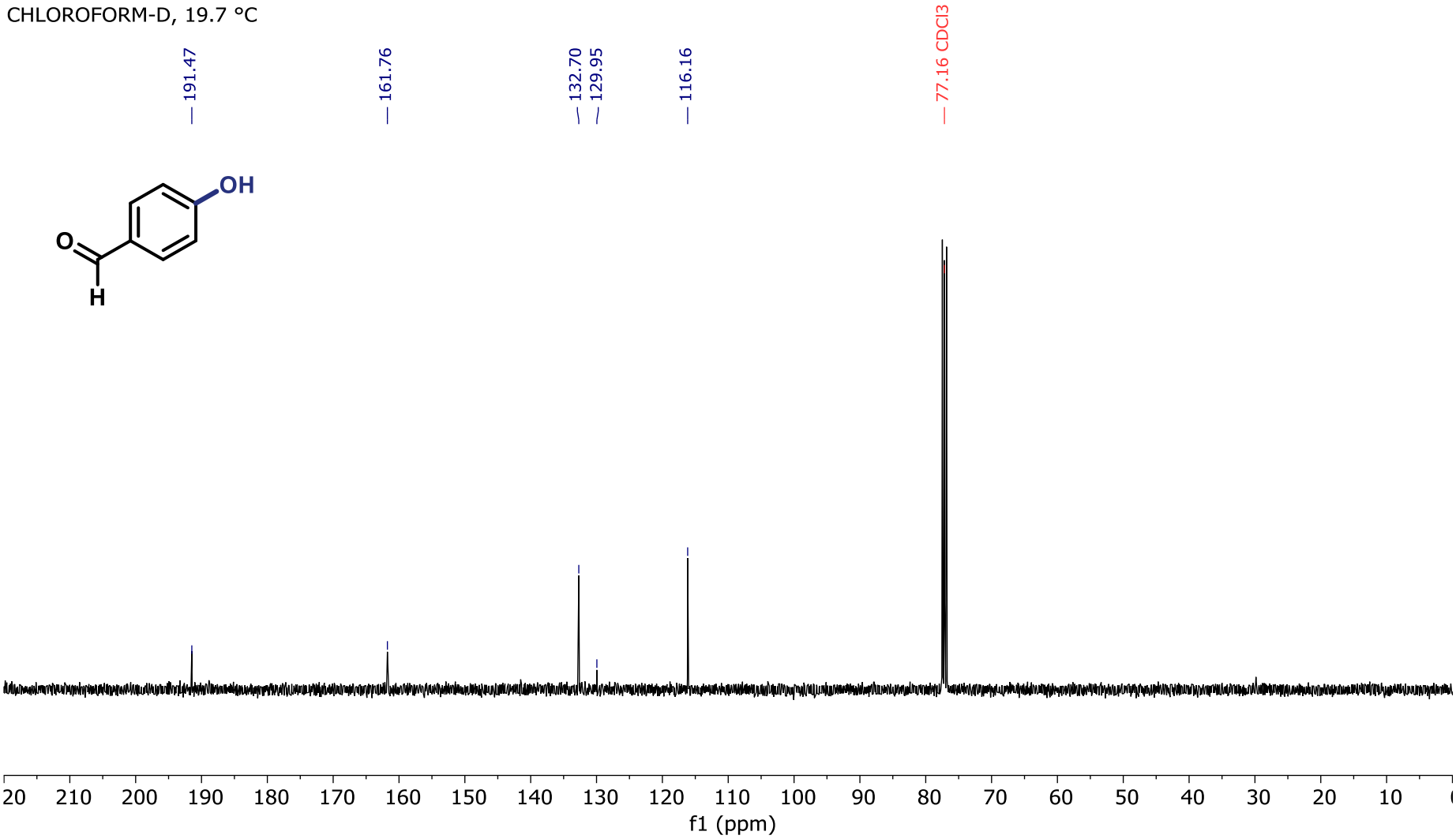

^{1}H NMR of 2-hydroxybenzaldehyde (8e)

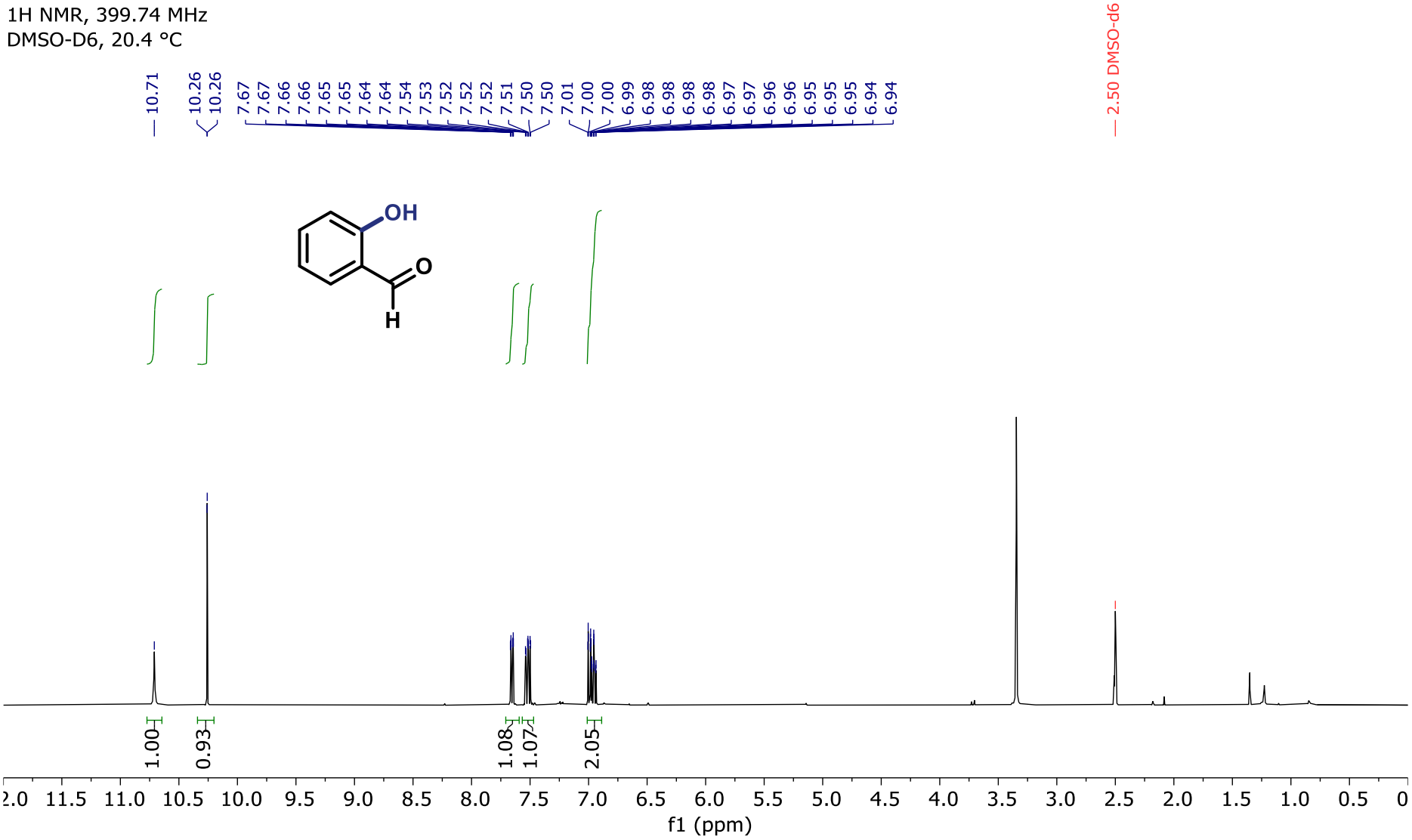

^{13}C NMR of 2-hydroxybenzaldehyde (8e)

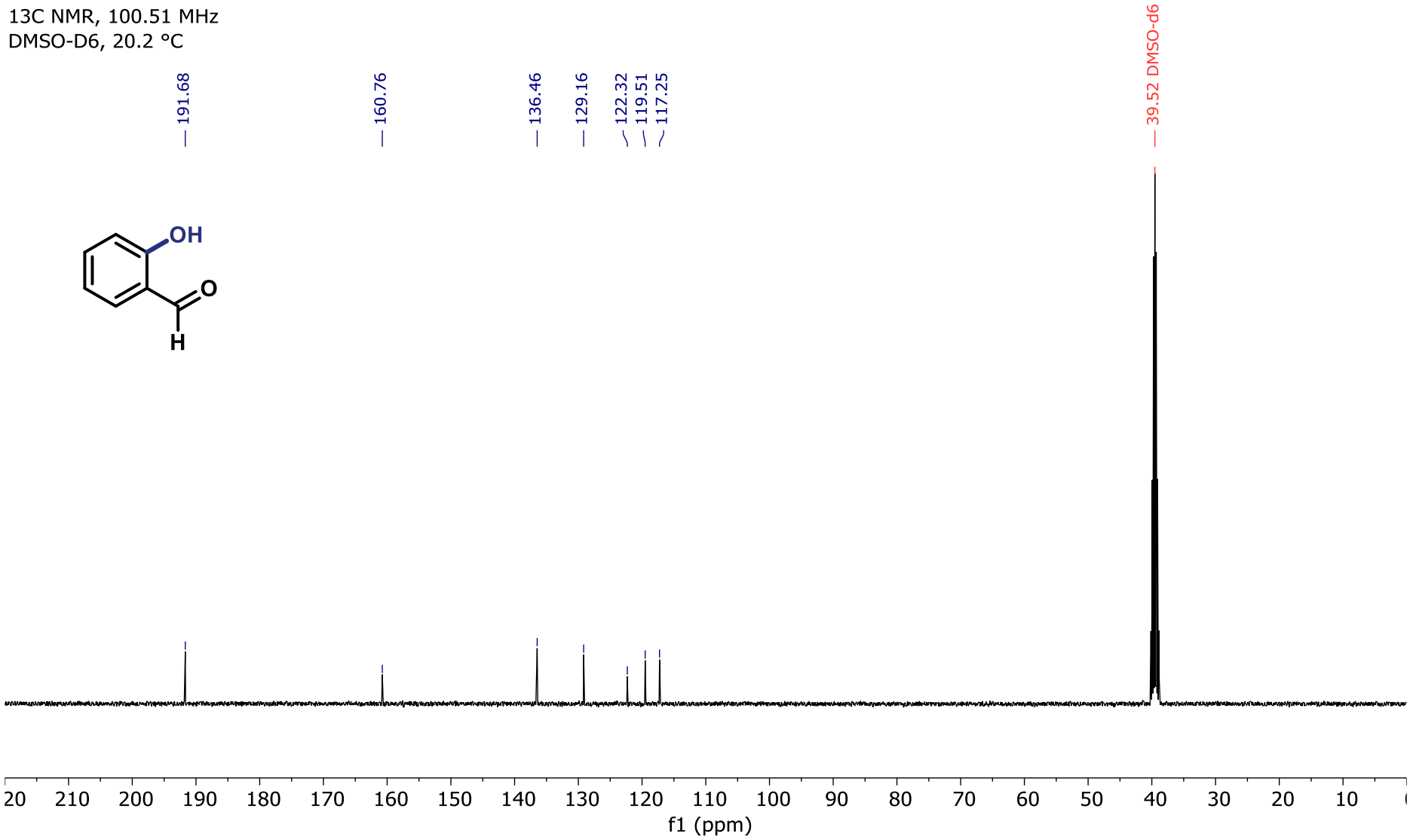

^{1}H NMR used to determine the yield of 2-hydroxybenzaldehyde (8e)

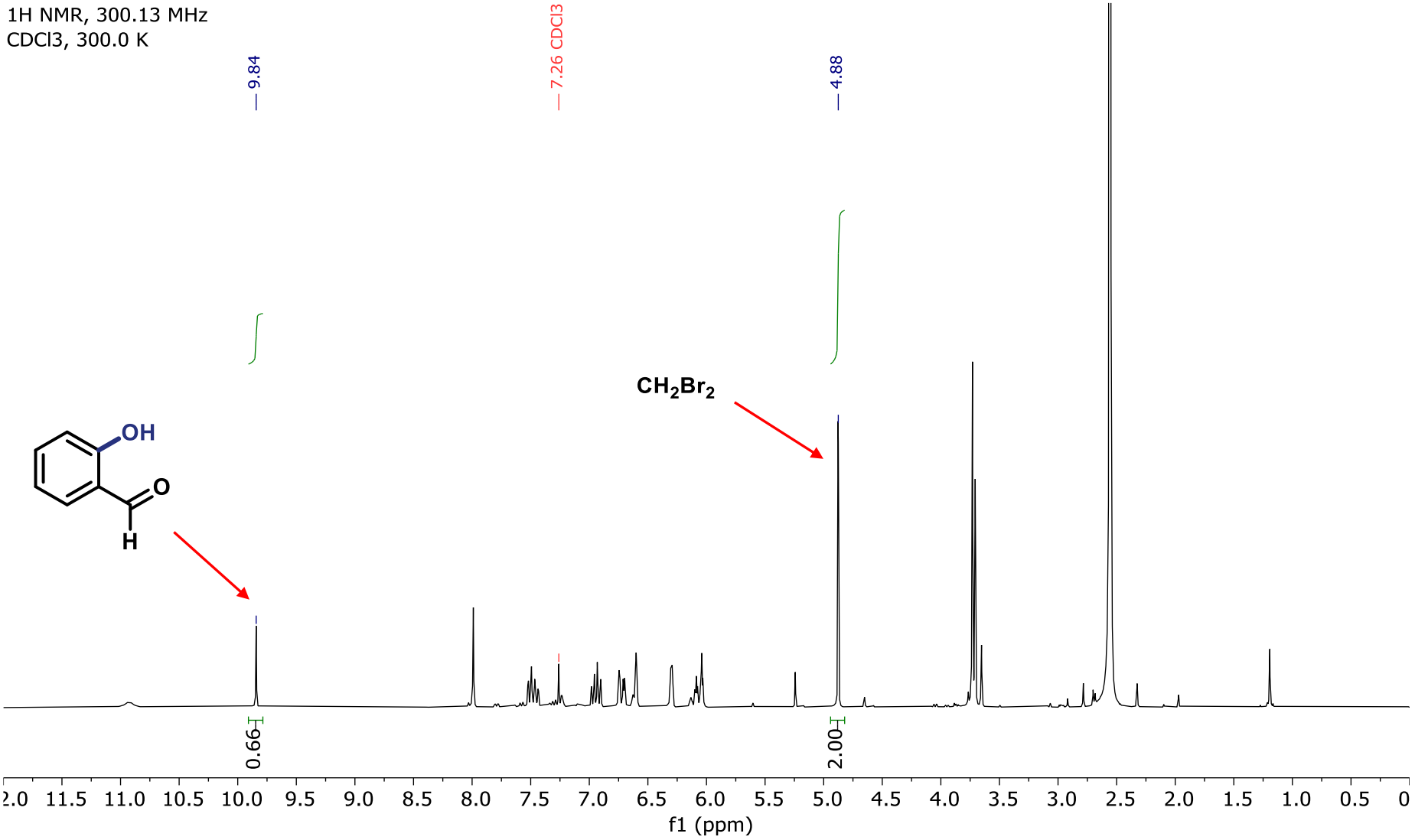

^{1}H NMR of 3'-hydroxyacetophenone (8f)

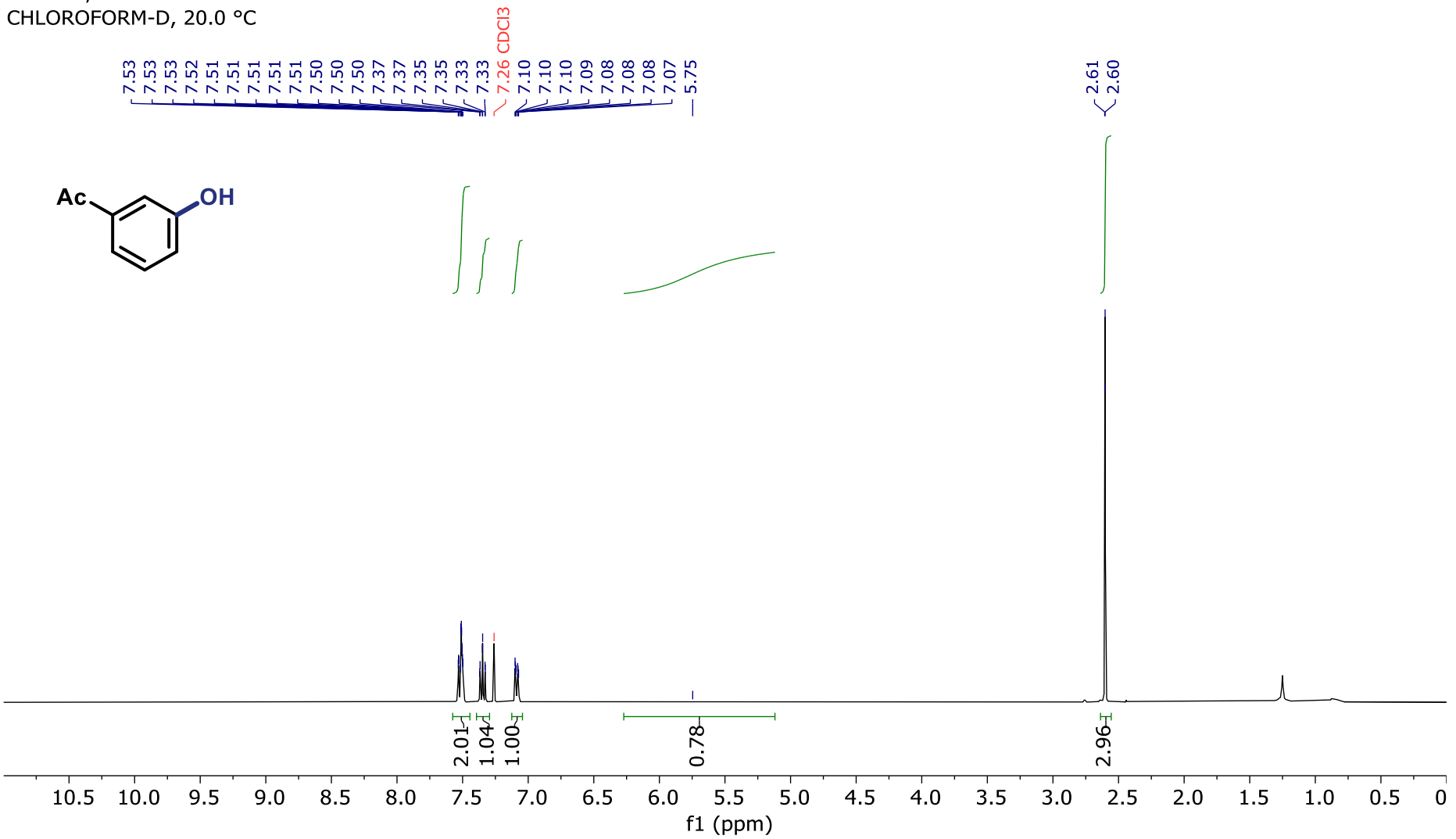

^{13}C NMR of 3'-hydroxyacetophenone (8f)

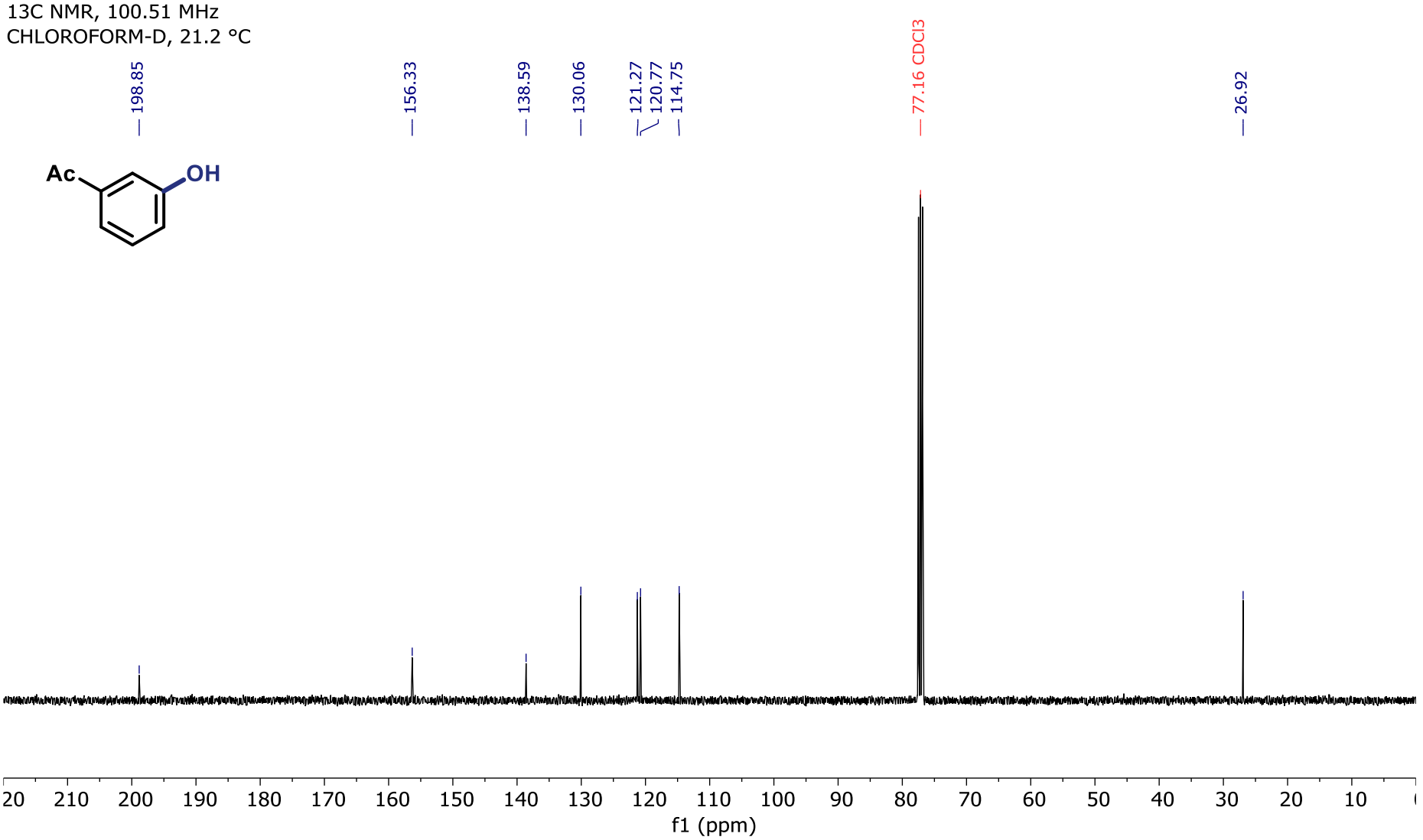

^{1}H NMR of 4-hydroxybenzonitrile (8g)

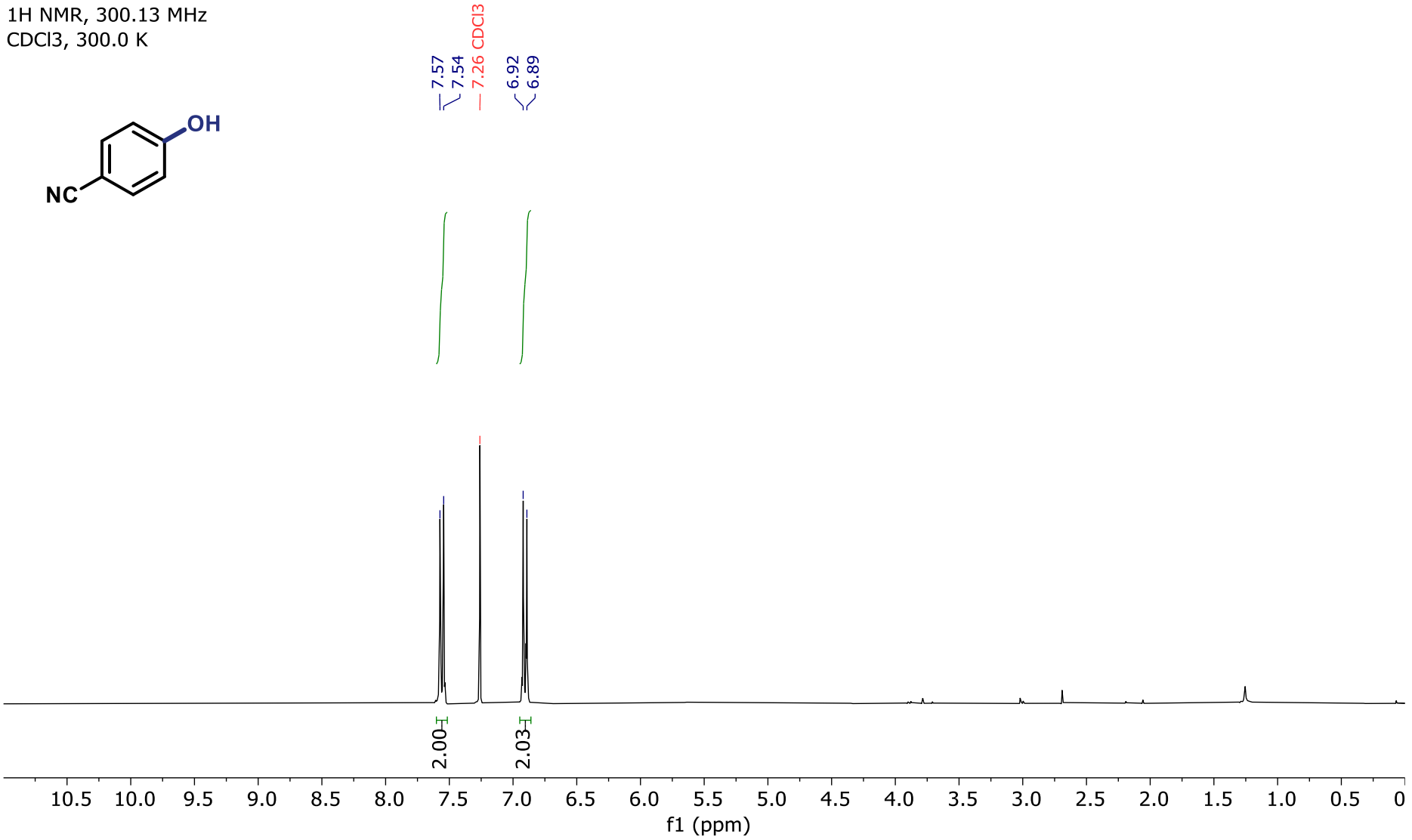

^{13}C NMR of 4-hydroxybenzonitrile (8g)

13C NMR, 100.51 MHz
CHLOROFORM-D, 20.6 °C

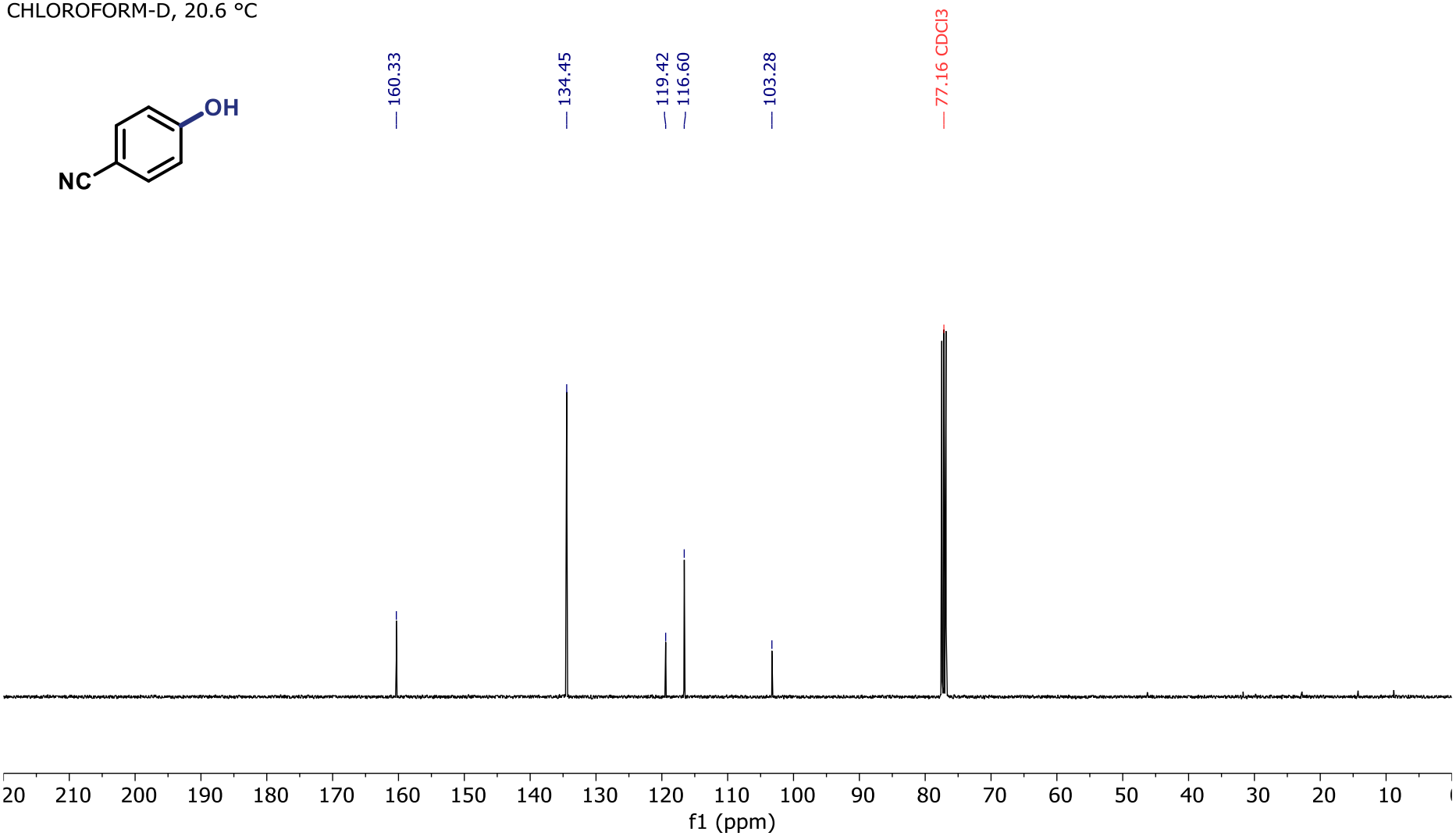

^{1}H NMR of 3-hydroxybenzonitrile (8h)

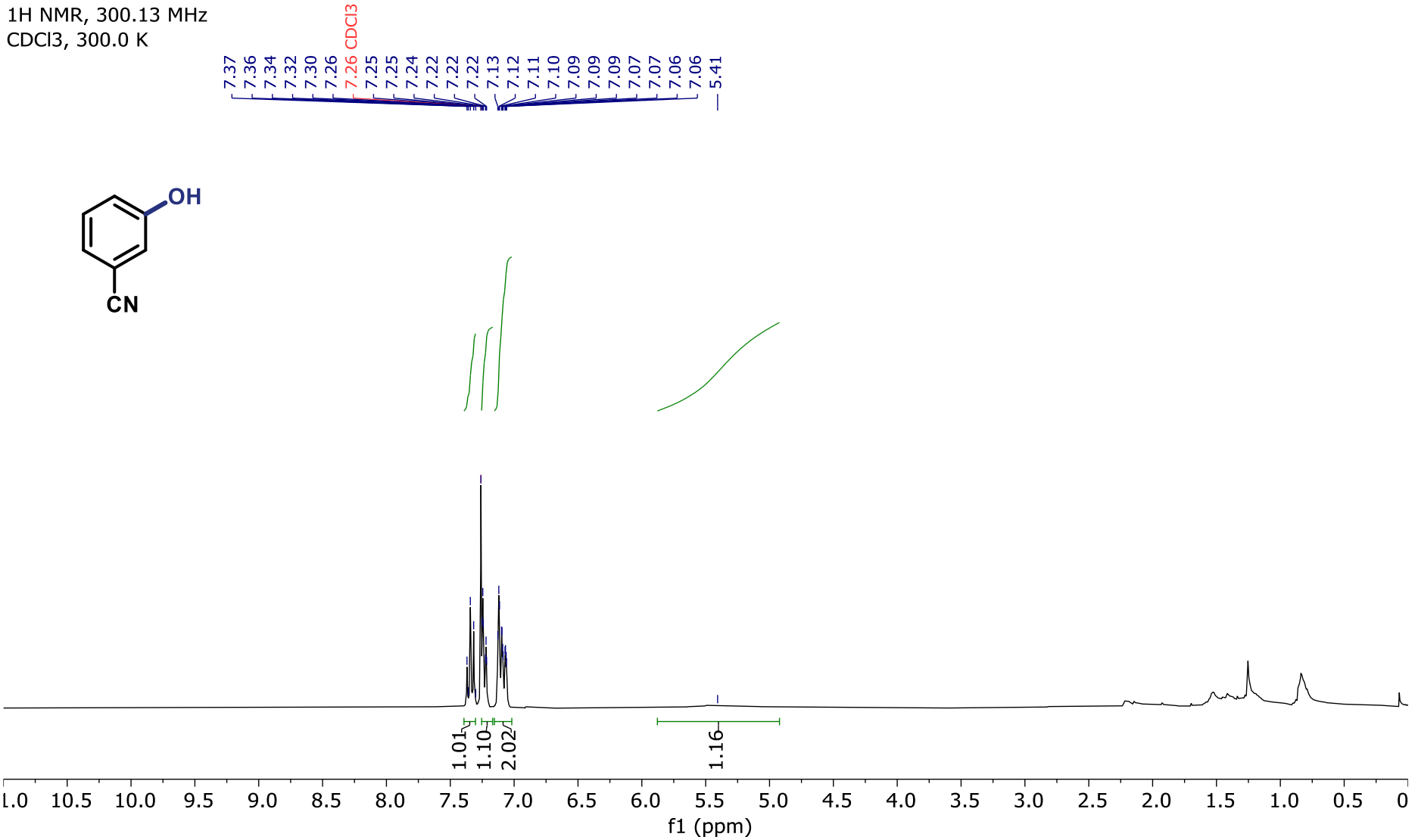

^{13}C NMR of 3-hydroxybenzonitrile (8h)

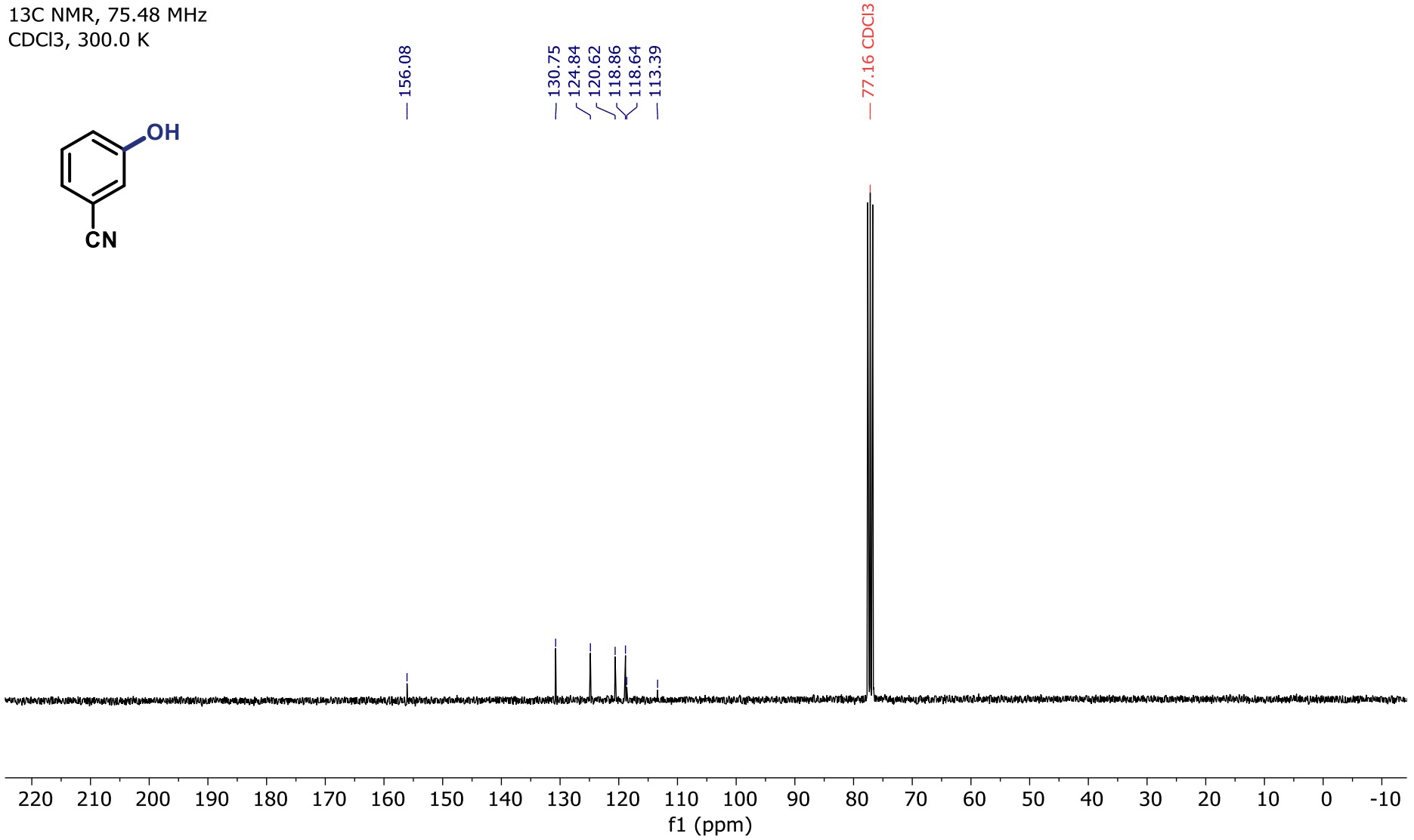

^{1}H NMR of 4-(methylsulfonyl)phenol (8i)

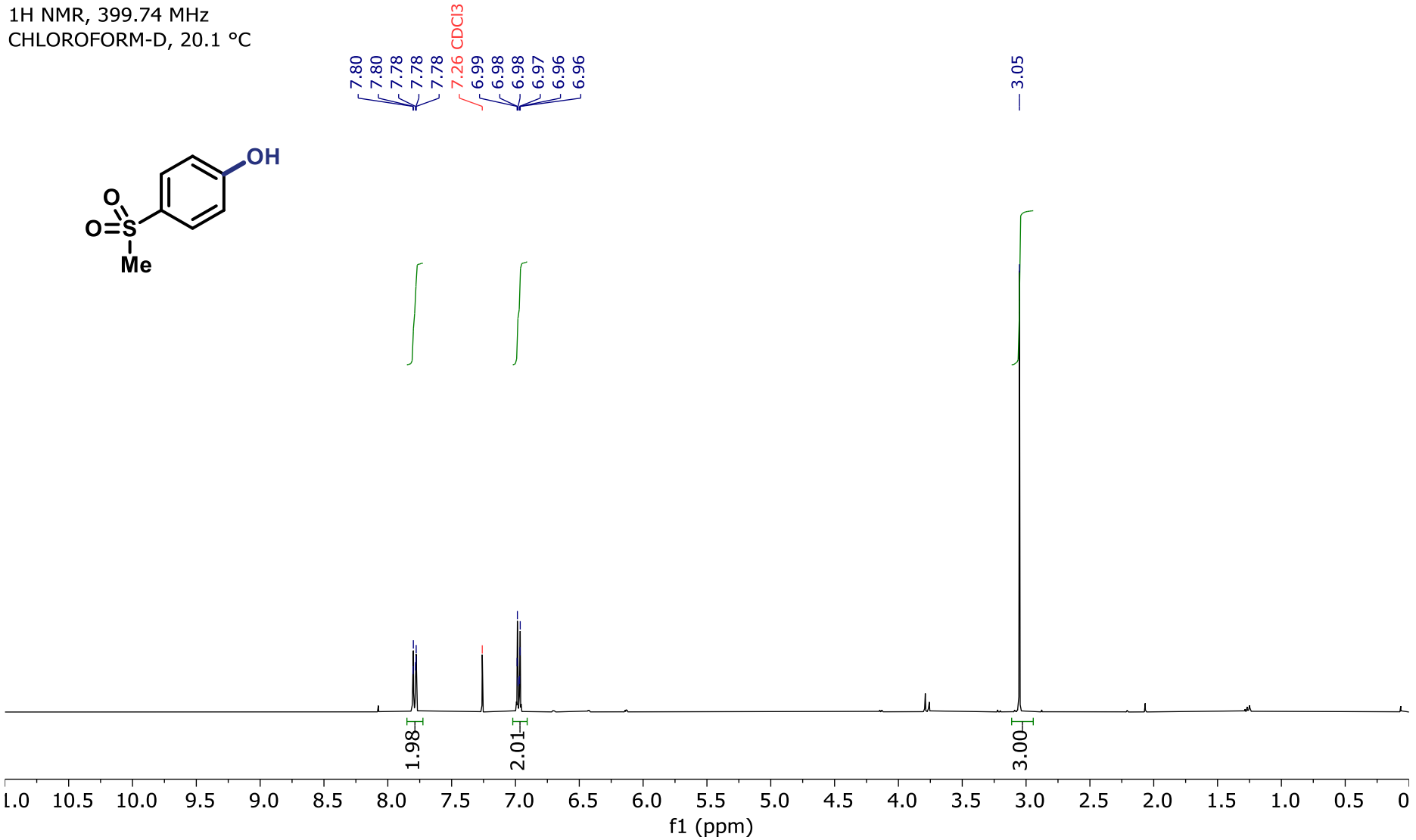

^{13}C NMR of 4-(methylsulfonyl)phenol (8i)

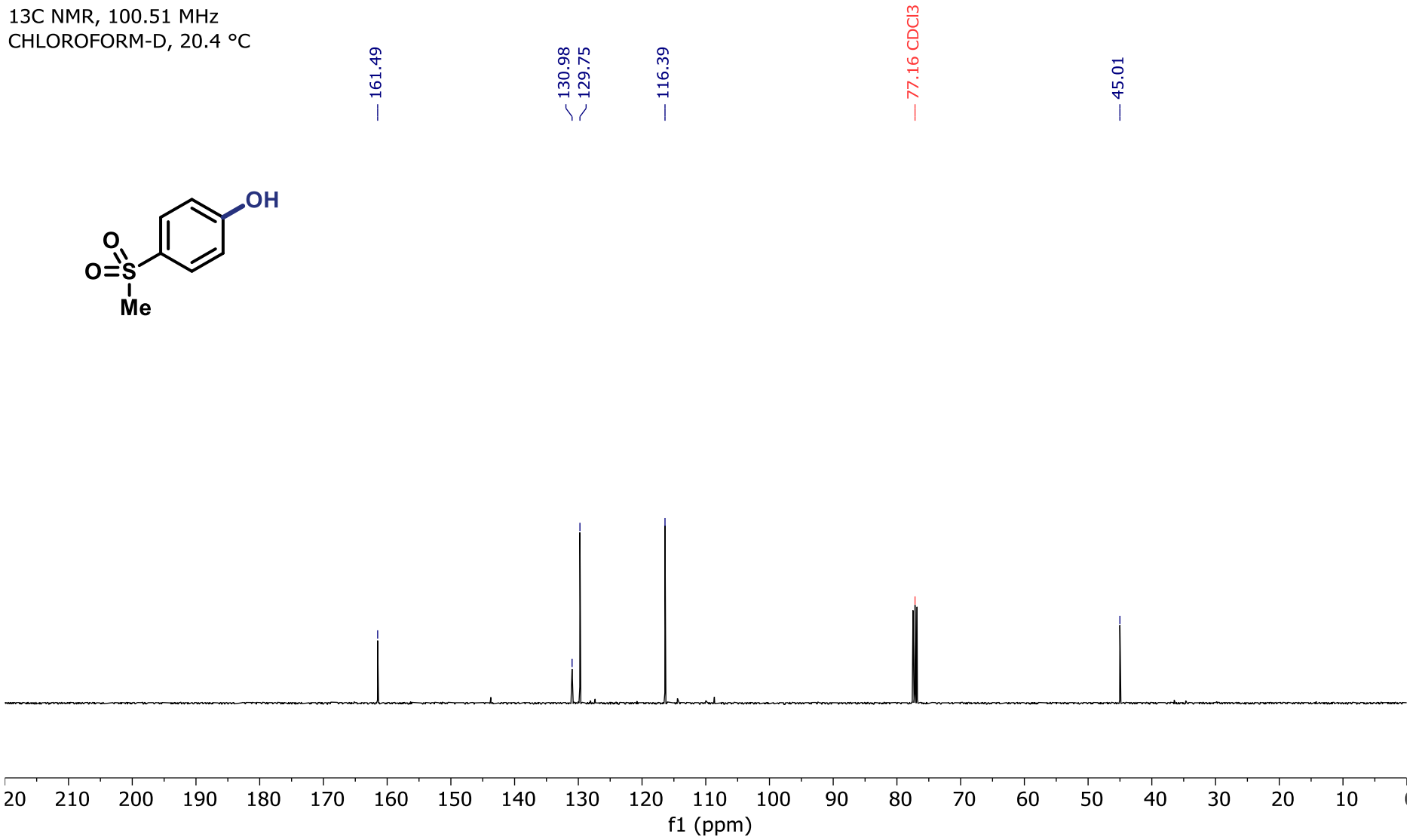

^{1}H NMR of 3-(methylsulfonyl)phenol (8j)

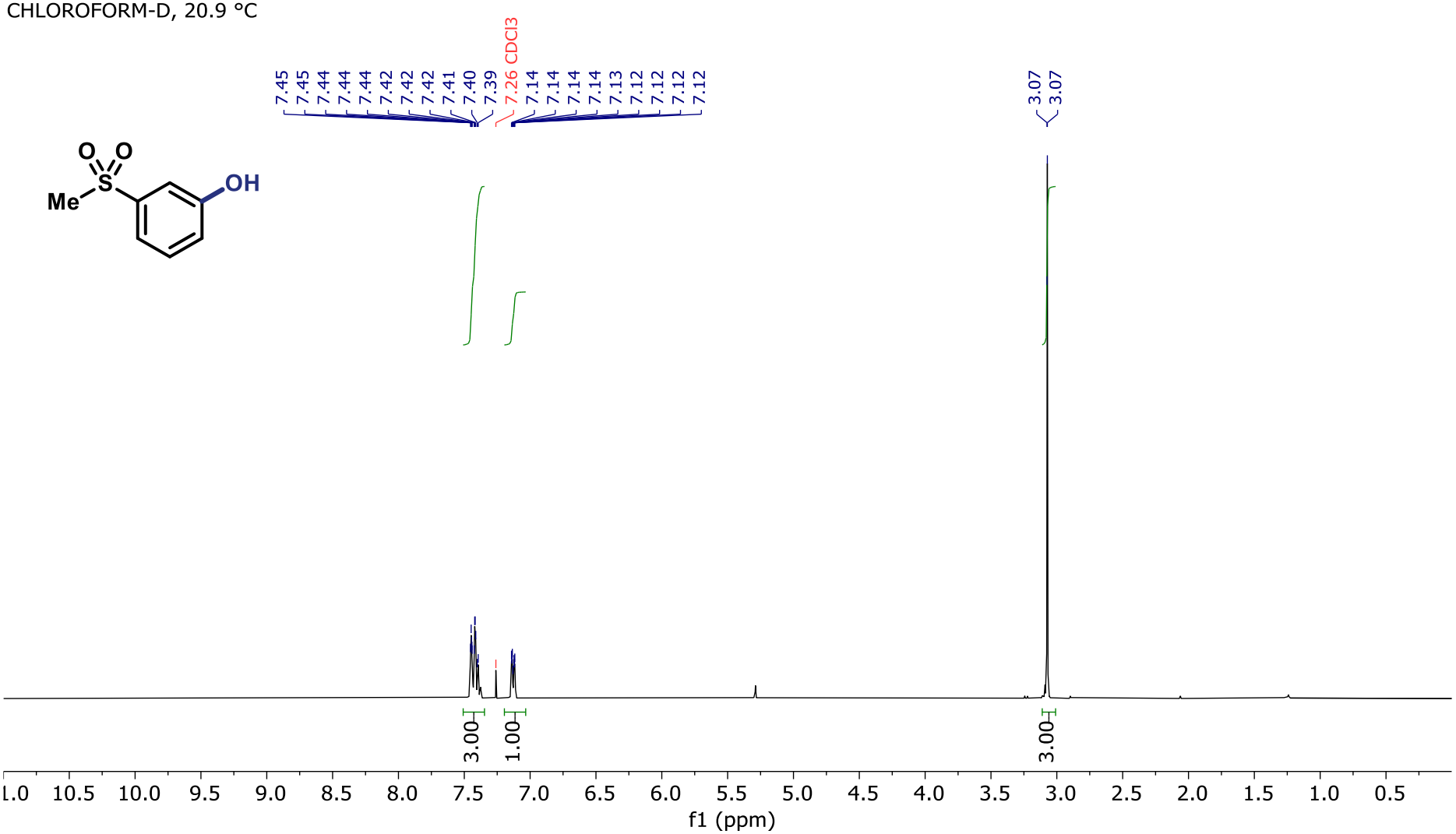

^{13}C NMR of 3-(methylsulfonyl)phenol (8j)

13C NMR, 100.51 MHz
CHLOROFORM-D, 21.2 °C

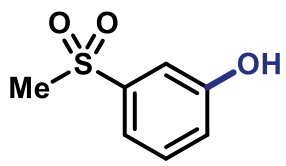

^{1}H NMR of 3,5-bis(trifluoromethyl)phenol (8k)

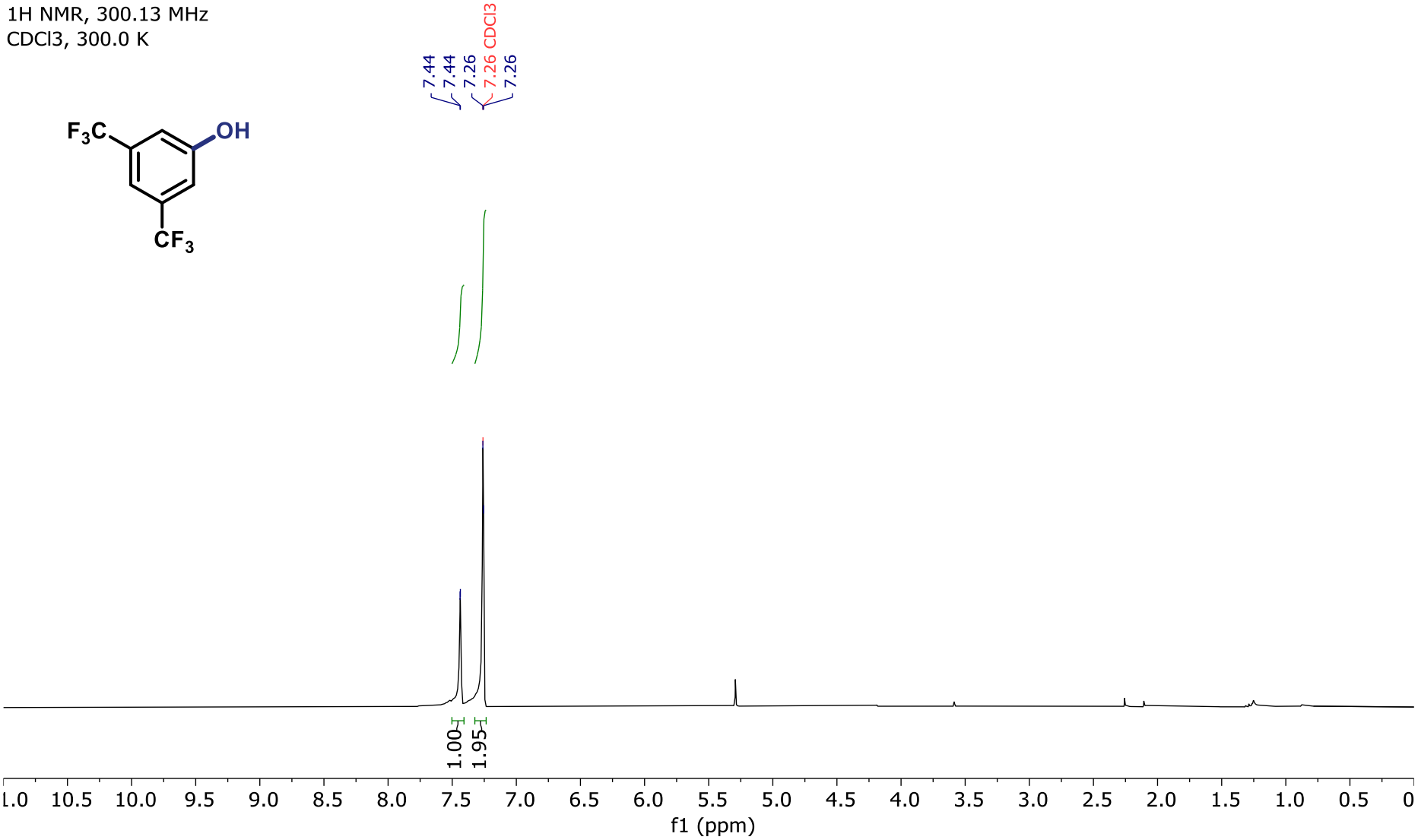

^{19}F NMR of 3,5-bis(trifluoromethyl)phenol (8k)

19F NMR, 282.40 MHz
CDCl3, 300.0 °C

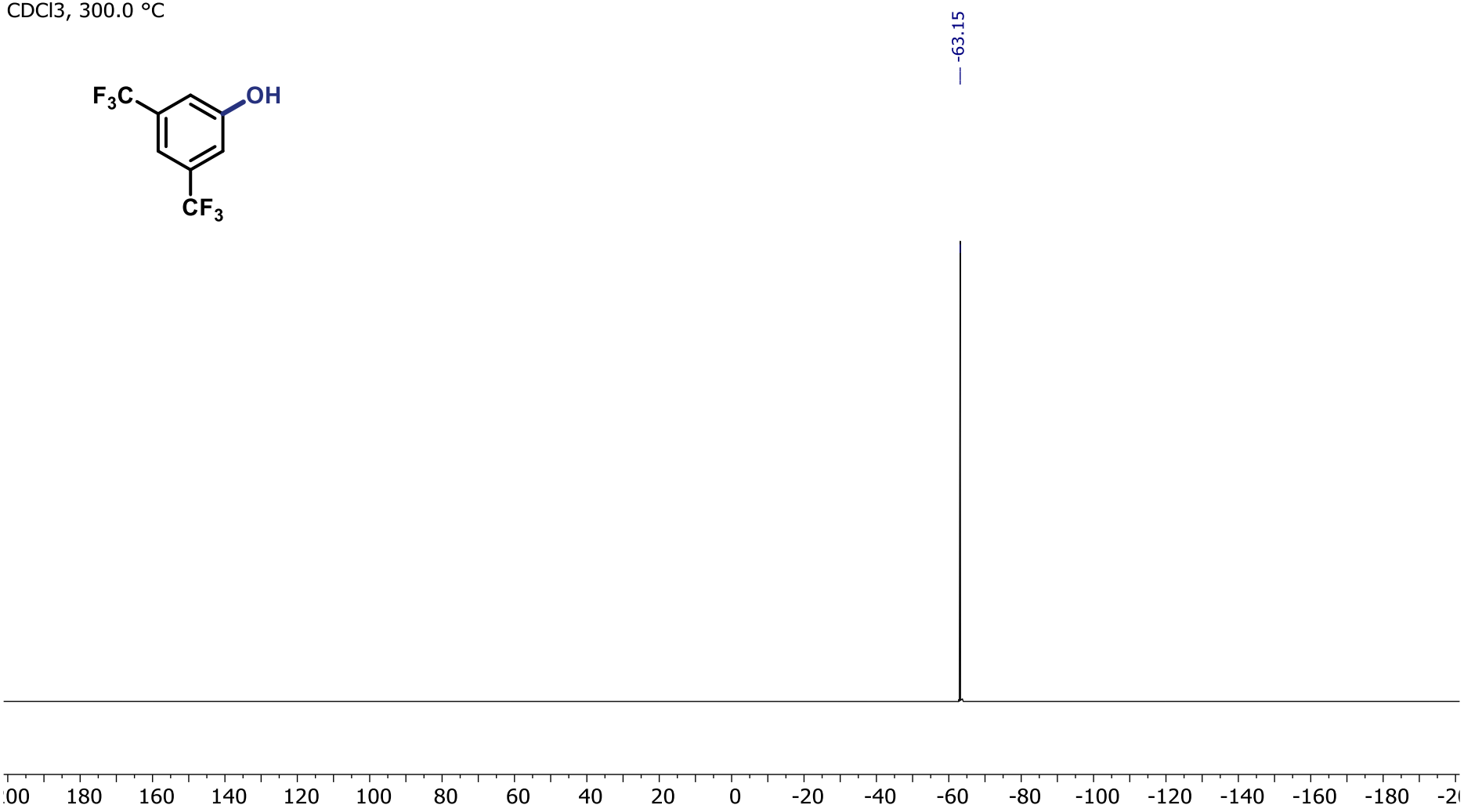

^{1}H NMR of 4-hydroxybenzotrifluoride (8l)

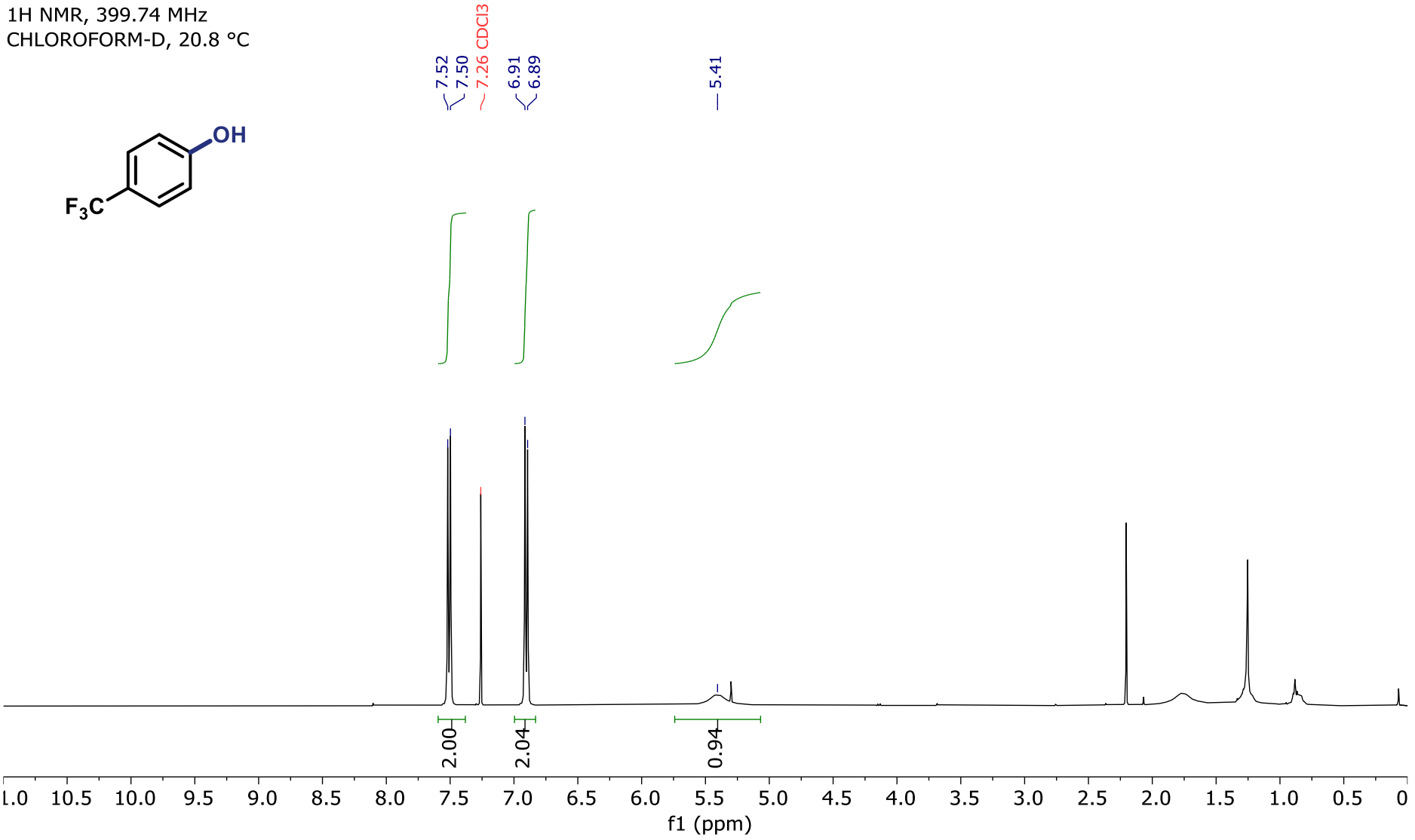

^{19}F NMR of 4-hydroxybenzotrifluoride (8l)

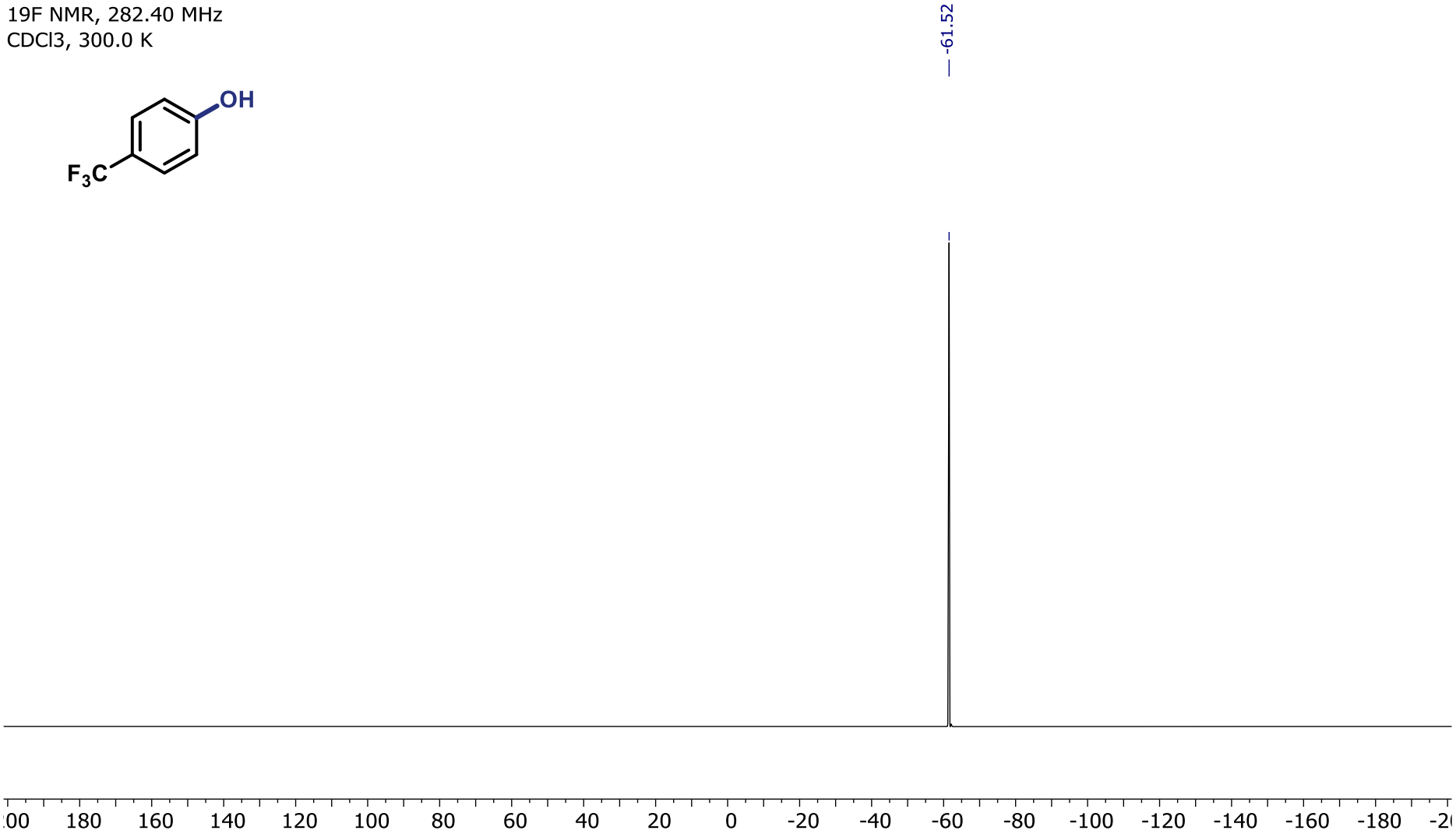

^{19}F NMR used to determine the yield of 4-hydroxybenzotrifluoride (8l)

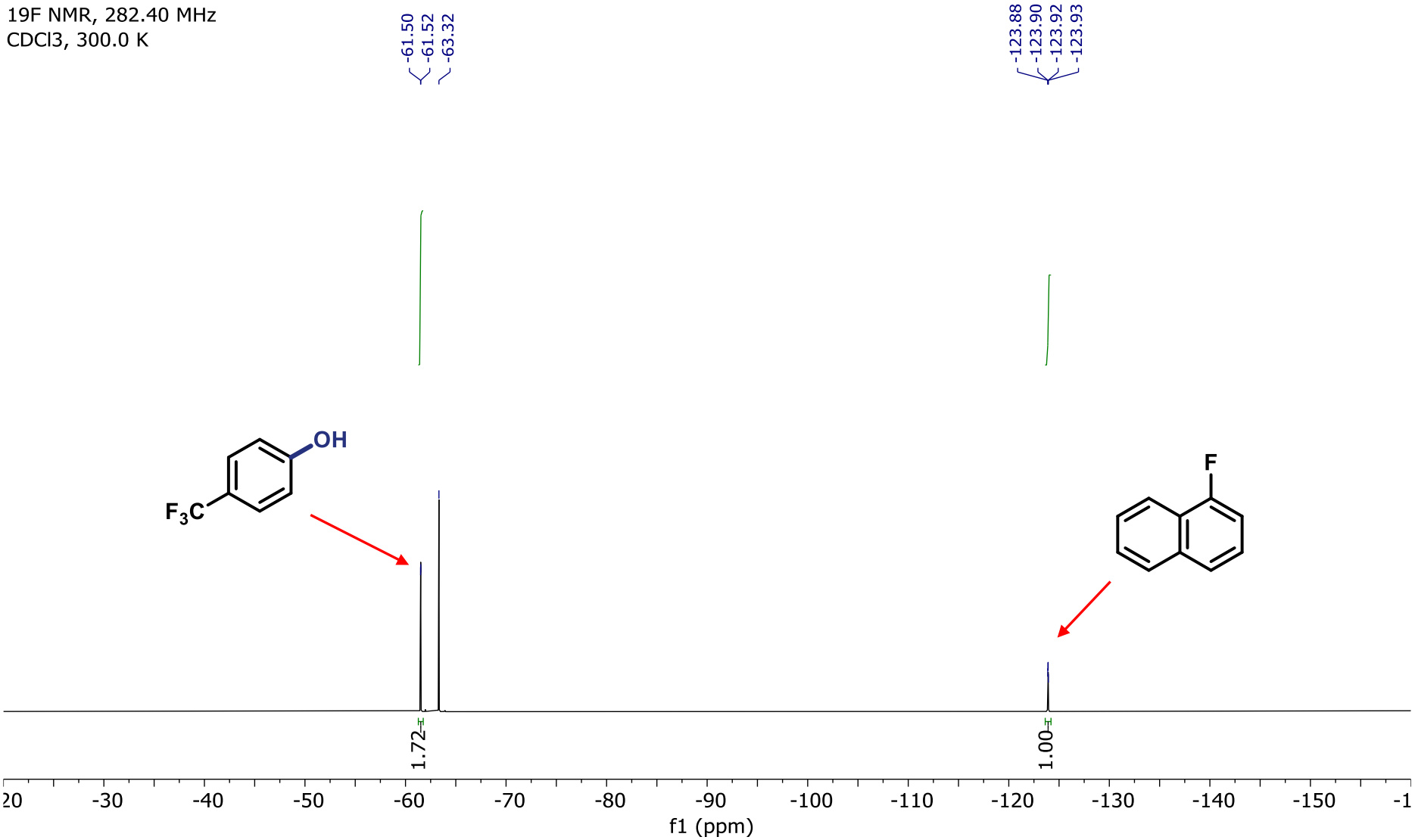

^{1}H NMR of 4-nitrophenol (8m)

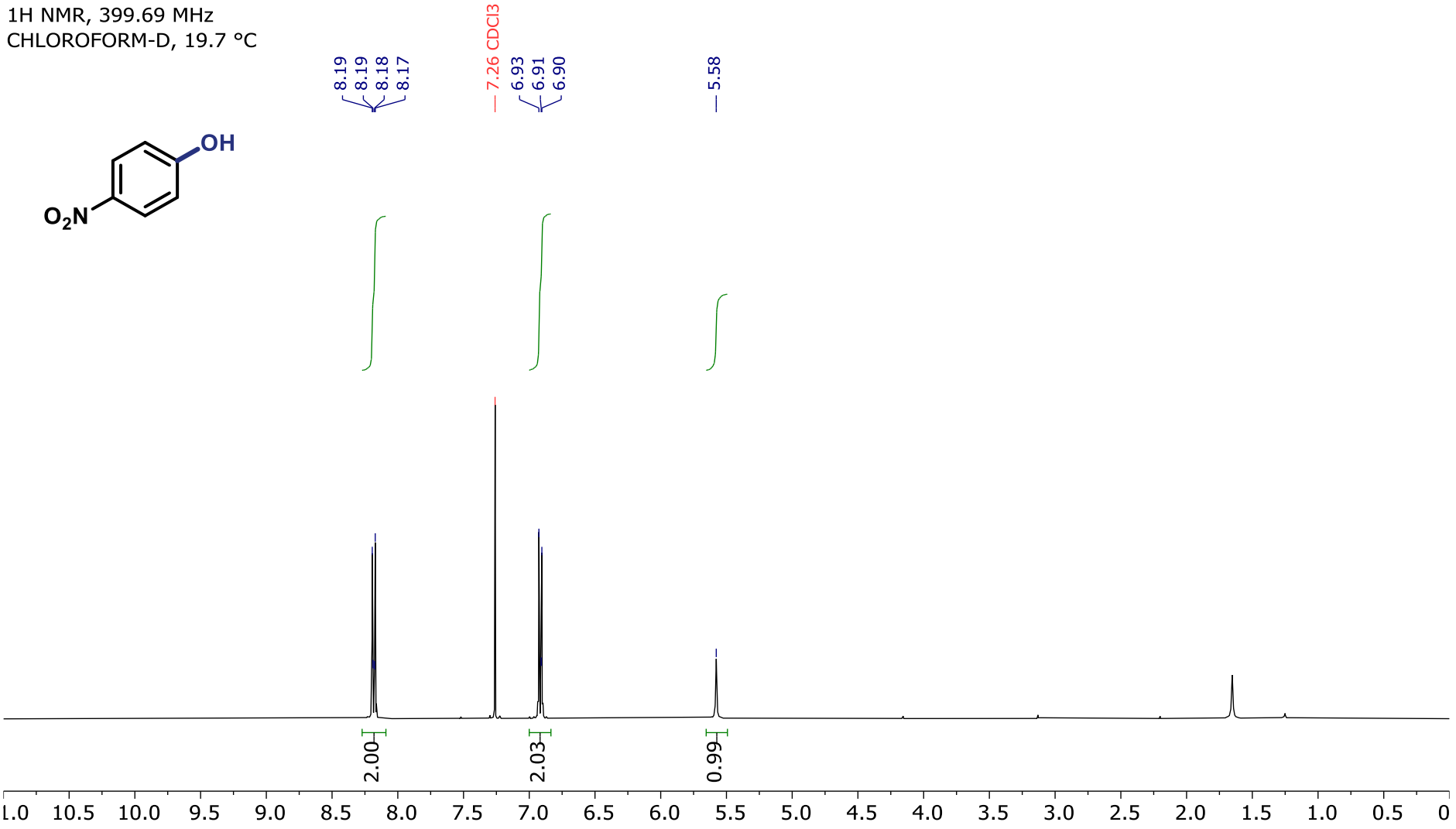

^{13}C NMR of 4-nitrophenol (8m)

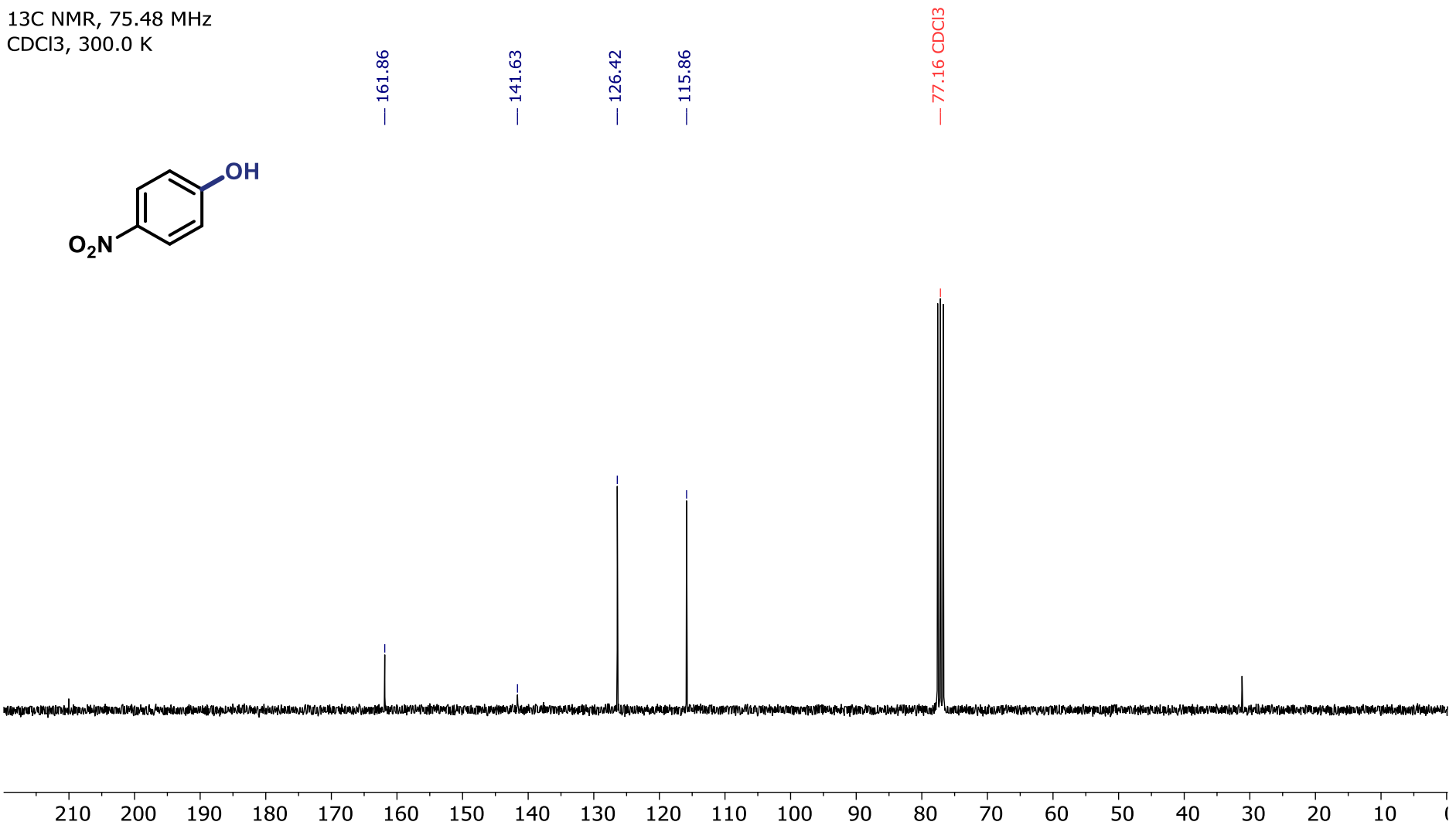

^{1}H NMR of 2-nitrophenol (8n)

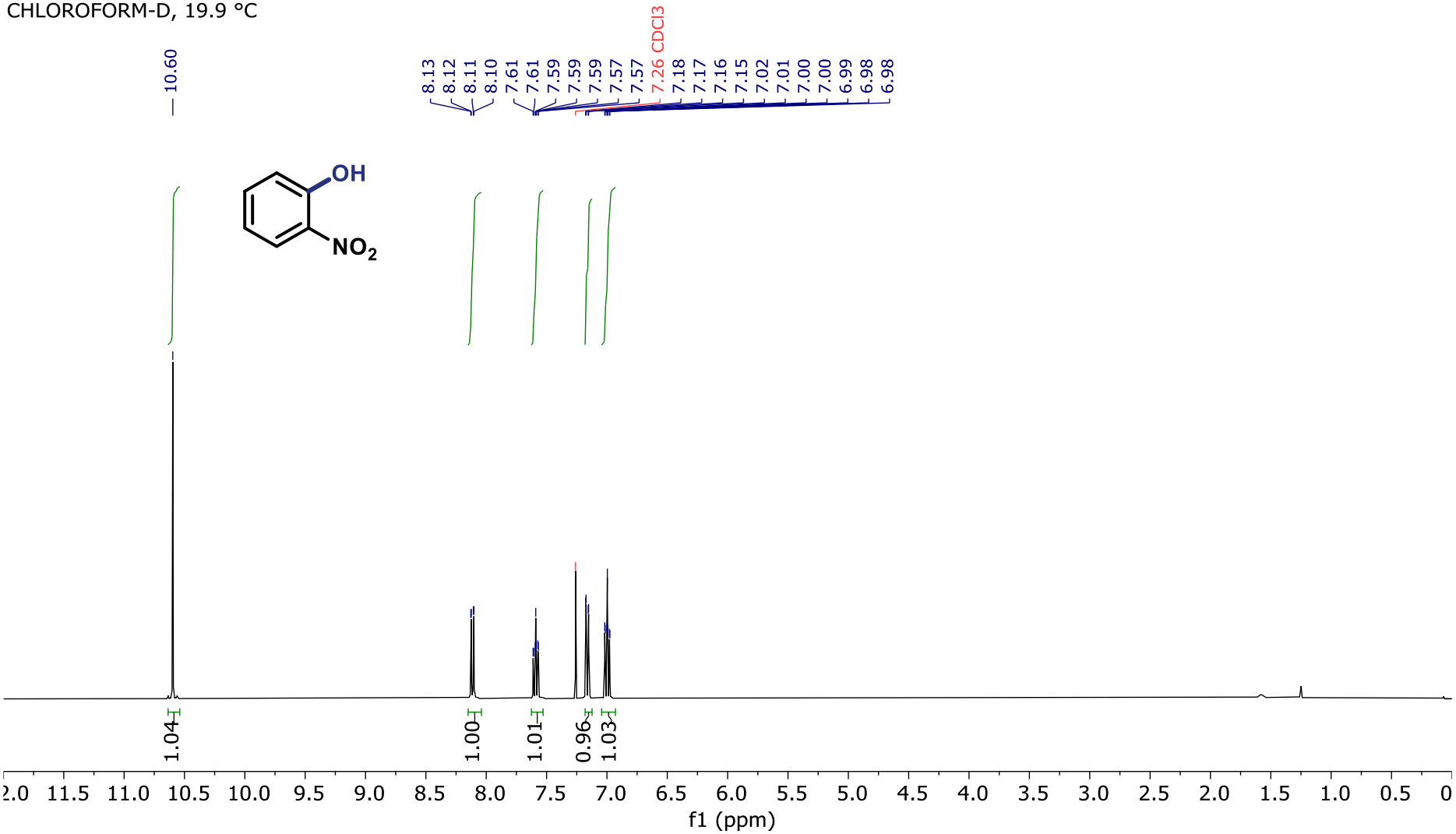

^{13}C NMR of 2-nitrophenol (8n)

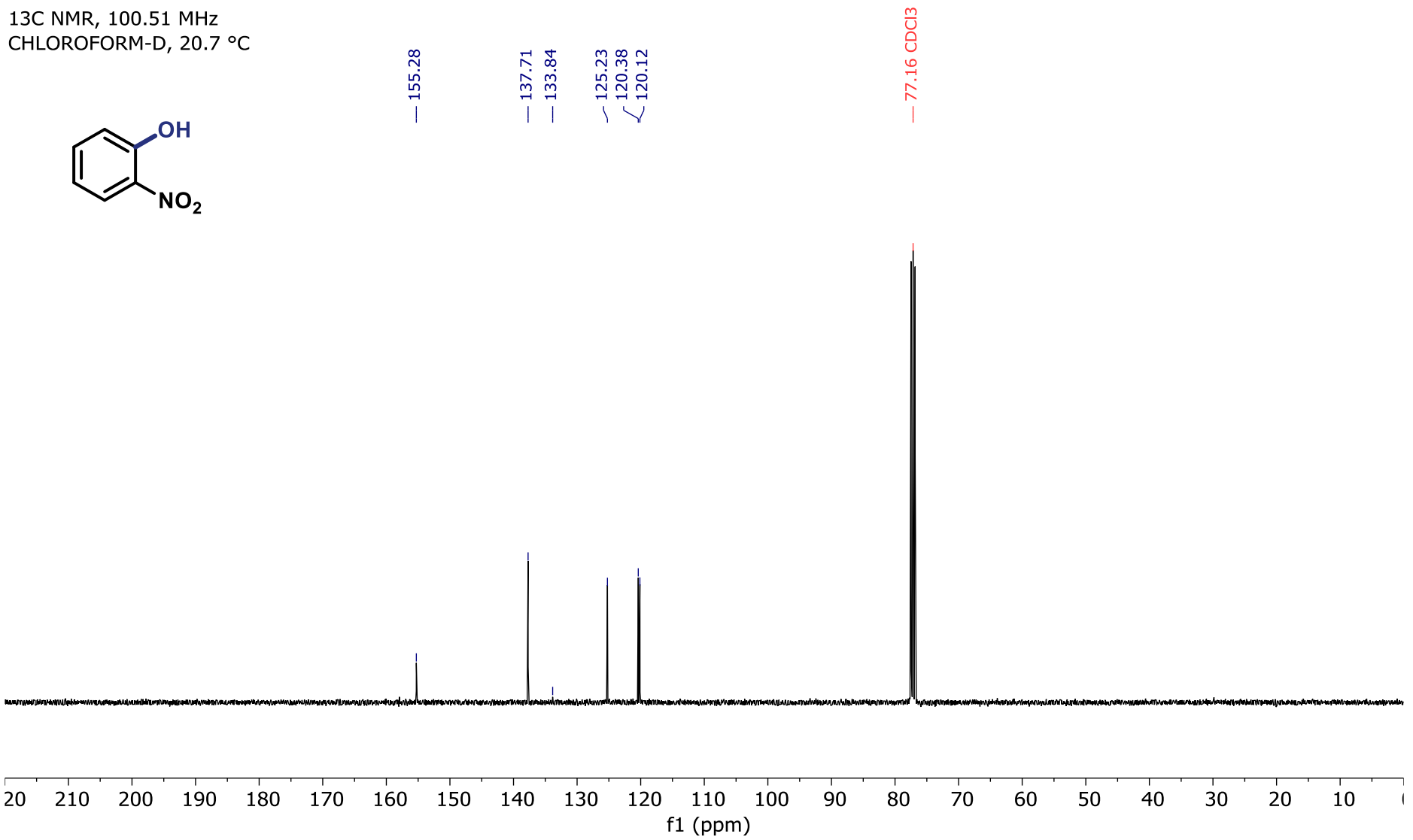

^{1}H NMR of 1-naphthol (8o)

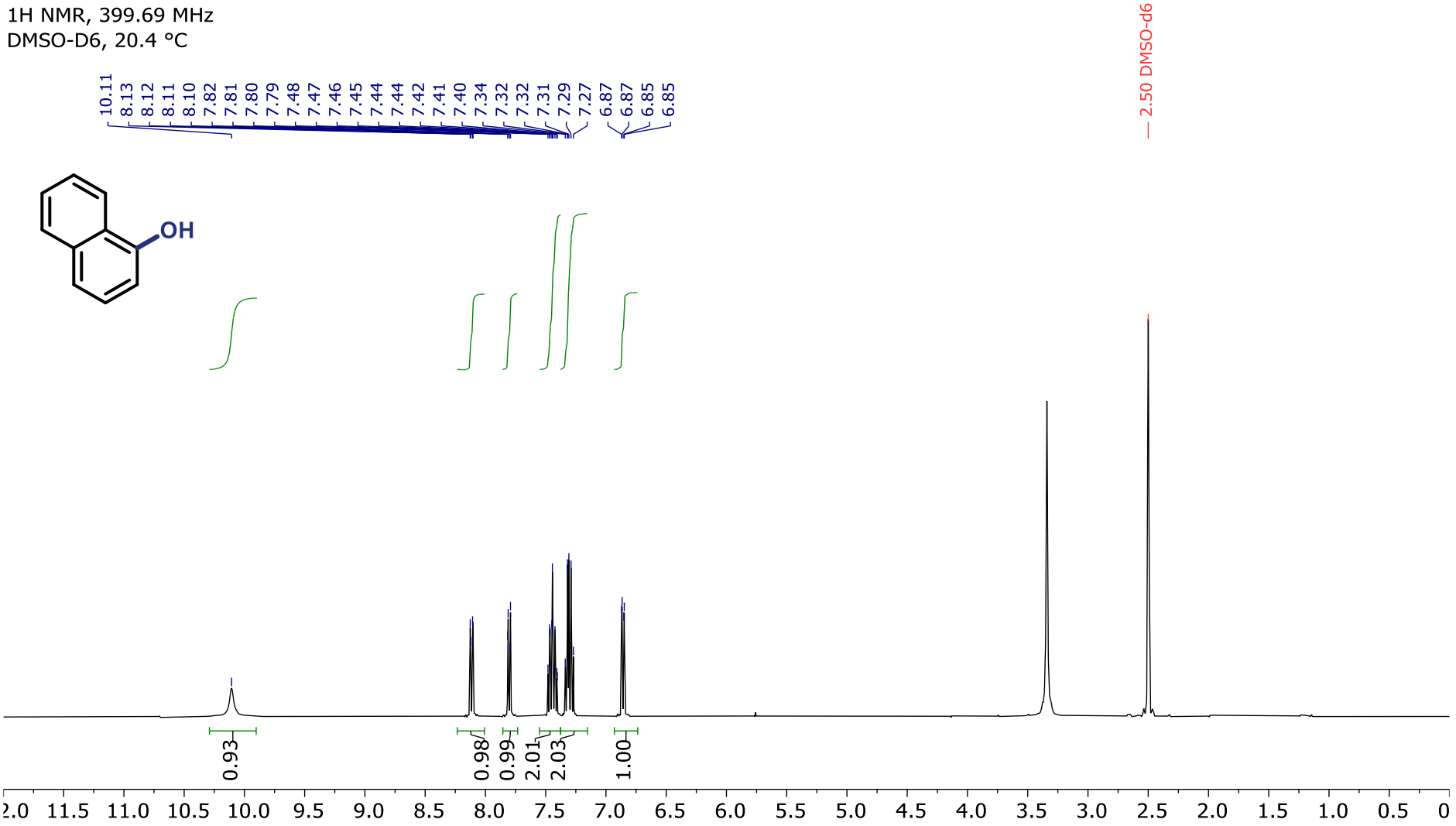

^{13}C NMR of 1-naphthol (8o)

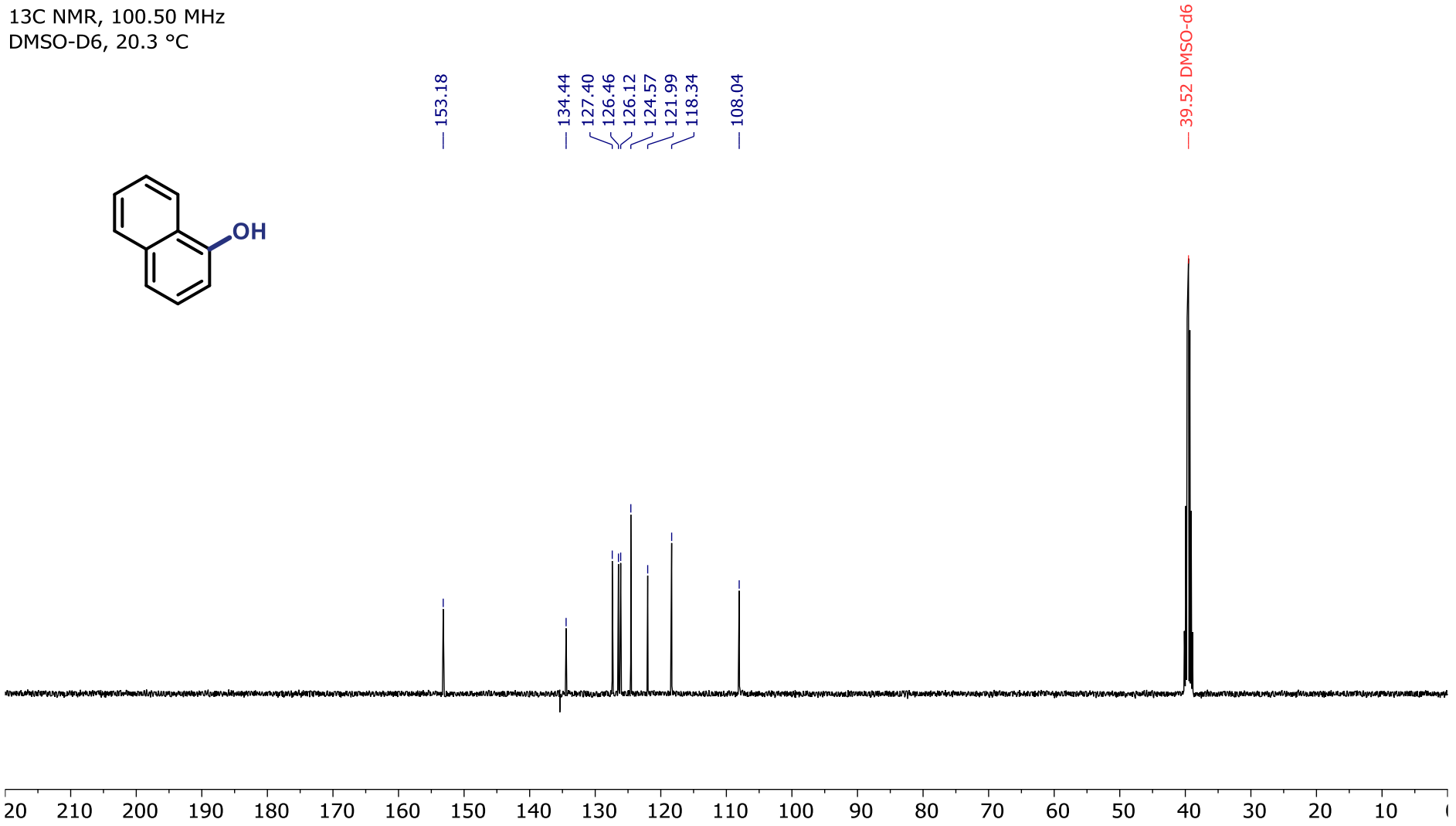

^{1}H NMR of 4-phenylphenol (8p)

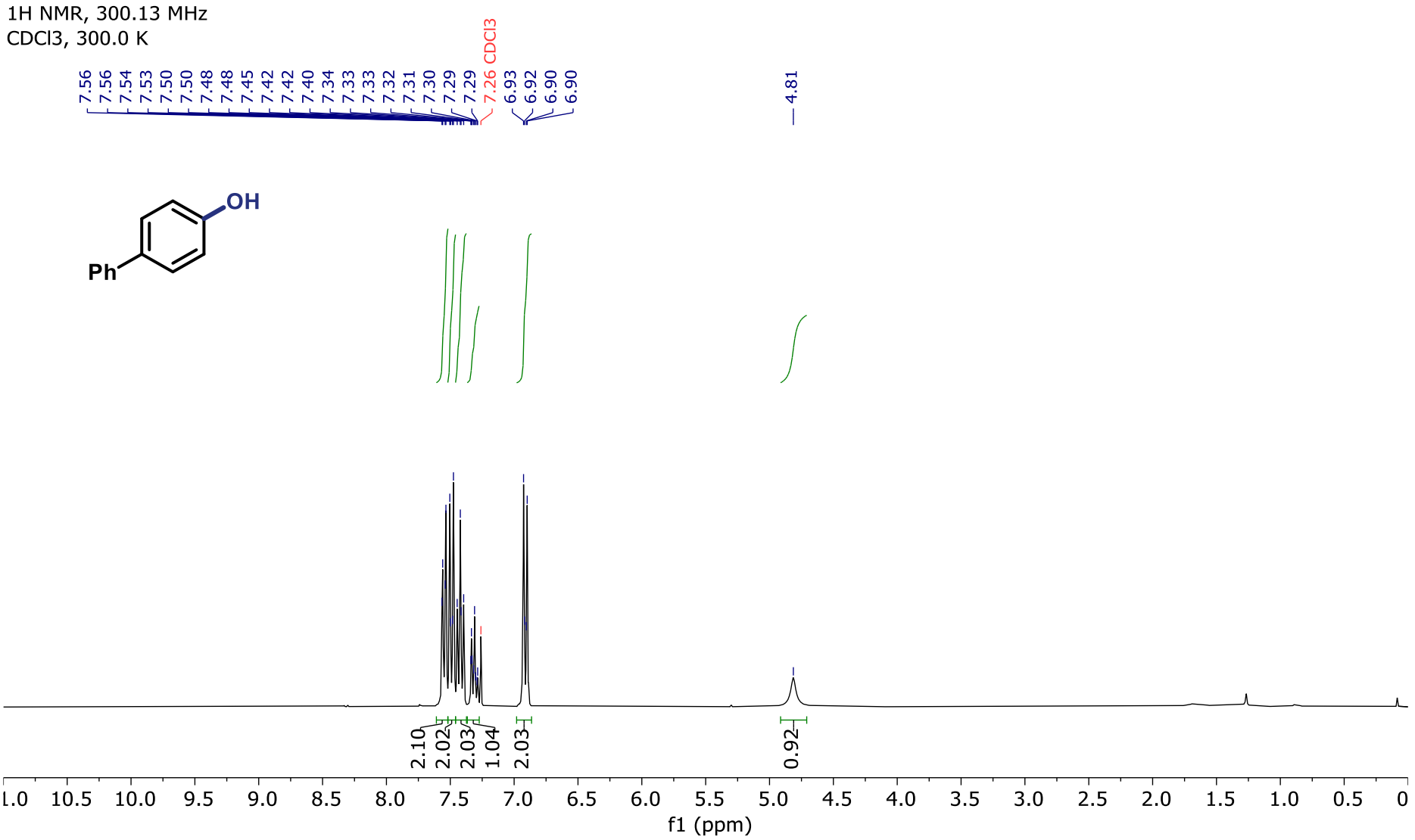

^{13}C NMR of 4-phenylphenol (8p)

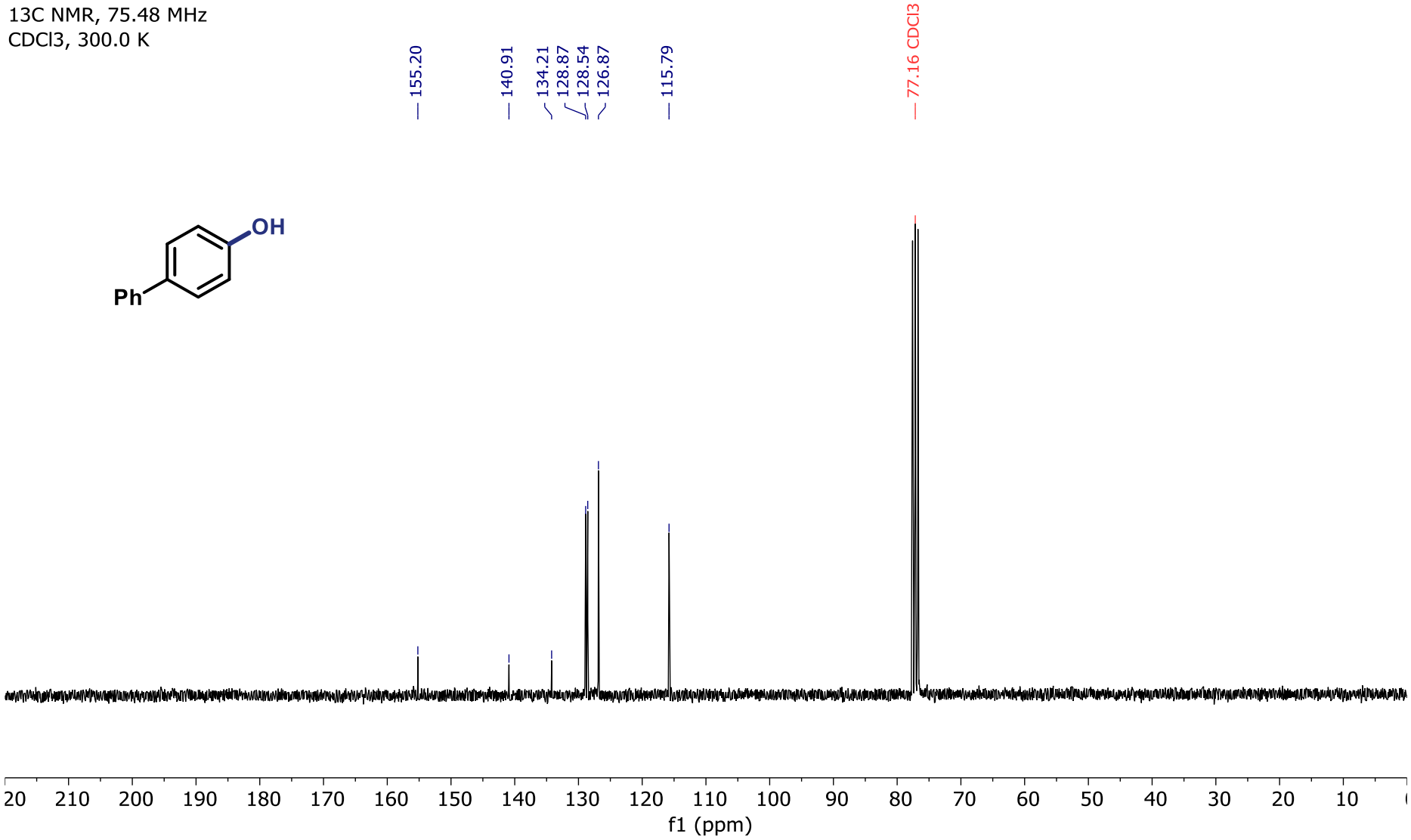

^{1}H NMR of 2-hydroxy-4-bromobiphenyl (8q)

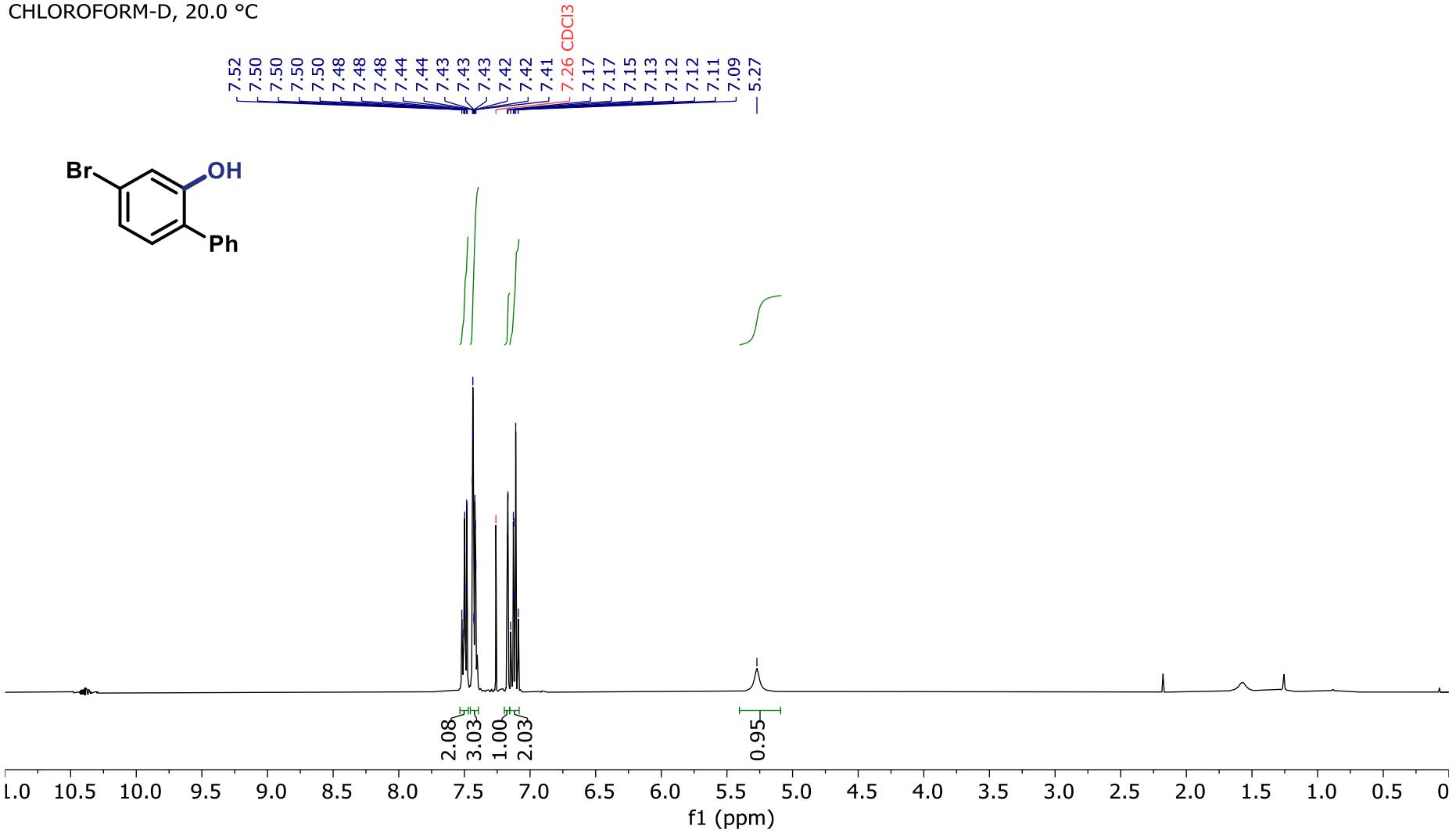

^{13}C NMR of 2-hydroxy-4-bromobiphenyl (8q)

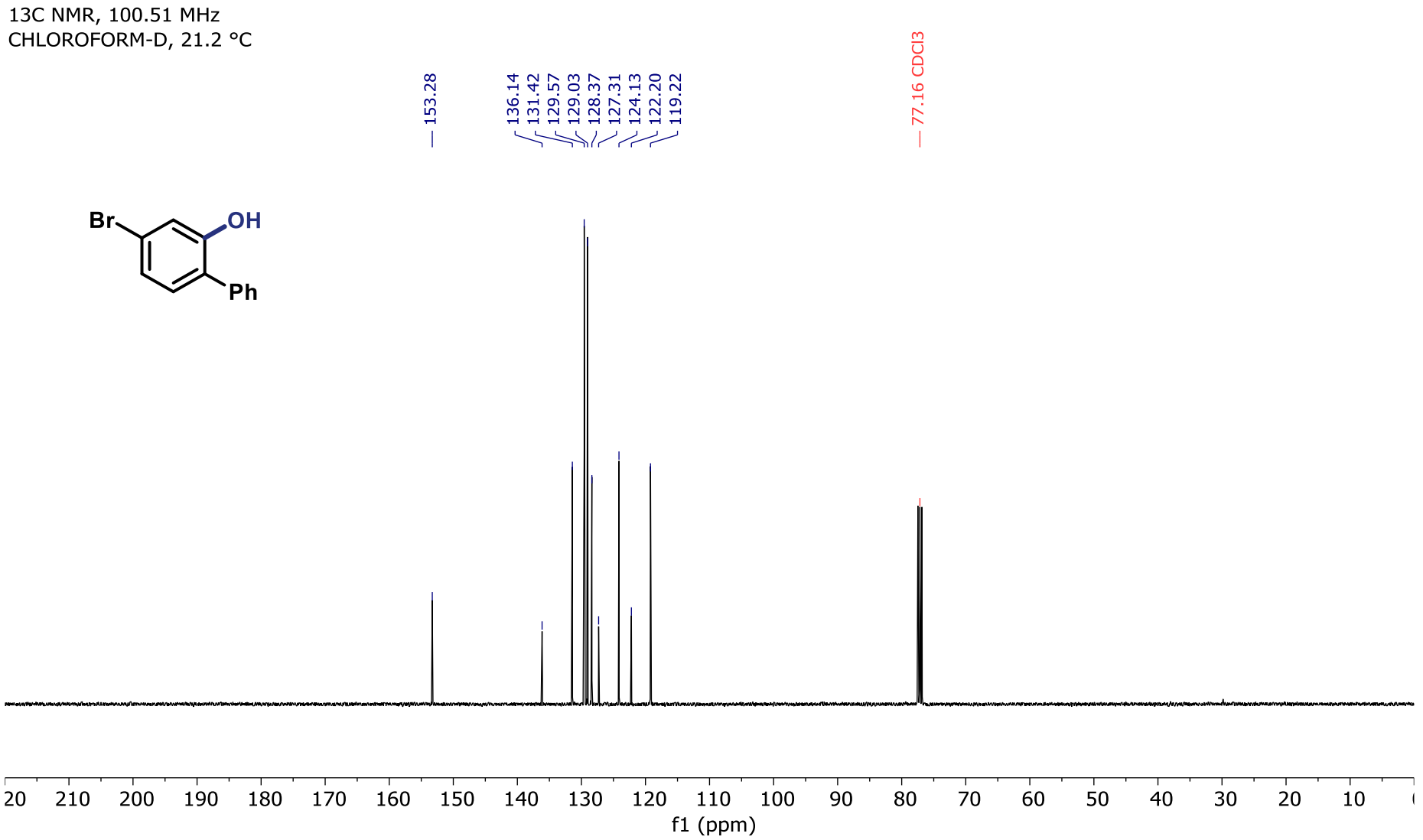

^{1}H NMR of 4-bromo-2-hydroxyacetophenone (8r)

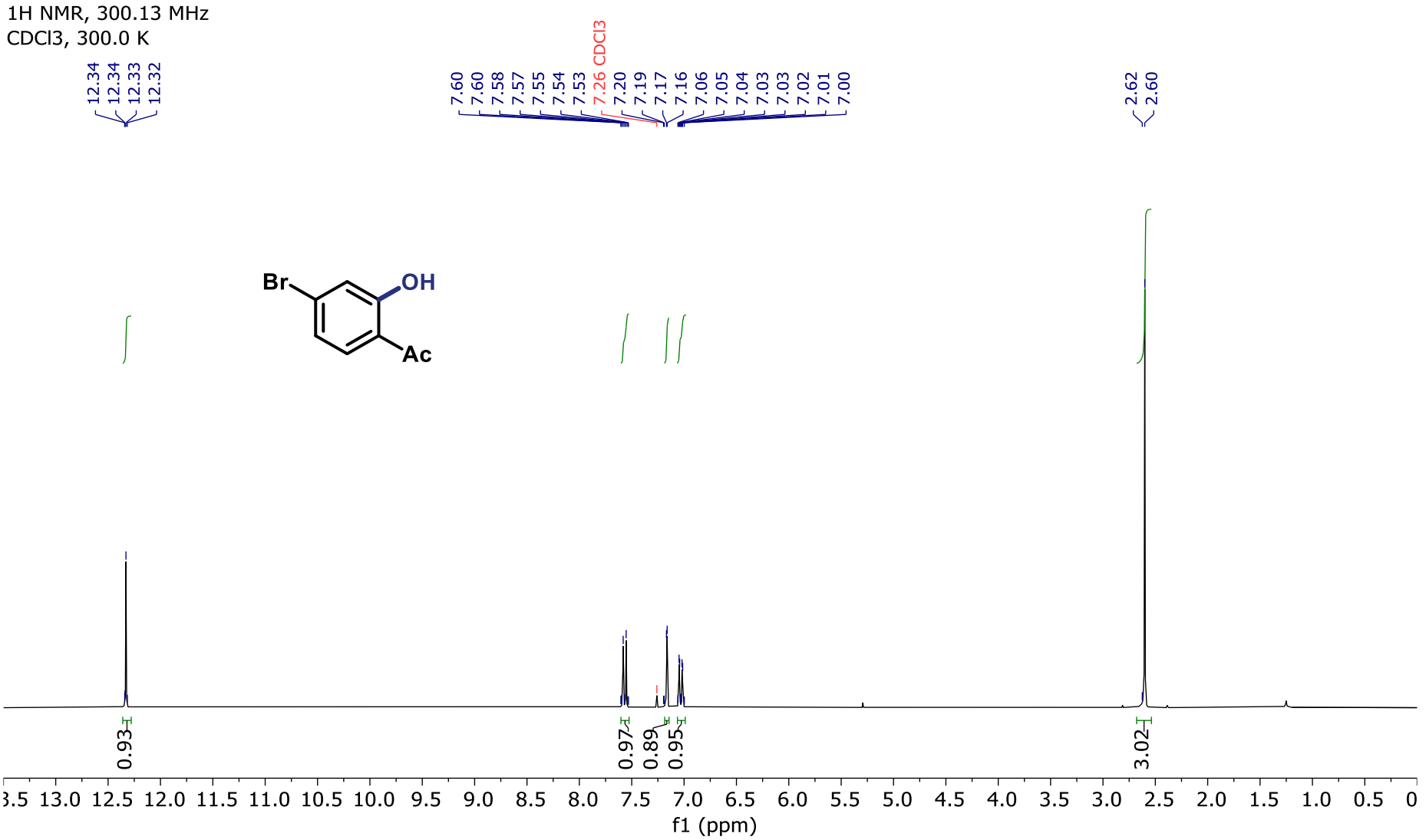

^{13}C NMR of 4-bromo-2-hydroxyacetophenone (8r)

13C NMR, 75.48 MHz
CDCl3, 300.0 °C

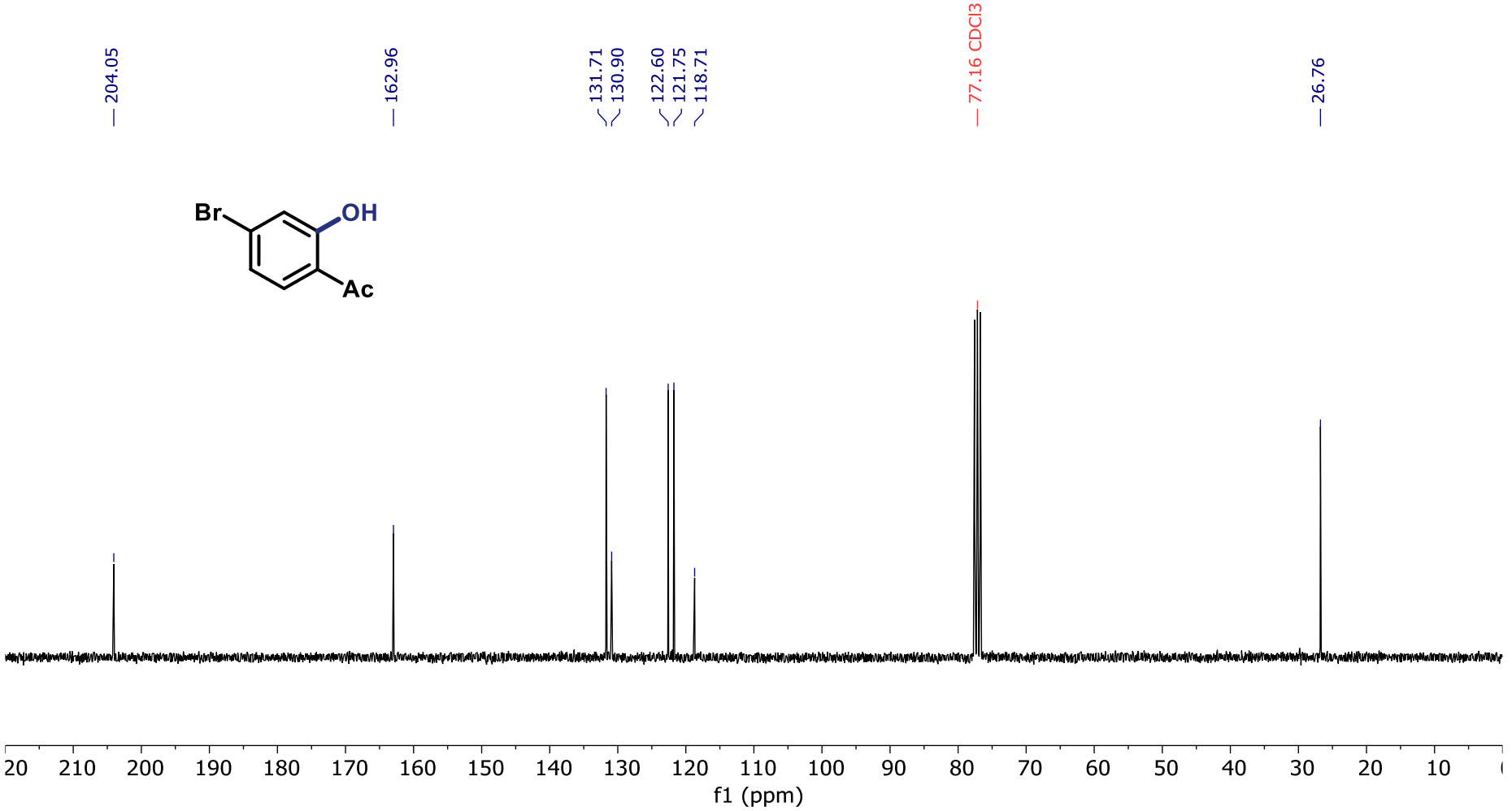

^{1}H NMR of 5-hydroxy-2-trifluoromethyl pyridine (8s)

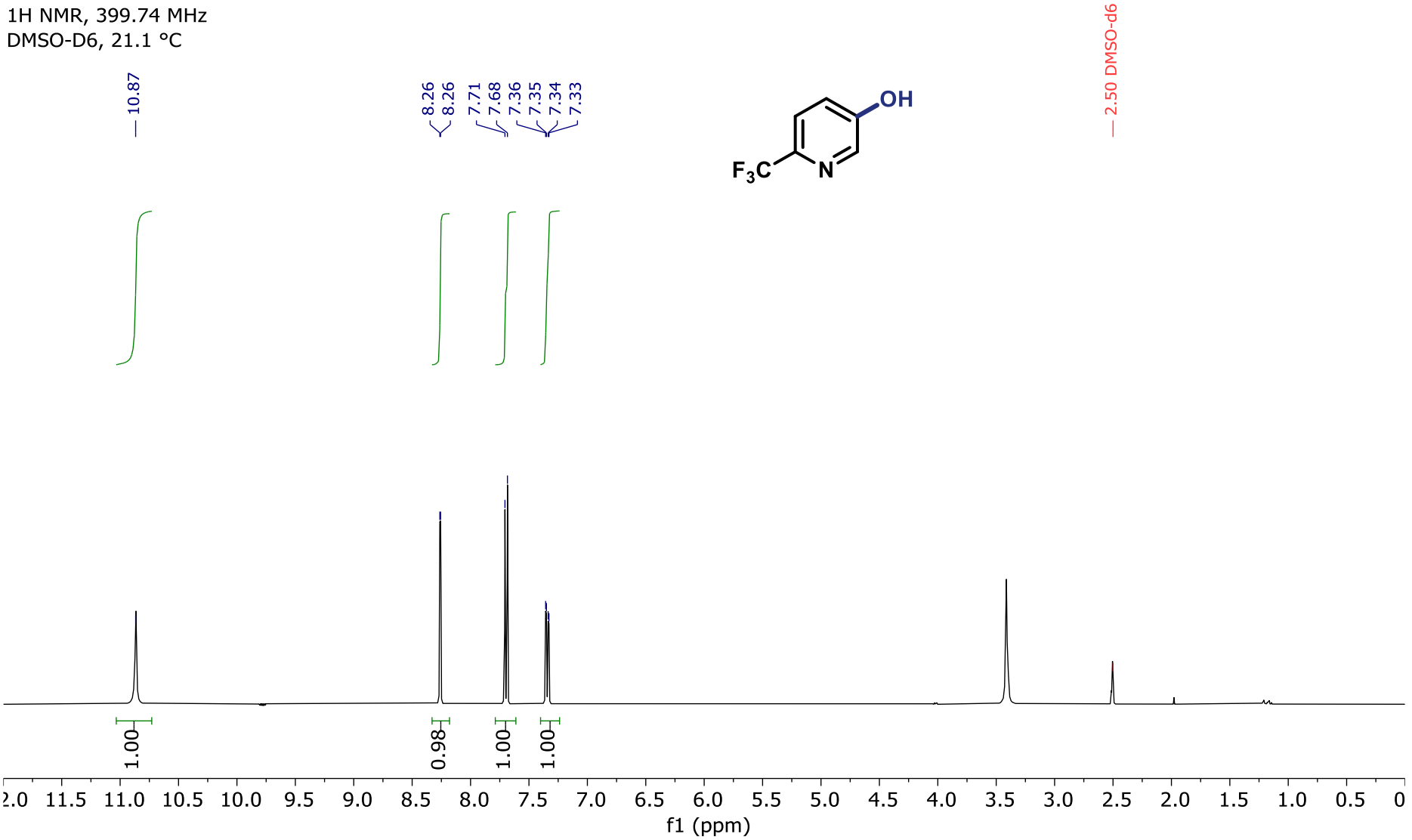

^{13}C NMR of 5-hydroxy-2-trifluoromethyl pyridine (8s)

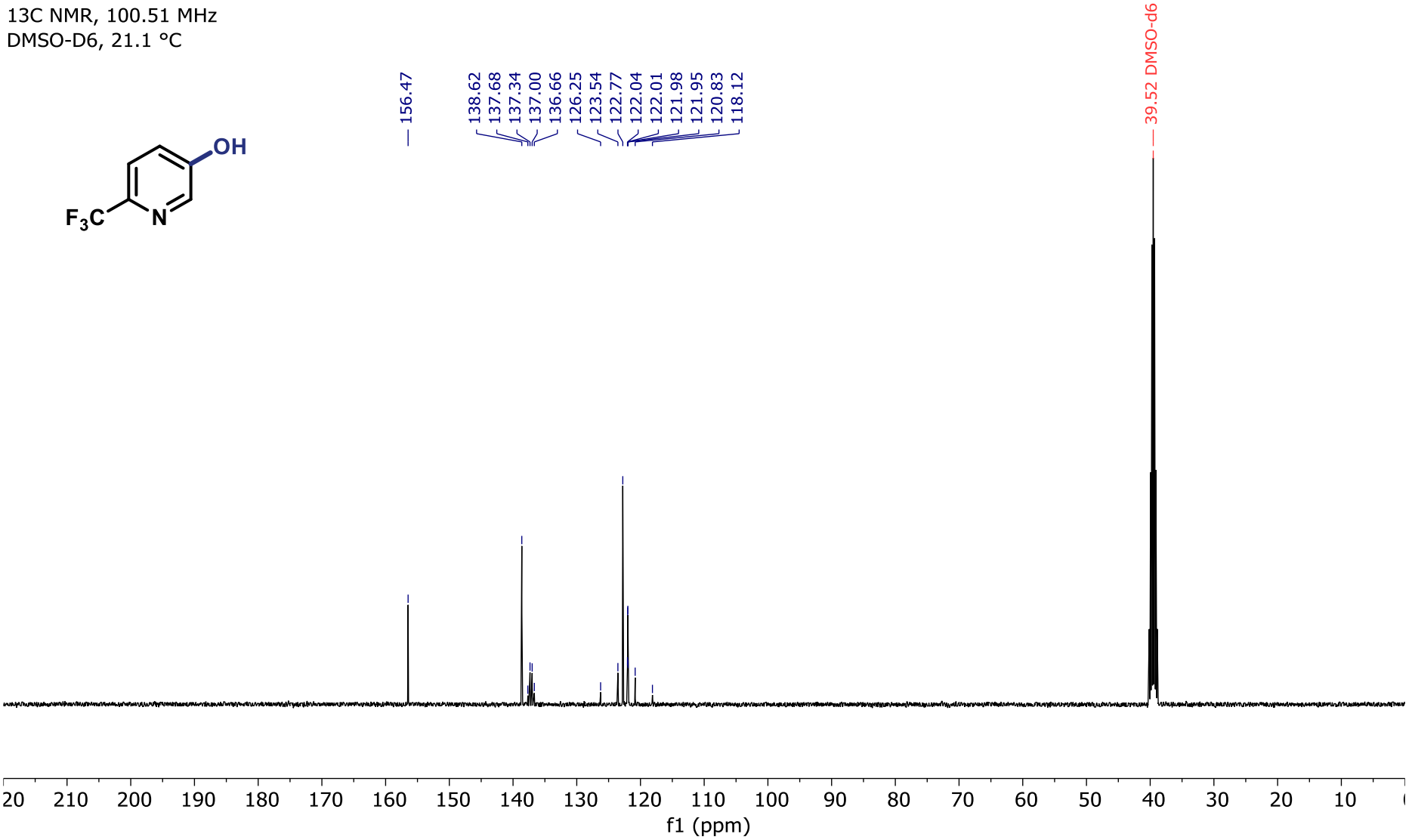

^{19}F NMR of 5-hydroxy-2-trifluoromethyl pyridine (8s)

19F NMR, 282.40 MHz
DMSO, 300.0 °C

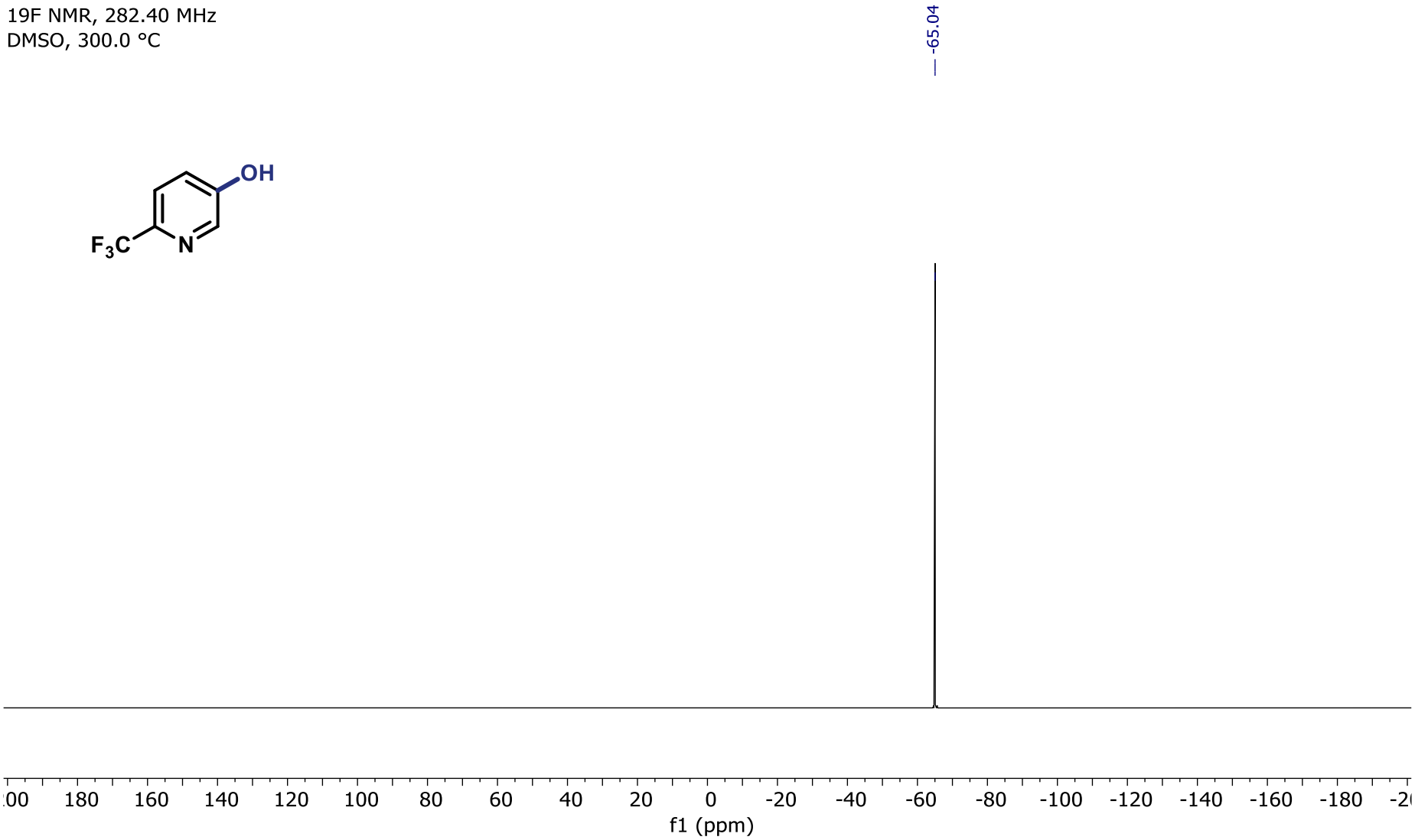

^{1}H NMR of 5-hydroxyquinoline (8t)

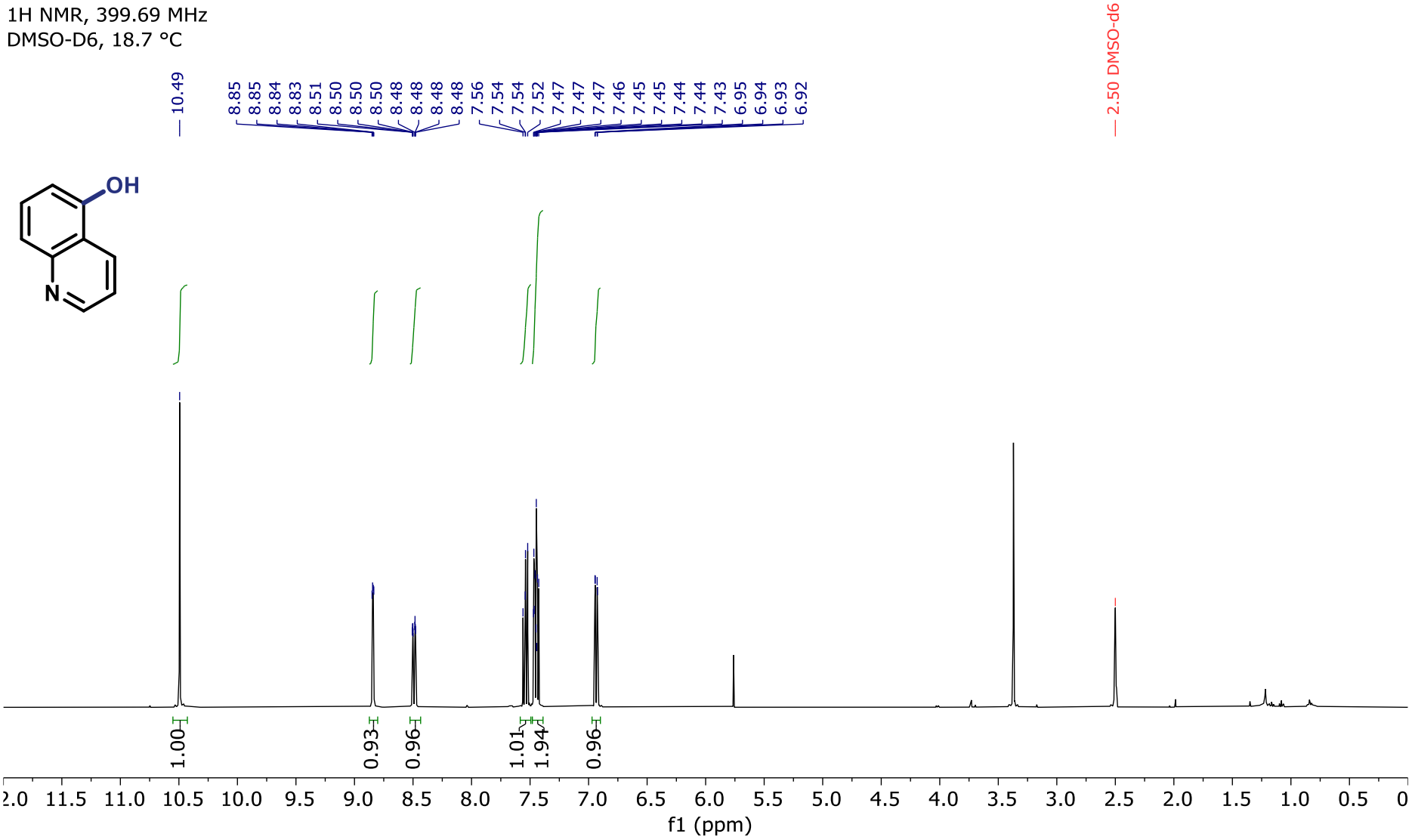

^{13}C NMR of 5-hydroxyquinoline (8t)

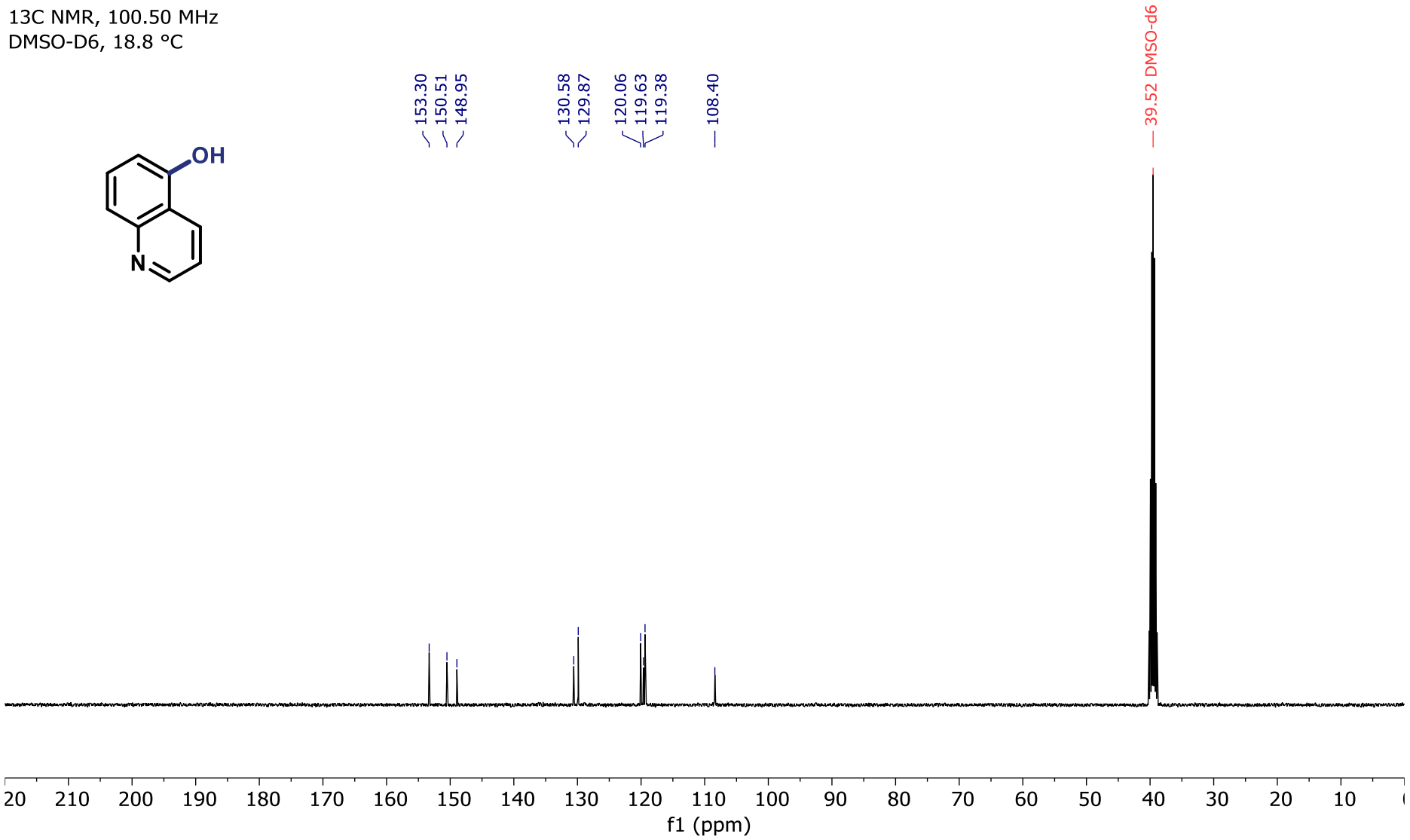

^{1}H NMR of 6-hydroxyquinoline (8u)

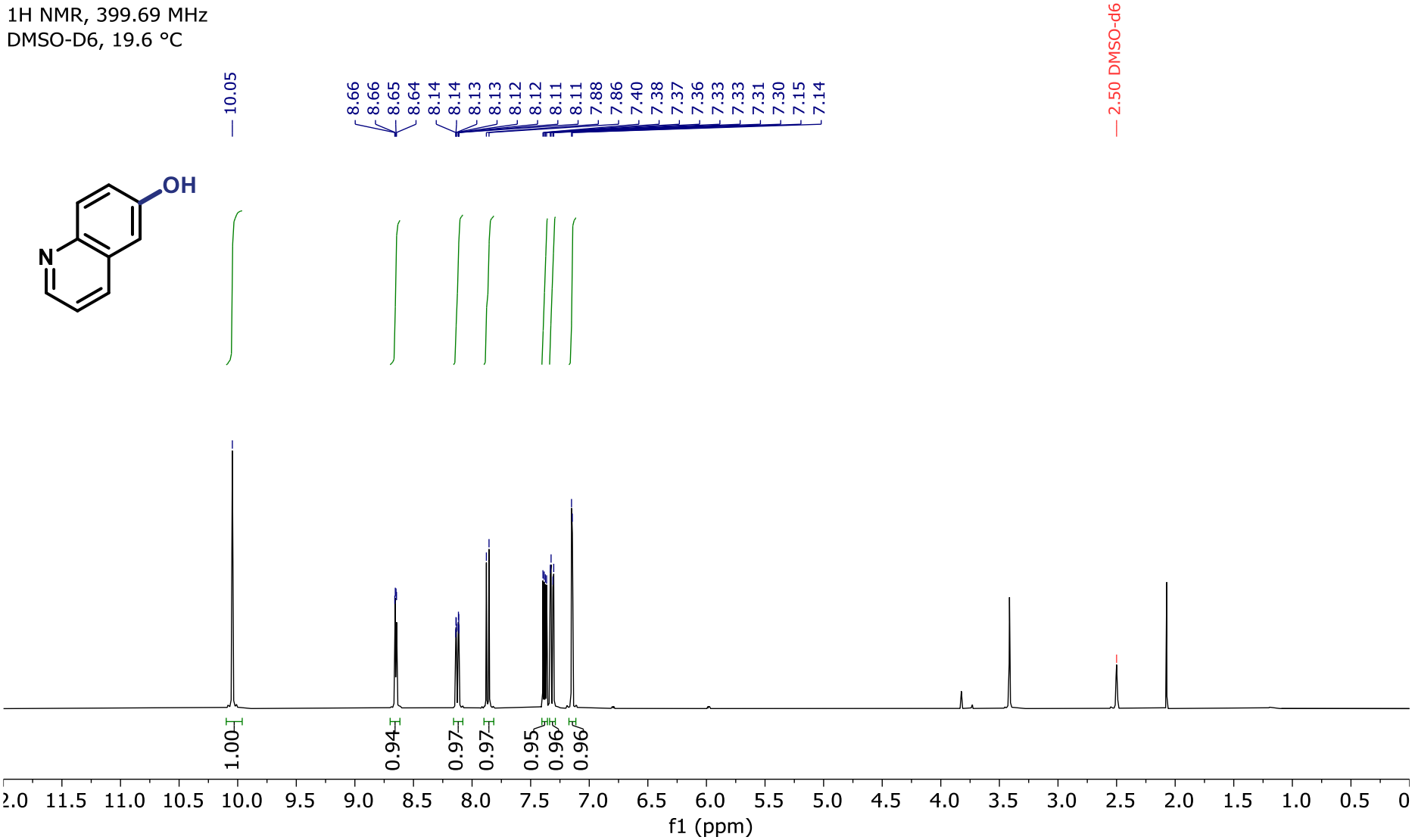

^{13}C NMR of 6-hydroxyquinoline (8u)

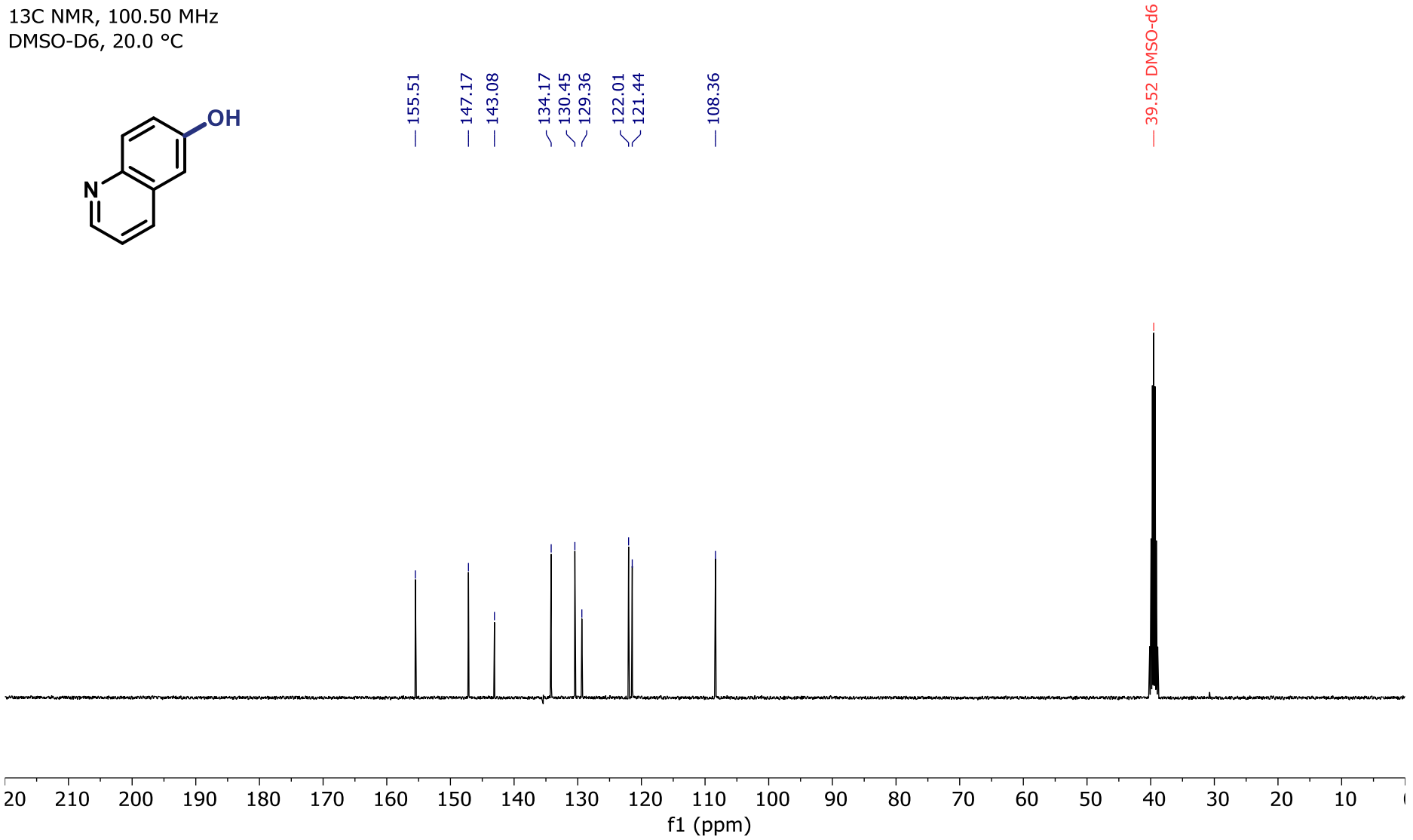

^{1}H NMR of 6-bromo-5-methylpyridin-3-ol (8v)

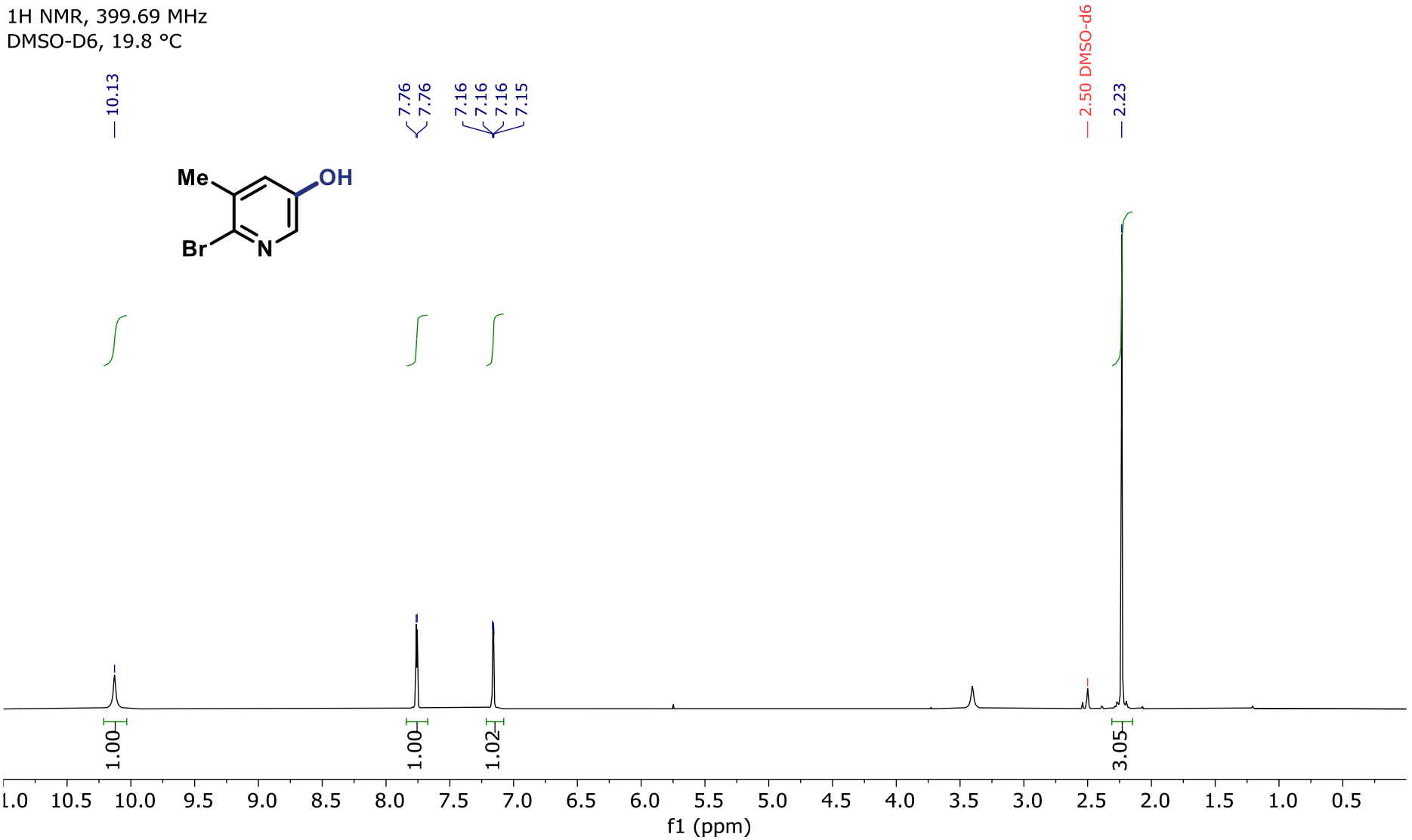

^{13}C NMR of 6-bromo-5-methylpyridin-3-ol (8v)

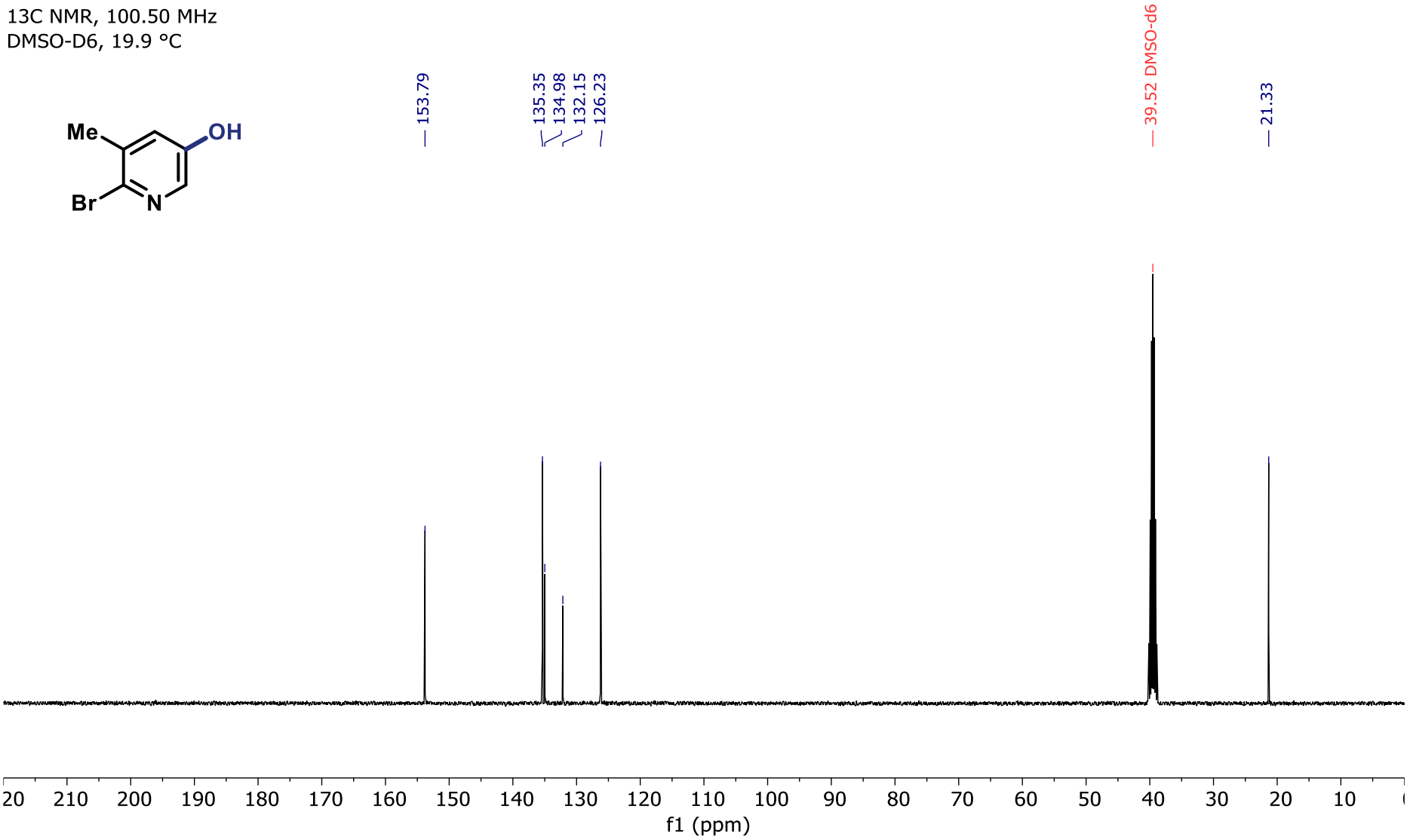

^{1}H NMR of hydroxy-Fenofibrate derivative (8w)

1H NMR, 399.74 MHz
CHLOROFORM-D, 20.1 °C

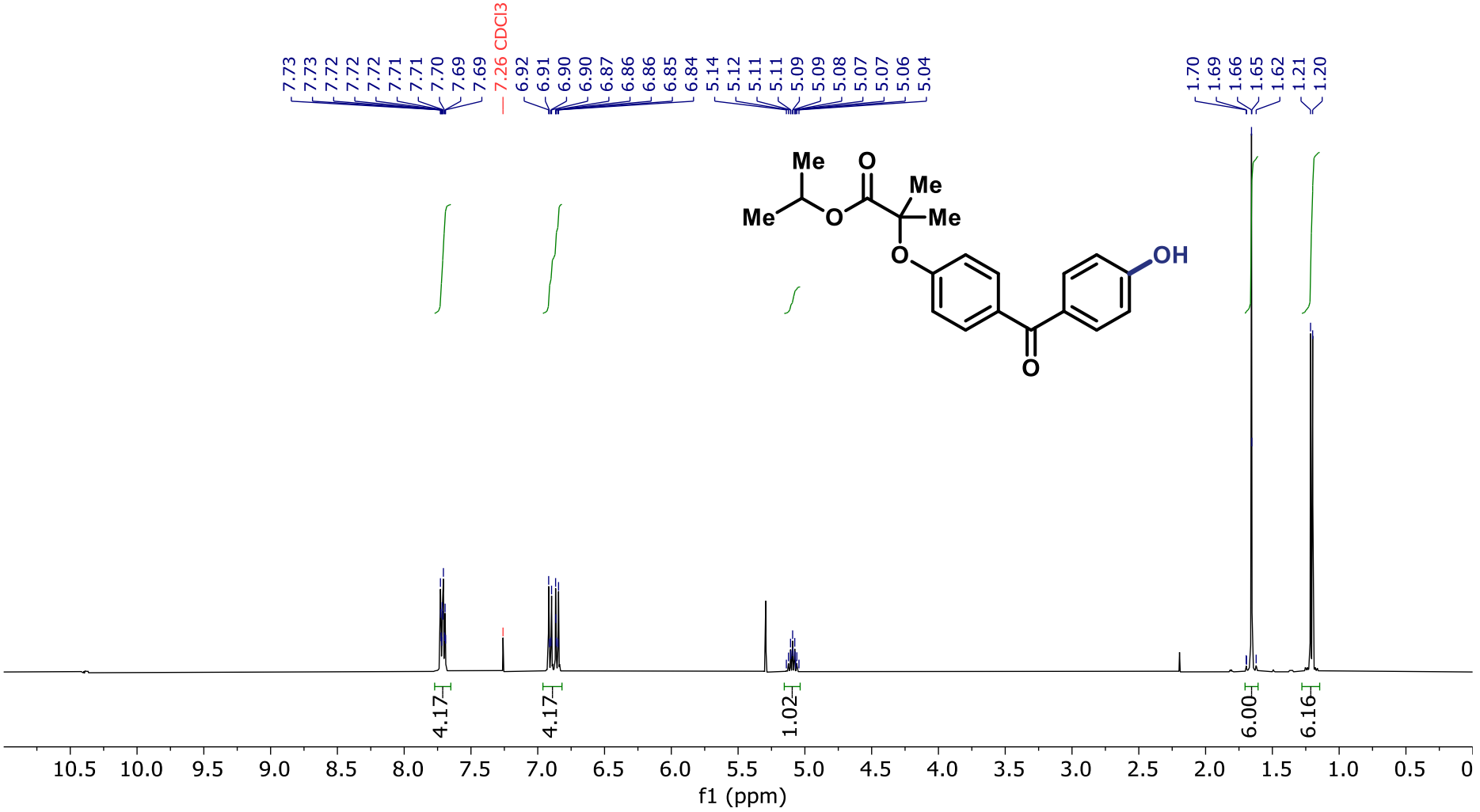

^{13}C NMR of hydroxy-Fenofibrate derivative (8w)

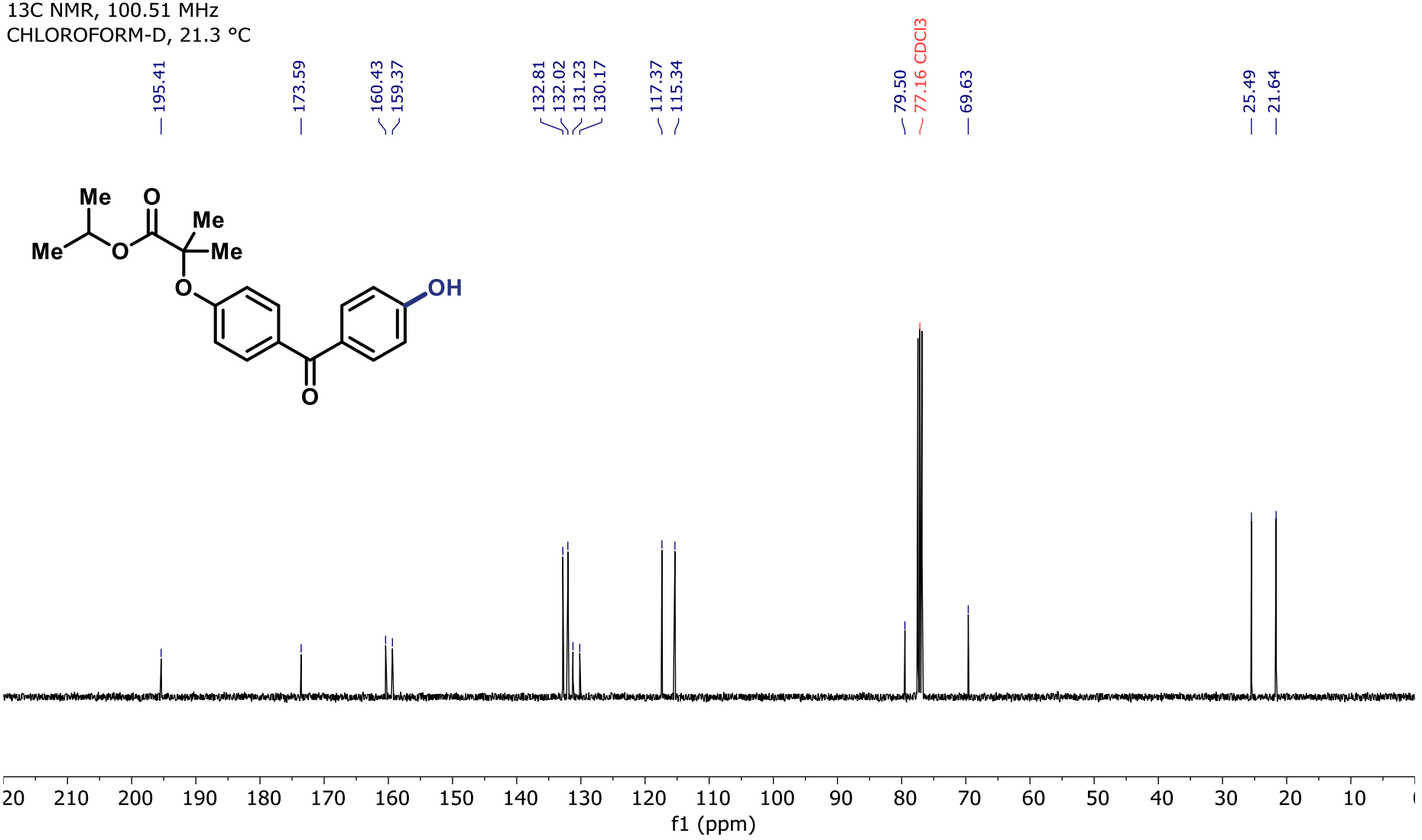

^{1}H NMR of hydroxy-Iloperidone derivative (8x)

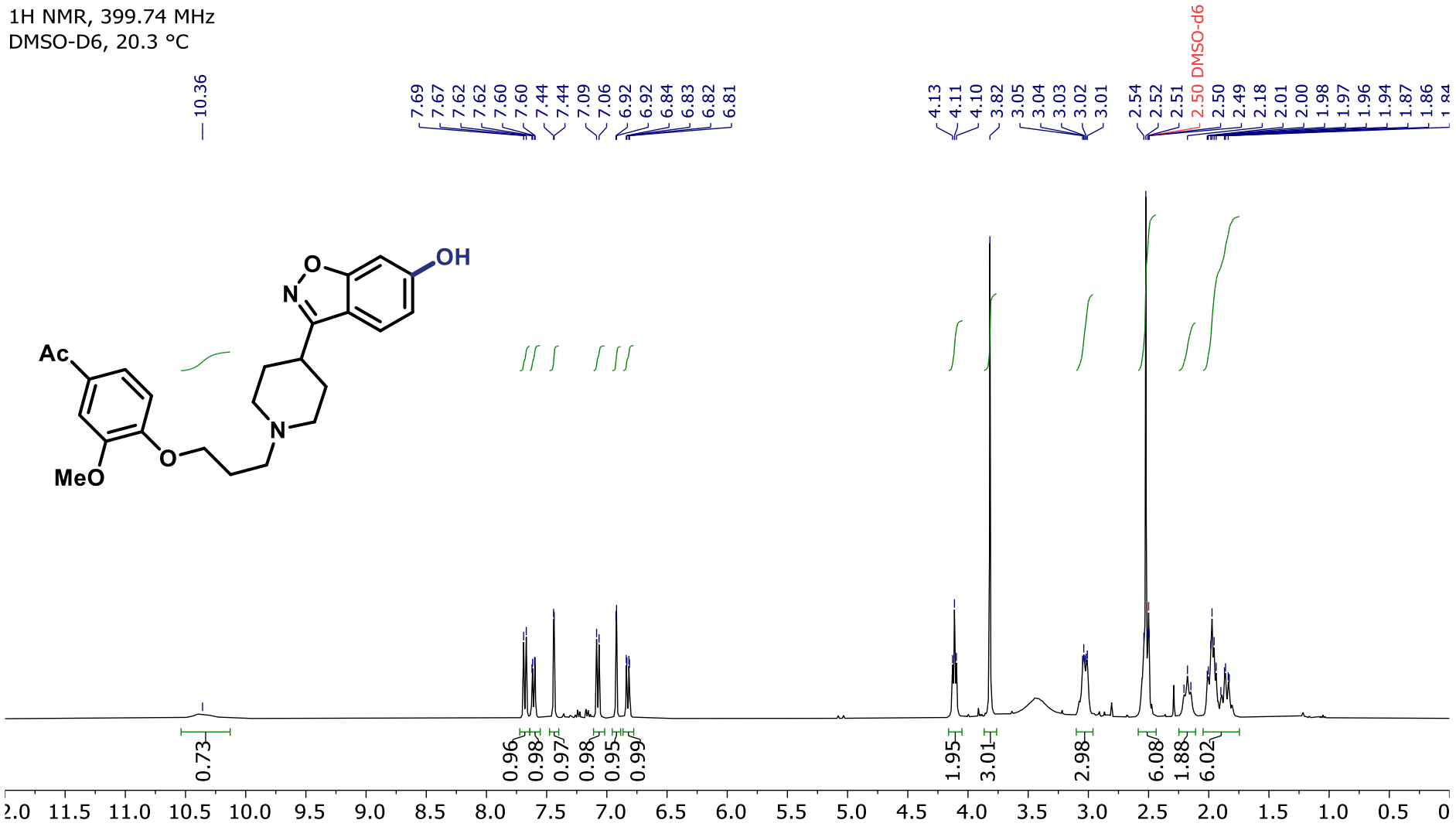

^{13}C NMR of hydroxy-Iloperidone derivative (8x)

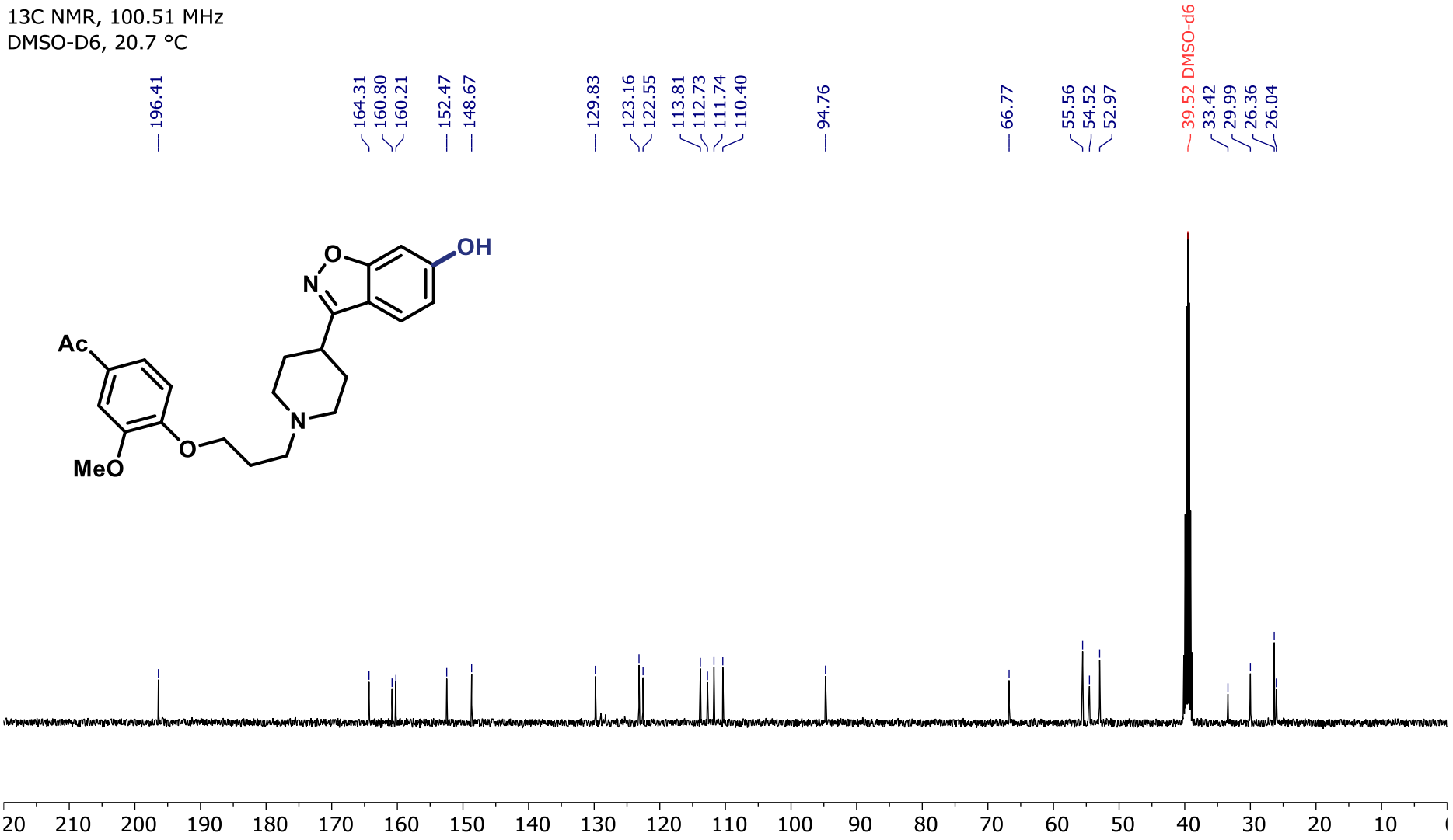

^{1}H NMR of hydroxy-Etoricoxib derivative (8y)

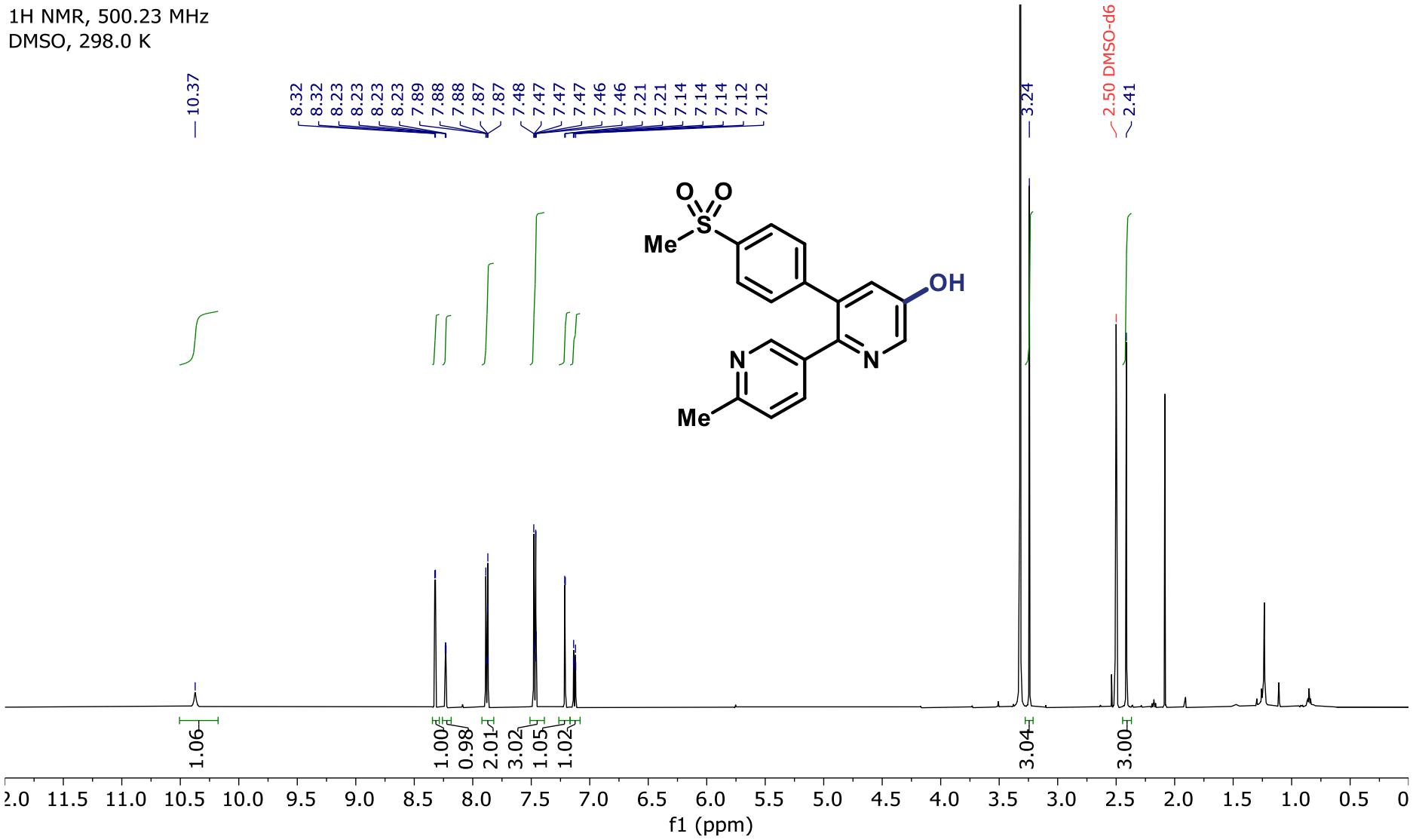

^{13}C NMR of hydroxy-Etoricoxib derivative (8y)

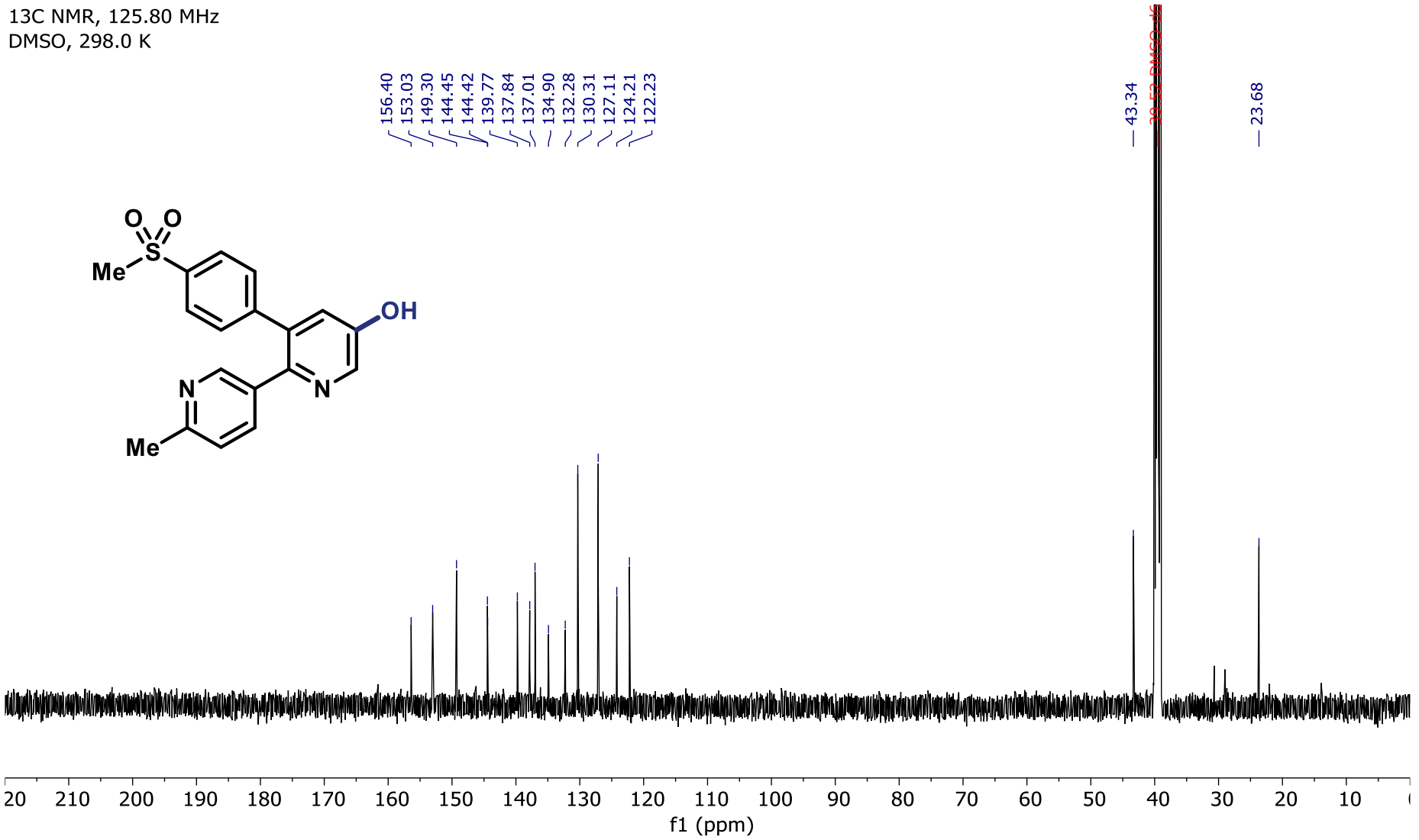

^{1}H NMR of hydroxy-Blonanserin derivative (8z)

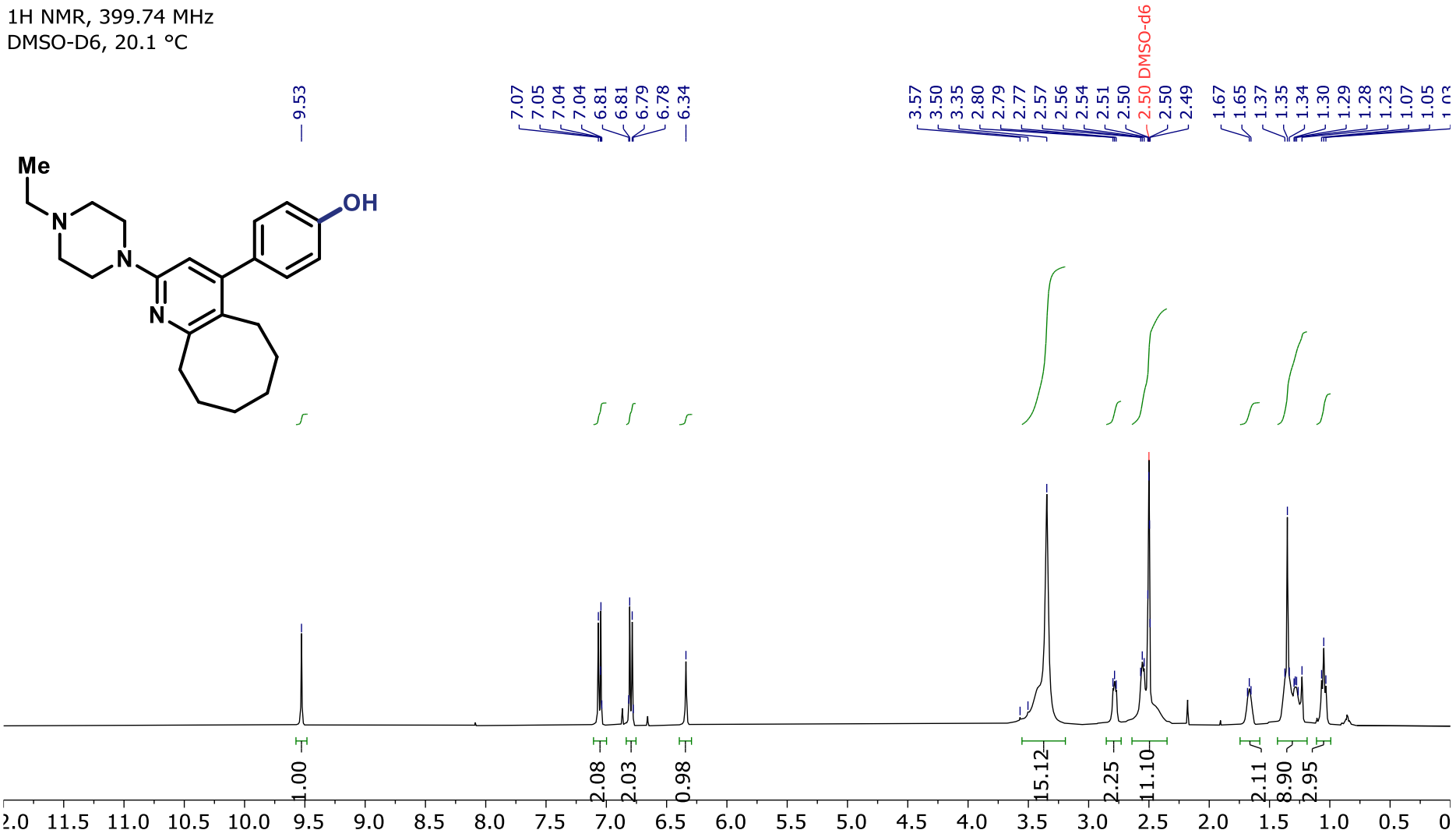

^{13}C NMR of hydroxy-Blonanserin derivative (8z)